STUDY OF A WIND POWERED WATER

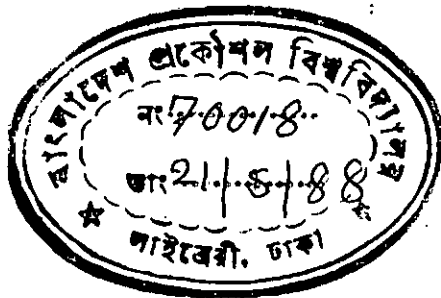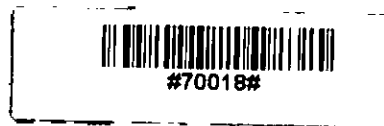PUMPING SET FOR BANGLADESH

by

IMTIAZ KAMAL

A Thesis Submitted to the Department of
Mechanical Engineering in partial fulfilment
of the requirements for the degree of

Master of Science

in

Mechanical Engineering

January, 1988

#70018#

Bangladesh University of Engineering and Technology,

Dhaka, Bangladesh.

STUDY OF A WIND POWERED WATER
PUMPING SET FOR BANGLADESH

A Thesis

by

Imtiaz Kamal

Approved as to the Style and Content:

Dr. Md. Quamrul Islam
Associate Professor
Department of Mechanical
Engineering, BUET, Dhaka.

Chairman

Dr. Dipak Kanti Das
Professor and Head
Department of Mechanical
Engineering, BUET,
Dhaka.

Member

Dr. Md. Abu Taher Ali
Professor
Department of Mechanical
Engineering, BUET,
Dhaka.

Member

Dr. Md. Abdur Razzaq Akhanda
Associate Professor
Department of Mechanical
Engineering, BUET,
Dhaka.

Member

Prof. Dr. Md. Fazli Ilahi
MCE Department
ICTVTR, - OIC
Dhaka.

Member (external)

CERTIFICATE OF RESEARCH

This is to certify that the work presented in this thesis is the outcome of the investigation carried out by the candidate under the supervision of Dr. Md. Quamrul Islam, Associate Professor of the Department of Mechanical Engineering, BUET, Dhaka.

Supervisor

Candidate

CANDIDATE'S DECLARATION

This is to certify that this work
has been done by me and has not
been submitted elsewhere for the
award of any Degree or Diploma.

Candidate

ABSTRACT

The aim of this study is to analyse the performance of a Horizontal Axis Wind Turbine coupled with a piston pump. Considering average wind velocity at Chittagong, the rotor configuration for twist and chord is determined by applying the momentum theory and the blade element theory, assuming no drag, no tilting or coning. The forces and moments on the blade and the tower top are calculated by obtaining the optimal aerodynamic shape of the blade.

In the present analysis, three types of blade shape have been considered : optimum-chord optimum-twist, linear-chord linear-twist, linear-chord zero-twist. Considering the aerodynamic performances, it has been observed that a linear-chord linear-twist blade is comparable to the optimum designed blade while offering a considerable reduction in manufacturing time and cost. The effect of coning angle, tilt angle, and of several wind conditions e.g. wind gradient, wind shift and tower shadow are discussed. The principal objectives of this study are to design a rotor optimised for peak performance and predict its characteristics and comparing the results with the results of existing wind turbines. For the designed rotational speed and

power of the turbine, a suitable piston pump is designed. The behaviour of the pump and also the behaviour of the rotor coupled with the designed pump are studied.

The effects of different acceleration of the Piston, and of valve behaviour are discussed. The starting behaviour of rotor is analysed with and without leakhole on the piston valve.

ACKNOWLEDGEMENT

To

my   parents

LIST OF SYMBOLS

a   axial interference factor

a'   tangential interference factor

a_p acceleration of Piston Pump

$a_{P_{max}}$ maximum acceleration of Piston Pump

a_w acceleration of water column

A   turbine disc area, AR^2

A_p area of the piston

A_v Area of valve

B   number of blades

C   chord of the blade

C_a acceleration co-efficient $\dfrac{\frac{1}{2} \Omega^2 S}{g}$

C_D blade drag coefficient, $\dfrac{dD}{\frac{1}{2} \rho C W^2 dr}$

C_L blade lift coefficient, $\dfrac{dL}{\frac{1}{2} \rho C W^2 dr}$

C_{L_d} design lift Coefficient

C_p power coefficient, $\dfrac{P}{\frac{1}{2} \rho A V_\alpha^3}$

C_Q torque coefficient, $\dfrac{Q}{\frac{1}{2} \rho A V_\alpha^2 R}$

C_T thrust coefficient, $\dfrac{T}{\frac{1}{2}\, \rho\, A\, V_\alpha^2}$

D drag force

D_p Diameter of Piston

D_v Diameter of valve

dA blade element area, C dr

dC_P elemental power coefficient, $\dfrac{dP}{\frac{1}{2}\, \rho\, A\, V_\alpha^3}$

dC_Q elemental thrust coefficient, $\dfrac{dT}{\frac{1}{2}\, \rho\, A\, V_\alpha^2\, R}$

dD blade element drag force

dF_n blade element normal force

dF_t blade element tangential force

dP blade element power

dL blade element lift force

dm differential mass

dN blade element normal force

dQ blade element torque

dT blade element thrust

E modulus of elasticity

F Prandtl's loss factor

F_{cl} static force

F_{hub} hub loss factor

F_{inst} instationary drag force

F_n normal force

F_p force on piston

F_{st} stationary drag force

F_t tangential force

F_{tip} tip loss factor

g acceleration due to gravity

H hub height from ground level

L lift force

m_v mass of valve

P turbine power

P_e amount of power to be extracted

p^+ pressure immediately in front of the rotor

p^- pressure immediately behind the rotor

P_α free stream pressure

P_{id} ideal power

$\bar{P}_{id}$ average ideal power

Q_{id} ideal torque of the rotor

$\bar{Q}_{id}$ average ideal torque of the rotor

Q_{mech} mechanical torque of the rotor

q discharge (m/sec)

q_{leak} flow through leak hole

Q_p torque of the pump

$\bar{Q}_p$ average torque of the pump

r	local blade radius
r_{Hub}	hub radius
R	rotor radius
R_e	effective radius
R_L	radial distance along the blade
Q	torque
Q_{S_t}	starting torque
S	stroke length
SH	shape of blade
$SH=1$	ideal case (optimum-chord optimum-twist)
$SH=2$	linearizing chord & twist angle between 0.5R & 0.9R
$SH=3$	linearizing chord between 0.5R & 0.9R but twist angle is zero.
T	thrust force
T^*	number of pump⅔
U	wind speed through turbine
V	wind velocity
$\bar{V}$	average wind velocity
V_d	design wind velocity
V_p	velocity of pump
V_w	velocity of water column
V_t	tangential wind velocity
V_α	undisturbed wind velocity
$V_{\alpha\,o}$	local wind velocity considering wind shear
W	relative wind velocity

X	dimensionless quantity, r/R
z	height of a particular point from ground level
z_{ref}	height of a reference point from ground level
z_p	displacement of the piston
z_v	displacement of valve
z_w	displacement of water column

SUBSCRIPTS

a	axial
c	centrifugal
d	design
D	drag
eff.	efficiency
g	gravity
idp*	ideal total pump(combination of three)
L	lift
max	maximum
min	minimum
n	normal
P	power
P*	pump
Q	torque
R	rotor
r	local
ref	reference
S_t	starting
T	tilt, twist, thrust
t	tangential
v	vertical
W	wake
β	coning

GREEK ALPHABETS

α angle of attack

α_d design angle of attack

α_T tilt angle

β coning angle

β_T blade twist angle

γ yawing angle

Γ circulation

η power law exponent

η_{eff} efficiency of windmill

η_{vol} volumetric efficiency of the pump

η_{mech} mechanical efficiency of the pum

θ_K blade azimuth angle

θ_p pitch angle

λ tip speed ratio

λ_d design tip speed ratio

λ_r local tip speed ratio

ρ air density

σ solidity, $BC/2\pi r$

ρ_w water density

ϕ angle of relative wind velocity

ψ angular position of rotor, Ωt

ω wake rotational velocity

Ω angular velocity of rotor

Ω^* angular velocity of pump

∇_S stroke volume

$\dot{\nabla}_v$ volume of the valve

∇_{cy} pump cylinder volume

μ a constant

CONTENTS

Wind energy systems have been utilized for centuries as a source of power, for more than a variety of applications. Among those windmills of Holland and the rural windmills of the early 20th century are most familiar. Due to the world wide energy crisis and the problems of environmental pollution as a result of energy conversion, wind is once again moving to the fore front. Recently, wind power is being seriously considered as a new potential source of electrical power generation and irrigation purposes.

Recent interest in wind machine has resulted in the reinvention and analysis of many of the wind power machines developed in past centuries. The advent of the digital computer makes the task of preparing general performance analysis for wind machines quite easy.

The success of wind power as an alternate energy source is a function of the economic production of wind power machines.

In this regard, the role of improved power output through the development of better aerodynamic performance offers some potential return

1.1   HISTORICAL BACKGROUND

Among the sources of energy which man exploited to his advantage
were the energy from wind and water. Two early uses of wind
energy were the windmills and the sail ships. The use of wind-
mills date back to 17th century B.C. when the Babylonian emperior
Hammurabi planned to use windmills for brine pumping.

Windmills were used in Persia and evidence is found that the
early Muslim Kingdoms saw extensive uses of windmills of vertical
axis type. Then comes horizental axis so called European windmills
whose applications were found in Germany and in the Netherlands
during the 13th century and onwards. Sketches of a six sail wind-
mill has also been found among the many sketches by Leonardo da
Vinci (1452 - 1519). The first propeller type blades were used
during this period. The earliest record of English windmills
dates back 1191 which were two type - "Postmill" and the
"Towermill".

In the fourteenth century, the Dutch had taken the lead in
improving the design of windmills and used them extensively
thereafter or draining the marshes and lakes of Rhine river
delta.

During early part of the twentieth century, two quite different
vertical designs were developed. One of the designs known as the

Savonius rotor was formed by cutting a cylinder into two semi cylindrical surfaces, moving these surfaces sideways along the cutting plane to form a rotor with cross section in the form of the letter "S", placing a shaft in the centre of the rotor and closing the end surfaces with circular end plates as shown in Figure 1.1.1. The other vertical windmill design patented in 1927 by George Darrieus consisted of two thin airfoils with one end mounted on the lower end of a vertical shaft end the other end mounted on the upper end of the same shaft, sketched in Figure 1.1.2. Another interesting wind machine that was built during that period was the Smith Putnam unit as shown in Figure 1.1.3. After a lengthy study in the 1930, S. Palmer Putnam had concluded that large machine was required to minimize the cost of electricity generated by the wind.

In Denmark, at the end of nineteenth century there were about 2500 industrial windmills in operation supplying a total of about 40,000 hp or 30 MW i.e. about 25% of the total power available to Danish industry at that time.

In 1931, the Russians built an advanced 100 kW wind turbine near Yalta on the Black Sea. The annual output of this machine was found to be about 28000 kWh per year. At one time in the 1930's the Russians consider building a larger system of 5MW rated

capacity but apparently this project was never implemented./‾9_7

In England in the late 1940's and during 1950's considerable

work was done on wind powered electrical generation plants.

In the 1950's the Enfield Cable Company built a wind powered

generator designed by a French named Andreau as shown in

Figure 1.1.4. The prepeller blades were hollow and when they

rotated acted as centrifugal pumps. The air entered through

the ports in the lower parts of the tower passed through an

air turbine which turned the electric generator went up through

the tower and went out the hollow tips of the blades. The

efficiency of the unit was found to be low compared other more

conventional horizontal axis wind power rotors. The main advan-

tage of this system is that the power generating equipment is

not supported aloft.

The French built and operated several large wind powered

electric generators in the period from 1958 to 1966. These

included three horizontal axis units each with three propeller

type blades. A unit of this kind was operated intermittently

near Paris from 1958 to 1963. This unit was designed to generate

800 kW in winds having speed of 37 mph. The Germans made a number

of improvements in the design of wind powered generators including

light weight constant speed rotors that were controlled by

variable pitch propellor blades with swept diameters as large as 110 feet. The largest unit generated 100 kW. These units operated successfully for more than 4000 hours during the period from 1957 to 1958.

1.2 FEASIBILITY OF WIND ENERGY PROJECT IN BANGLADESH

1.2.1 Feasibility

Modern society projects power as complementary to its dynamic existence. The availability of the usuable power is a significant factor for the progress of a country. But world today extracts almost all of its energy needs from petroleum fuel, the price of which is increased mainfold over the past few years.

Bangladesh, which is facing with tremendous economic hardships with its enormous illiterate population has some reserves of natural gas. Its viable reserves of fossil fuel, and its recently found petroleum reserve has not yet been of any mentionable value.

The growing price for power production has retarded our over-all national progress. Under the prevailing condition it has become a compulsion for a developing country like Bangladesh to search for cheap alternative sources of energy.

Nature offers us with few options, which are the solar energy, energy from ocean and rivers, geothermal energy and wind energy. Geothermal energy is not available in Bangladesh. Apart from the Karnaphuli river which

has already been harnessed, no other river fulfil the
necessary pre-conditions for the installation of hydro-
electric power plants.

The readily available natural sources of abundant
energy are the sun, the ocean and the wind. The tapping of
solar and the oceanic energy involved large initial cost and
advanced technical know - how which is likely to put a barrier
in the way of their utilization in our country. This leaves us
with the option of wind energy as an alternate non-polluting
energy source with good potentialities.

Bangladesh is an agriculture based country whose economic
structure is dependent on agro-product commodities. Due to
population explosion Bangaldesh needs more food. Having poor
economic structure she seeks new technic to improve the agri-
cultural productivity with her efforts. Wind energy can
contribute a lot both for irrigating its land and producing
electricity for sustaining its economic viability. One of the
solution to the above problems worthy of investigation may be
the local installation of windmills in the villages with a
view to meet the local power demands for agricultural and
household purposes.

In Bangladesh, windmills may find extensive use along the coastal areas and as well as the hilly areas of Chittagong, Chittagong hill tracts, Sylhet, Mymensingh and Comilla.

For the hilly region and for the seashore, the approximate airfoil shape of some hills as well as the tunnelling effect between two hills can be utilized with advantage. Apart from these hilly areas, the rest of Bangladesh is flat land. A windmill properly designed and located in the flat plain of the country can supply electrical energy for both domestic and agricultural purposes. The wind pattern in the dry northern region of Bangladesh should also be throughly studied in order to tap this natural resource for the above mentioned uses.

In designing the windmills, suitable safety measures should be considered so that even in the gusty winds and cyclones. Provisions should be made to protect the windmills against other natural calamities. Automatic operation of windmills, that is windmills have to be turned out of wind whenever the wind speed exceeds a certain limiting value is preferable.

1.2.2 Wind Pattern in Bangladesh.

Winds are available mainly during the monsoons and around one to two month before and after the monsoons. During the month starting from late October to the middle of the February, winds either remains calm or has too low speed to be of any use by a windmill.

Therefore, except for the above mentioned period of about four months, a windmill if properly designed and located, can be of economic use.

The peak rainfall occurs in this country during the months of June, July and August. From the analysis it can be seen that the peak wind speed for most of the stations occurs one to two months and in some cases three months before the peak rainfall occurs. Thus one good advantage of such wind behaviour is that, the peak winds are available during the hot and dry month of March, April and May. Windmills, during this period, may be used for pumping water for irrigation, if the water has been previously stored in reservoir. The wind energy distribution during the year in such that about 55% is available during the time when the need for water pumping is low and about 25% is available in the season when the need for water pumping is at its peak $\underline{/}$28$\underline{}$

Therefore, excess windmill energy can be utilized in the rainy season for flood control and storing excess water in suitable reservoirs.

1.3 AIM OF THE THESIS

i)   To study wind velocity at different zone of Bangladesh
     and to design suitable wind turbine considering the
     average wind velocity.

ii) Considering average velocity of Chittagong the rotor
     configuration for twist and chord is determined by
     applying momentum theory and blade element theory
     which is known as strip theory.

iii) Three types of blade shapes have been considered
     optimum chord-optimum twist, linear chord-linear
     twist and linear chord-zero twist.

iv) To design a rotor optimised for peak performance and
     predict its characteristics and comparing the results
     with the results of existing wind turbine.

v)   The theoretical results will be used for the design of
     positive displacement pump for irrigation purposes.

vi) To observe the behaviour of the pump and also the
     behaviour of the rotor coupled with designed pump.

CHAPTER 2 : LITERATURE SURVEY

2.1 GENERAL

The horizontal axis wind turbine extracts energy from the driving air and converts it into a mechanical power in contrast to a propeller which adds energy into the air from another energy source. Because of the similarity of the wind turbine and propeller, it is possible to use the same theoretical development for the performance analysis.

2.2 REVIEW OF EXISTING LITERATURE

Little experimental work has been done on wind turbines or models in order to visualize actual flow field and much of the general behaviour has been deduced from propeller technology. This is mainly because of the restricted interest and financial support for wind pump studies. Even with interest and support, prototype experiment is very difficult, wing and the size of the rotors and the steadiness of the wind over sufficiently long period. Models experiments are possible but are handicapped by the effect of wind tunnel walls blockage. In the following section the review of the existing literature which forms the foundation for the present analysis is presented. The propeller theory was based on two different independent approaches. One is the momentum theory approach and the other is the blade element theory approach.

The first description of the axial momentum theory was given by Rankine $\boxed{6}$ in 1865 and was improved later by Froude $\boxed{16}$. The basis of the theory is the determination of the forces acting on the rotor which produce the motion of the fluid. It also predicts the ideal efficiency of the rotor. Later on Betz $\boxed{36}$ included the rotational wake effects in the theory.

Modern propeller theory has developed from the concept of free vortices being shed from the rotating blades. These vortices define a slipstream and generate induced velocities. The theory can be attributed to the work of Lanchester $\boxed{37}$ and Flamm $\boxed{38}$ for the original concept. Later, Joukowaki $\boxed{7}$ introduced the induced velocity analysis. Prandtl $\boxed{24}$ and Goldstein $\boxed{31}$ developed separately the circulation distribution or tip loss analysis. Recently, Wilson, Lissaman and Walker $\boxed{46}$ have further analysed the aerodynamic performance of wind turbines. They have introduced a new method to apply tip loss which is sometimes referred as the linear method. This method is based on the assumption that the axial and tangential induced velocities are localised at the blade and only a fraction of these occur in the plane of the rotor.

Modified blade element theory or strip theory is the most frequently used theory for performance analysis of horizontal

axis wind turbine. The technique, which assumes local two dimensional flow at each radial rotor station, is a design analysis approach in which the airfoil sectional aerodynamics, chord and pitch angles are required in order to determine forces and the torque.

The application limit of the momentum theory is the state where reverse flow begins to occur downstream of the rotor. The operating states of a wind turbine can be classified theoretically into four categories namely, the propeller state, the windmill state, the turbulent wake state, and the vortex ring state. These states can occur simultaneously at different positions of a blade. In the helicopter analysis, several experimental studies have been made on the vortex ring state and on the turbulent wake state. Lock $\sqrt{26,27\_7}$ conducted wind tunnel tests using two model rotors and Glauert $\sqrt{15\_7}$ defined a characteristic curve ulitizing the data of Lock. While Gessow $\sqrt{12\_7}$ conducted a flight test of a helicopter to obtain a similar characteristic curve, and its approximate formula is given by Johnson $\sqrt{22\_7}$. Wilson $\sqrt{42\_7}$ has suggested linear algebraic expressions for the local thrust at high tip speed ratios where a wind turbine may operate in the vortex ring state. There is very little published literature on the performance of a wind turbine operating in the turbulent wake state. Yamane $\sqrt{45\_7}$

has introduced a performance prediction method for windmill
in the turbulent wake state utilizing the empirical characteris-
tic curve of Gessow or Lock and Glauert in combination with
blade element theory. Recently, Anderson $\underline{/5\_7}$ has published
the results of a vortex-wake analysis of a horizontal axis wind
turbine and he compared his results with those obtained from
the modified blade element theory. He suggests that unless
information is required about the wake, it is satisfactory to
use the blade element theory with a suitable model for tip loss.
The vortex-wake analysis has advantages over modified blade ele-
ment theory is that, it provides information on the radial flow
and the axial velocity deficit in the wake. The main disadvan-
tage of the vortex-wake analysis is the computational time
necessary to obtain a solution. Viterna $\underline{/14\_7}$ has suggested an
improved method to calculate the aerodynamic performance of a
horizontal axis wind turbine at tip speed ratios where aerody-
namic stall can occur as the blade experiences high angles of
attack.

Walker $\underline{/41\_7}$ has developed a method to determine the blade
shapes for maximum power. According to his method, the blade
chord and twist are continuously varied at each radial station
until the elemental power coefficient has been maximized. This
is obtained when every radial element of the blade is operating

at the airfoil's maximum lift to drag ratio. This results in the lift coefficient and angle of attack being identical at each radial element. Anderson $\sqrt{4\_7}$ has compared near-optimum and optimum blade shapes for turbines operating at both constant tip speed ratio and constant rotational speed. Shepherd $\sqrt{34\_7}$ has suggested a simplified method for design and performance analysis of a horizontal axis wind turbine which can be carried out on a hand-held calculator by elimination of iteration processes. It is based on the use of the ideal and optimised analysis to determine the blade geometry. It requires only fixed values of the axial interference factors and corresponding optimised rotational induction factors.

Jansen $\sqrt{21\_7}$ worked on the theories that form the basis for calculation of the design and the behaviour of a windmill. A modification of the Prandtl model of tip losses is derived. This modification takes the relatively heavy loading of the windmill rotor into account. It is argumented that, in contrast with propeller design, a maximum energy extraction is reached by enlarging the chords of the blades near the tips. Selection, design and construction of several rotors and of a test unit are described in his report. He concluded that with simple materials high power coefficients are possible.

Glasgow $\underline{/}$13$\underline{/}$ carried out tests on MOD-O wind turbines considering downwind and upwind wind direction. As a result of the tests, it is shown that while mean flatwise bending moments were unaffected by the placement of the rotor, cyclic flatwise bending tended to increase with wind speed for the downwind rotor while remaining somewhat uniform with wind speed for the upwind rotor, reflecting the effect of increased flow disturbances for a downwind rotor. Nacelle yaw moments are higher for the upwind rotor but do not indicate significant design problems for either configuration.

Powells $\underline{/}$30,45$\underline{/}$ investigated the effects of tower shadow on a downwind two-bladed horizontal axis wind turbine. A rotor aeroelastic simulation is used to predict the blade responses to tower shadow and subsequently to estimate increased blade fatigue damage. He suggested to reduce the effect of tower shadow by making the tower more aerodynamically smooth, thereby reducing the flow disturbance. However, because of changes in wind direction, it is necessary to have an aerodynamic tower fairing which is free to move in yaw with the turbine nacelle.

CHAPTER 3: DESCRIPTION OF EXISTING THEORIES

The main purpose of a wind turbine is to utilize energy from the air flow & then transform it into mechanical energy which later may be transformed into other forms of energy. The performance calculation of wind turbines are mostly based upon a steady flow, in which the influence of the turbulence of the atmospheric boundary layer is neglected.

For the design & evaluation of wind turbines the availability of computation tools is essential. Most existing theoretical models are based on the combination of momentum theory & blade element theory. This combined theory is known as modified blade element theory or strip theory. It has been assumed that the strip theory approaches will be adequate for wind machines performance analysis. The basic theoretical development of the strip theory is presented in this chapter. Effects of wake rotation, tip and hub losses & equations for maximum power are also presented.

3.1   AXIAL MOMENTUM THEORY

3.1.1   Non-rotating Wake

The axial momentum theory has been presented by Rankine in 1865 and modified later by Froude (4). The basis of the theory is the determination of the forces acting on a rotor to produce the motion of the fluid. The theory has been useful in predicting ideal efficiency of a rotor and may also be applied for wind turbine.

The necessary assumptions needed for momentum theory are:

a) Uniform flow

b) incompossible and inviscid fluid

c) infinite number of blades

d) thrust loading is uniform over the disc

e) non-rotating wake

f) static pressure for ahead and for behind the rotor are equal to the undisturbed ambient static pressure

Considering the control volume in Fig. 3.1.1, where the upstream and downstream control volume planes are infinitely far removed from the turbine plane, the conservation of mass may be expressed as:

$$\rho A_1 V_\alpha = \rho A U = \rho A_2 V \quad \text{(Continuity Equation)} \quad (3.1.1)$$

where

V_α = undisturbed wind velocity

U = Wind velocity through the rotor

V = wind velocity far behind the rotor

A = turbine disc area

A_1 = cross-sectional area of incoming wind

A_2 = wake cross-sectional area

The thrust force T on the rotor is given by the change of momentum of the flow:

$$T = m(V_\alpha - V) = \rho AU(V_\alpha - V) \text{ (Momentum theory)} .. \quad (3.1.2)$$

Now applying Bernoulli's Equation:

for upstream of the rotor: $P_\alpha + \tfrac{1}{2}\rho V_\alpha{}^2 = P^+ + \tfrac{1}{2}\rho U^2$ (3.1.3)

for downstream of the rotor: $P_\alpha + \tfrac{1}{2}\rho V^2 = P^- + \tfrac{1}{2}\rho U^2$ (3.1.4)

Subtracting equation (3.1.4) from equation (3.1.3), one obtains

$$P^+ - P^- = \tfrac{1}{2}\rho (V_\alpha^2 - V^2) \qquad (3.1.5)$$

The thrust on the rotor can be expressed from the pressure difference over the rotor area:

$$T = (P^+ - P^-)A \qquad (3.1.6)$$

and the expression for the thrust from equation (3.1.6).

$$T = \tfrac{1}{2} \rho A (V_\alpha^2 - V^2) \qquad\qquad (3.1.7)$$

Equating the eqn. (3.1.7) with equation (3.1.2)

$$\tfrac{1}{2} \rho A (V_\alpha^2 - V^2) = \rho A U (V_\alpha - V)$$

$$U = \frac{V_\alpha + V}{2} \qquad\qquad (3.1.8)$$

The velocity at the rotor U is often defined in terms of an axial interference factor a as

$$U = (1-a) V_\alpha \qquad\qquad (3.1.9)$$

Balancing equations (3.1.8) & (3.1.9), the wake velocity can be expressed as:

$$U = (1-2a) V_\alpha \qquad\qquad (3.1.10)$$

The change is kinetic Energy of the mass flowing through the rotor area is the power absorbed by the rotor:

$$P = m \quad KE = \tfrac{1}{2} \rho A U (V_\alpha^2 - V^2) \qquad\qquad (3.1.11)$$

With equations (3.1.9) & (3.1.10), the expression, for power becomes:

$$P = 2 \rho \, AV_\alpha^3 \ a(1-a)^2 \qquad\qquad (3.1.12)$$

Maximum power occurs when, $\frac{dP}{da} = 0$.

Therefore, $\frac{dP}{da} = 2 \ \rho AV_\alpha^3 \ (1-4a+3a^2) = 0$

which leads to an optimum interference factor

$$a = \frac{1}{3}$$

Putting this value in eqn. (3.1.12), maximum power becomes

$$P_{max} = \frac{16}{27}(\tfrac{1}{2} \, \rho AV_\alpha^3 \ ) \qquad\qquad (3.1.13)$$

The quantity factor $\frac{16}{27}$ is called the Betz-coefficient (20) and represents the maximum fraction which an ideal rotor can extract from flow.

If we denote

$$C_p = \frac{P}{\tfrac{1}{2} \, \rho \, V_\alpha^3 \, A} \qquad\qquad (3.1.14)$$

From (3.1.13)

$$C_{P_{max}} = \frac{P_{max}}{\frac{1}{2} \rho A V_{\alpha}^2} = \frac{16}{27} = 0.593$$

The fraction is related to the power of an undisturbed flow arriving at an area A, whereas in reality the mass flow rate through A is not AV_{α} but AU. Hence the maximum power can be written as

$$\eta_{eff} = \frac{P_{max}}{\frac{1}{2} \rho A U V_{\alpha}^2} = \frac{16}{27} \cdot \frac{3}{2} = \frac{8}{9} \qquad (3.1.15)$$

This modelling does not take into account additional effects of wake rotation. As the initial stream is not rotational, interaction with a rotating windmill will cause the wake to rotate in opposite direction.

Since generating torque implies tangential forces & thus momentum changes in the air in tangential direction, the flow is entirely axial is only acceptable for very high speed devices. The higher the torque that is generated, the higher the tangential momentum in the air downstream will be. Apart from other losses that occur in reality, we have the first reason why a C_p of 59.3% cannot be realized in a real construction.

3.1.2   Effect of Wake Rotation on Momentum Theory

Considering this effect the assumption is made that at the upstream of the rotor the flow is entirely axial and the downstream flow rotates with an angular velocity ω but remains irrotational. This angular velocity is considered to be small in comparison to the angular velocity Ω of the wind turbine. This assumption maintains the approximation of axial momentum theory that the pressure in the wake is equal to the free stream pressure.

The wake rotation is opposite in direction of the rotor and represents an additional loss of kinetic energy for the wind rotor. Power is equal to the product of the torque Q acting on the rotor and the angular velocity Ω of the rotor. In order to obtain the maximum power it is necessary to have a high angular velocity and low torque because high torque will result in large wake rotational energy. The angular velocity ω of the wake and the angular velocity Ω of the rotor are related by an angular interference factor a':

$$a' = \frac{\text{angular velocity of the wake}}{\text{twice the angular velocity of the rotor}} = \frac{\omega}{2\Omega}$$

$$\cdots\cdots\qquad (3.1.16)$$

The annular ring through which a blade element will pass is illustrated in Figure 3.1.3.

Using the relation for momentum flux through the ring the axial thrust force dT can be expressed as

$$dT = d\dot{m} \; (V_{\alpha} - V) = \rho \; dA \; U \; (V_{\alpha} - V) \tag{3.1.17}$$

Inserting equations (3.1.9) and (3.1.10)

$$U = (1 - a) V_{\alpha} \tag{3.1.9}$$

$$V = (1 - 2a) V_{\alpha} \tag{3.1.10}$$

and expressing the area of the annular ring dA as

$$dA = 2 \pi r \; dr \tag{3.1.18}$$

the expression for the thrust becomes

$$dT = 4 \pi r \rho V_{\alpha}^{2} \; a \; (1 - a) \; dr \tag{3.1.19}$$

The thrust force may also be calculated from the pressure difference over the blades by applying Bernoulli's equation. Since the relative angular velocity changes from Ω to $(\Omega + \omega)$, while the axial components of the velocity remain unchanged, Bernoulli's equation gives

$$P^{+} - P^{-} = \tfrac{1}{2} \rho \; (\Omega + \omega)^{2} \; r^{2} - \tfrac{1}{2} \rho \; \Omega^{2} \; r^{2}$$

or, $P^+ - P^- = \rho \ (\ \Omega + \tfrac{1}{2}\omega) \ \omega r^2$

The resulting thrust on the annular element is given by

$$dT = (P^+ - P^-) \ dA$$

or, $dT = \rho \ (\ \Omega + \tfrac{1}{2}\omega) \ \omega r^2 \ 2\pi \ r \ dr$

To omit ω

$$dT = 4a' \ (1 + a') \ \tfrac{1}{2}\rho \ \Omega^2 \ r^2 \ 2\pi \ r \ dr \qquad (3.1.20)$$

Balancing equation (3.1.20) and equation (3.1.19), leads to the expression

$$\frac{a \ (1 - a)}{a' \ (1 + a')} = \frac{\Omega^2 \ r^2}{V_\alpha^2} = \lambda^2_r \qquad (3.1.21)$$

where λ_r is known as the local tip speed ratio which is given by

$$\lambda_r = \frac{r\Omega}{V_\alpha} \qquad (3.1.22)$$

To derive an expression for the torque acting on the rotor the change in angular momentum flux dQ through the annular ring is considered.

$$dQ = d\dot{m} \ V_t \ r$$

$$\text{or,} \quad dQ = \omega \ r \ \rho \ dA \ U \ r$$

where V_t is the wake tangential velocity.

Considering equations (3.1.9), (3.1.16) and (3.1.18), the expression for the torque acting on the annular ring is given by

$$dQ = 4 \ \pi \ r^3 \ \rho \ V_\alpha \ (1 - a) \ a' \ \Omega \ dr \qquad (3.1.23)$$

The generated power through the annular ring is equal to $dP = \Omega \cdot dQ$, so the total power becomes

$$P = \int_0^R \Omega \ dQ \qquad (3.1.24)$$

Introducing the tip speed ratio λ as

$$\lambda = \frac{\Omega \ R}{V_\alpha} \qquad (3.1.25)$$

Equation for total power from equations (3.1.23) and (3.1.24) becomes

$$P = \int_0^R 4 \ \pi \ r^3 \ \rho \ V_\alpha \ (1 - a) \ a' \ \Omega^2 \ dr$$

This can be written as

$$P = \frac{1}{2} \rho A V_{\alpha}^3 \frac{8}{\lambda^2} \int_0^{\lambda} a' (1 - a) \lambda_r^3 \, d\lambda_r \qquad (3.1.26)$$

where A is the turbine swept area which is given by $A = \pi R^2$. The power coefficient is defined as

$$C_p = \frac{P}{\frac{1}{2} \rho A V_{\alpha}^3} \qquad (3.1.14)$$

Inserting equation (3.1.26) power coefficient can be written as

$$C_p = \frac{8}{\lambda^2} \int_0^{\lambda} a' (1 - a) \lambda_r^3 \, d\lambda_r \qquad (3.1.27)$$

Rearranging equation (3.1.21)

$$a' = -\frac{1}{2} + \frac{1}{2} \sqrt{1 + \frac{4}{\lambda_r^2} a (1 - a)} \qquad (3.1.28)$$

Substituing this value in equation (3.1.27) and taking the derivative equal to zero, the relation between λ_r and a for maximum power becomes

$$\lambda_r^2 = \frac{(1 - a)(4a - 1)^2}{(1 - 3a)} \qquad (3.1.29)$$

Introducing equation (3.1.29) into equation (3.1.21) the rela-
tionship between a and a' becomes:

$$a' = \frac{1 - 3a}{4a - 1} \quad \text{(For detail see Appendix-}c\text{)} \quad (3.1.30)$$

This relation will be used later on for design purposes.

3.2   BLADE ELEMENT THEORY

Since the wind turbine that extracts the energy in the momentum theory is not specified, the momentum theory can not give information on

- blade chords and angles
- influence of friction
- influence of number of blades

With the blade element theory the forces acting on a differential element of the blade may be calculated. Then integration is carriedout over the length of the blade to determine the performance of the entire rotor. The assumptions underlying the blade element theory are:

1. There is no interference between adjacent blade element along each blade.

2. The forces acting on a blade element are solely due to the lift and drag characteristics of the sectional profile of the element.

3. The pressure in the far wake is equal to the free stream pressure.

The aerodynamic force components acting on the blade element are the lift force dL perpendicular to the resulting velocity vector and the drag force dD acting in the direction of the resulting velocity vector. The following expressions for the sectional lift and drag forces may be introduced:

$$dL = C_L \tfrac{1}{2} \rho W^2 C \, dr \qquad (3.2.1)$$

$$dD = C_D \tfrac{1}{2} \rho W^2 C \, dr \qquad (3.2.2)$$

The thrust and torque experienced by the blade element are

$$dT = dL \cos \phi + dD \sin \phi \qquad (3.2.3)$$

$$dQ = (dL \sin \phi - dD \cos \phi) \, r \qquad (3.2.4)$$

Assuming that the rotor has B blades, the expressions for the thrust and torque become

$$dT = B \, C \, \tfrac{1}{2} \rho W^2 (C_L \cos \phi + C_D \sin \phi) \, dr$$

$$\text{or,} \, dT = B \, C \, \tfrac{1}{2} \rho W^2 C_L \cos \phi \left(1 + \frac{C_D}{C_L} \tan \phi\right) dr \qquad (3.2.5)$$

$$\text{and} \quad dQ = B \, C \, \tfrac{1}{2} \rho W^2 (C_L \sin \phi - C_D \cos \phi) \, r \, dr$$

$$\text{or,} \quad dQ = B \, C \, \tfrac{1}{2} \rho W^2 C_L \sin \phi \left(1 - \frac{C_D}{C_L} \frac{1}{\tan \phi}\right) r \, dr \qquad (3.2.6)$$

According to the Figure 3.2.1 the expression for relative velocity W can be written as

$$W = \frac{(1 - a) V_\alpha}{\sin \phi} = \frac{(1 + a') \Omega \, r}{\cos \phi} \qquad (3.2.7)$$

Introducing the following trigonometric relations based on
Figure 3.2.1

$$\tan \phi = \frac{(1 - a) \, V_,}{(1 + a') \, \Omega \, r} = \frac{1 - a}{1 + a'} \cdot \frac{1}{\lambda \, r} \qquad (3.2.8)$$

$$\text{and} \quad \beta_T = \phi - \alpha \qquad (3.2.9)$$

and the local solidity σ as

$$\sigma = \frac{B \, C}{2 \, \pi \, r} \qquad (3.2.10)$$

The equations of the blade element theory become

$$dT = (1 - a)^2 \, \frac{\sigma \, C_L \, \cos \phi}{\sin^2 \phi} \, (1 + \frac{C_D}{C_L} \, \tan \phi) \, \tfrac{1}{2} \, \rho \, V_\alpha^2 \, 2 \, \pi \, r \, dr \qquad (3.2.11)$$

$$dQ = (1 + a')^2 \, \frac{C_L \, \sin \phi}{\cos^2 \phi} \, (1 - \frac{C_D}{C_L} \, \frac{1}{\tan \phi}) \, \tfrac{1}{2} \, \rho \, ^2 \, r^3 \, 2 \, \pi \, r \, dr \qquad (3.2.12)$$

3.3 STRIP THEORY

From the axial momentum and blade element theories a series of relationships can be developed to determine the performance of a wind turbine.

By equating the thrust, determined from the momentum theory equation (3.1.19) to equation (3.2.11) of blade element theory for an annular element at radius r,

$$dT_{momentum} = dT_{blade\ element}$$

or,
$$\frac{a}{1-a} = \frac{\sigma\ C_L\ Cos\ \phi}{4\ Sin^2\phi}\ (1 + \frac{C_D}{C_L}\ tan\phi\ )$$
(3.3.1)

Equating the angular momentum, determined from the momentum theory equation (3.1.23), with equation (3.2.12) of blade element theory one obtains

$$dQ_{momentum} = dQ_{blade\ element}$$

or,
$$\frac{a'}{1+a'} = \frac{\sigma\ C_L}{4\ Cos\ \phi}\ (1 - \frac{C_D}{C_L}\ \frac{1}{tan\ \phi}\ )$$
(3.3.2)

Equations (3.3.1) and (3.3.2), which determine the axial and angular interference factors contain drag terms. It has been suggested in (45) that the drag terms should be omitted in

calculations of a and a' on the basis that the retarded air due to drag is confined to thin helical sheets in the wake and have little effects on the induced flow. Omitting the drag terms the interference factors a and a' may be calculated with the following equations.

$$\frac{a}{1-a} = \frac{\sigma\ C_L\ Cos\ \phi}{4\ Sin^2\phi} \qquad\qquad (3.3.3)$$

$$\frac{a'}{1+a'} = \frac{\sigma\ C_L}{4\ Cos\ \phi} \qquad\qquad (3.3.4)$$

Considering the equations (3.3.3) and (3.2.11), elemental thrust can be written as

$$dT = 4\ a\ (1-a)\ (1+\frac{C_D}{C_L}\ tan\ \phi)\tfrac{1}{2}\ \rho\ V_\alpha^2\ \ 2\ \pi\ r\ \ dr$$

$$\qquad\qquad\qquad\qquad \ldots\ldots\ldots \qquad (3.3.5)$$

From equations (3.3.4) and (3.2.12), elemental torque can be obtained as

$$dQ = 4\ a'\ (1-a)\ (1-\frac{C_D}{C_L}\ \frac{1}{tan\ \phi})\ \tfrac{1}{2}\ \rho\ V_\alpha\ \Omega\ 2\ \pi\ r^3\ dr$$

$$\qquad\qquad\qquad\qquad \ldots. \qquad (3.3.6)$$

Elemental power is given by

$$dP = dQ\ \Omega$$

or, $\quad dP = 4\ a'\ (1 - a)\ (1 - \dfrac{C_D}{C_L}\ \dfrac{1}{\tan\phi})\ \tfrac{1}{2}\ \rho\ V_\infty.\Omega^2\ 2\ \pi\ r^3\ dr$

$$\ldots\ldots \qquad (3.3.7)$$

Introducing the local tip speed ratio λ_r with :

$$\lambda_r = \dfrac{\Omega\ r}{V_\infty} \qquad\qquad (3.1.22)$$

Equations of total thrust, torque and power become

$$T = \tfrac{1}{2}\ \rho\ A\ V_\infty^2\ \dfrac{8}{\lambda^2}\ \int_0^\lambda a\ (1 - a)\ (1 + \dfrac{C_D}{C_L}\tan\phi\ )\ \lambda_r\ d\ \lambda_r$$

$$\ldots\ldots \qquad (3.3.8)$$

$$Q = \tfrac{1}{2}\ \rho\ A\ V_\infty^2\ R\ \dfrac{8}{\lambda^3}\ \int_0^\lambda a'\ (1 - a)\ (1 - \dfrac{C_D}{C_L}\ \dfrac{1}{\tan\phi})\ \lambda_r^3\ d\ \lambda\ r$$

$$\ldots\ldots \qquad (3.3.9)$$

and

$$P = \tfrac{1}{2}\ \rho\ A\ V_\infty^3\ \dfrac{8}{\lambda^2}\ \int_0^\lambda a'\ (1 - a)\ (1 - \dfrac{C_D}{C_L}\ \dfrac{1}{\tan\phi}\ )\ \lambda_r^3\ d\ \lambda\ r$$

$$\ldots\ldots \qquad (3.3.10)$$

where $\quad A = \pi R^2$

This equations are valid only for a wind turbine having infinite number of blades. The effect of the finite blade number will be discussed in the next section.

3.4   TIP AND HUB LOSSES

In the preceding sections the rotor was assumed to be possessing an infinite number of blades with an infinitely small chord. In reality, however, the number of blades is finite. According to the theory discussed previously, the wind imparts a rotation to the rotor, thus dissipating some of its kinetic energy or velocity and creating a pressure difference between one side of the blade and the other. At tip and hub, however, this pressure difference leads to secondary flow effects. The flow becomes three-dimensional and tries to equalize the pressure difference as shown in Figure 3.4.1. This effect is more pronounced as one approaches the tip. It results in a reduction of the torque on the rotor and thus in a reduction of the power output.

Several alternate models to take this loss into account exist and are outlined in (46). The method suggested by Prandtl will be used here.

The correction factor suggested by Prandtl is

$$F_{tip} = \frac{2}{\pi} \cos^{-1} e^{-f} \quad \text{where} \quad f = \frac{B}{2} \frac{R-r}{R \sin}$$

Hence, a correction factor F for total losses is applied as

$$F = F_{tip} \cdot F_{hub} \tag{3.4.1}$$

The loss factor F may be introduced in several ways for the

rotor performance calculations. In the method adopted by Wilson
and Lissaman ((45), the interference factors a and a' are
multiplied with F, and thus the axial and tangential veloci-
ties in the rotor plane as seen by the blades are modified.
It is further assumed that these corrections only involve
the momentum formulas.

Thus the thrust and torque from momentum theory become

$$dT = 4 \pi r \rho V_\alpha^2 a F (1 - a F) dr \qquad (3.4.2)$$

$$dQ = 4 \pi r^3 \rho V_\alpha a' F (1 - a F) \Omega dr \qquad (3.4.3)$$

The results of the blade element theory remain unchanged

$$dT = (1 - a)^2 \frac{\sigma C_L \cos\phi}{\sin^2\phi}(1 + \frac{C_D}{C_L} \tan\phi) \frac{1}{2} \rho V_\alpha^2 2 \pi r dr$$

$$\cdots \cdot \qquad (3.2.11)$$

$$\text{and } dQ = (1 + a')^2 \frac{\sigma C_L \tan\phi}{\cos\phi}(1 - \frac{C_D}{C_L} \frac{1}{\tan\phi}) \frac{1}{2} \rho \Omega^2 r^4 2 \pi dr$$

$$\cdots \cdots \qquad (3.2.12)$$

Equation (3.2.12) can also be written as

$$dQ = (1 - a)^2 \frac{\sigma C_L}{\sin\phi} (1 - \frac{C_D}{C_L} \frac{1}{\tan\phi}) \frac{1}{2} \rho V_\alpha^2 2 \pi r^3 dr \qquad (3.4.4)$$

Balancing the equation (3.4.2) with (3.2.11) one finds

$$a F (1 - a F) = \frac{\sigma C_L \cos\phi (1 - a)^2}{4 \sin^2 \phi} (1 + \frac{C_D}{C_L} \tan \phi) \qquad (3.4.5)$$

and considering the equations (3.4.3) and (3.4.4)

$$a' F (1 - a F) = (1 - a)^2 \frac{\sigma C_L}{4 \sin \phi} (1 - \frac{C_D}{C_L} \frac{1}{\tan \phi}) \qquad (3.4.6)$$

Omitting the drag terms in equations (3.4.5) and (3.4.6) the following expressions yield

$$a F (1-a F) = \frac{\sigma C_L \cos \phi (1-a)^2}{4 \sin^2 \phi} \qquad (3.4.7)$$

$$a' F (1 - a F) = \frac{\sigma C_L (1 - a)^2}{4 \sin \phi} \qquad (3.4.8)$$

From the equations (3.4.7) and (3.4.8), the final expressions for elemental thrust and torque become

$$dT = 4 a F (1 - a F) (1 + \frac{C_D}{C_L} \tan \phi) \rho V_\alpha^2 \pi r dr$$

$$\dots \dots \qquad (3.4.9)$$

and

$$dQ = 4 a' F (1 - a F) (1 - \frac{C_D}{C_L} \frac{1}{\tan \phi}) \rho V_\alpha^2 \pi r^2 dr$$

$$\dots \dots \qquad (3.4.10)$$

3.5   EQUATIONS FOR TOTAL THRUST, TORQUE AND POWER COEFFICIENTS

Elemental thrust, torque and power coefficients are defined as

$$dC_T = \frac{dT}{\frac{1}{2} \rho A V_\alpha^2} \qquad (3.5.1)$$

$$dC_Q = \frac{dQ}{\frac{1}{2} \rho A V_\alpha^2 R} \qquad (3.5.2)$$

and $\quad dC_p = \dfrac{dP}{\frac{1}{2} \rho A V_\alpha^3} = \dfrac{\Omega\, dQ}{\frac{1}{2} \rho A V_\alpha^3}$

or, $\quad dC_p = \dfrac{dQ\; \Omega\, R}{\frac{1}{2} \rho A V_\alpha^2 \, R\, V_\alpha} = dC_Q\, \lambda \qquad (3.5.3)$

Considering the equations (3.4.9) and (3.5.1), elemental thrust coefficient can be written as

$$dC_T = \frac{8}{R^2}\, a\, F\, (1 - a\, F)\, (1 + \frac{C_D}{C_L}\, \tan\phi)\, r\, dr \qquad (3.5.4)$$

Again from equations (3..4.10) and (3.5.2), elemental torque coefficient is given by

$$dC_Q = \frac{8}{R^3}\, a'\, F\, (1 - a\, F)\, (1 - \frac{C_D}{C_L}\, \frac{1}{\tan\phi})\, r^2\, dr \qquad (3.5.5)$$

Elemental power coefficient can be obtained from equation (3.5.3) as

$$dC_p = \frac{8 \cdot \Omega}{R^2 V_{\infty}} \, a' \, F \, (1 - a \, F) \, (1 - \frac{C_D}{C_L} \, \frac{1}{\tan \phi}) \, r^2 \, dr \qquad (3.5.6)$$

Finally, total thrust, torque and power coefficients can be obtained by the following equations:

$$C_T = \frac{8}{R^2} \int_0^R a \, F \, (1 - a \, F) \, (1 + \frac{C_D}{C_L} \, \tan \phi) \, r \, dr \qquad (3.5.7)$$

$$C_Q = \frac{8}{R^3} \int_0^R a' \, F \, (1 - a \, F) \, (1 - \frac{C_D}{C_L} \, \frac{1}{\tan \phi}) \, r^2 \, dr \qquad (3.5.8)$$

$$C_p = \frac{8 \Omega}{R^2 \, \overline{V_{\infty}}} \int_0^R a' \, F \, (1 - a \, F) \, (1 - \frac{C_D}{C_L} \, \frac{1}{\tan \phi}) \, r^2 \, dr$$

$$\ldots \ldots \qquad (3.5.9)$$

3..6   EQUATIONS FOR MAXIMUM POWER

For maximum power output the relation between a and a' may be expressed by the equation (3.1.30) as:

$$a' = \frac{1 - 3a}{4a - 1}$$

Introducing the equations of interference factors as follows:

$$\frac{a}{1 - a} = \frac{\sigma C_L \cos\phi}{4 \sin^2\phi} \qquad (3.3.3)$$

$$\frac{a'}{1 + a'} = \frac{\sigma C_L}{4 \cos\phi} \qquad (3.3.4)$$

From equations (3..1.30), (3,3.3) and (3.3.4), the following expression yields:

$$\sigma C_L = 4 (1 - \cos\phi) \qquad (3.6.1)$$

Considering the local solidity σ as

$$\sigma = \frac{B C}{2 \pi r} \qquad (3.2.10)$$

equation (3.6.1) transforms into

$$C = \frac{8 \pi r}{B C_L} (1 - \cos\phi) \qquad (3.6.2)$$

Local tip speed ratio σ_r is given by

$$\sigma_r = \frac{\Omega\, r}{V} \tag{3.1.22}$$

Putting the value of a' from equation (3.1.30) and value of $\sigma\, C_L$ from equation (3.6.1) in the equation (3.3.4)

$$\frac{1 - 3a}{a} = \frac{4(1 - \cos\phi)}{4\cos\phi} = \frac{1 - \cos\phi}{\cos\phi} \tag{3.6.3}$$

$$a = \frac{\cos\phi}{2\cos\phi + 1} \tag{3.6.3}$$

Putting the value of a in eqn. (3.1.30)

$$a' = \frac{1 - \cos\phi}{2\cos\phi - 1} \tag{3.6.4}$$

Putting the value of a & a' from eqn. (3.6.3) & (3.6.4) in eqn. (3.2.8)

$$\lambda_r = \frac{\sin\phi\,(2\cos\phi - 1)}{(1 - \cos\phi)(2\cos\phi + 1)} \tag{3.6.5}$$

and this can be reduced as'

$$\phi = \tfrac{2}{3}\tan^{-1}\frac{1}{\lambda_r} \tag{3.6.6}$$

Equation of blade twist angle can be written as:

$$\beta_T = \cdot \phi - \alpha \quad , \tag{3.2.5}$$

Equations (3.6.2), (3.1.22), (3.6.6) and (3.2.9) will be used to calculate the blade configurations.

CHAPTER 4: DEVELOPMENT OF EXISTING THEORIES

In the previous chapter the calculation method is restricted to a wind turbine in a steady uniform free stream wind. In reality the wind velocity is neither uniform nor steady or unidirectional.

This means that effects on load and performance due to wind shear, wind shift, tower shadow, coning and tilting must be considered. The procedure for calculating the performance of each blade segment for an apparent wind speed W and angle of attack α are different from the ones previously used and no longer axially symmetric. The individual streamtubes can no longer be taken as annuli but must be of small area dA perpendicular to the wind direction. Within each area dA the wind velocity is considered as constant.

The procedure used is similar to the case of a uniform wind velocity along the rotor axis and is based on a combination of momentum theory and blade element theory.

4.1   EXPRESSION FOR PERFORMANCE ANALYSIS

4.1.1 Momentum Theory

A small radial element subtended by a small angle $d\theta$ in the plane of the rotor is shown in the Figure 4.1.1.

Introducing the angular interference factor a' from equation (3.1.16) as

$$a' = \frac{\omega}{2\,\Omega}$$
(3.1.16)

and using the small segment in Figure 4.1.6, the thrust can be written as

$$dT = dm.(V_{\alpha} - V)$$

$$\text{or, } dT = (V_{\alpha} - V) \quad U \ dA$$
(4.1.1)

Equation (3.1.9) is expressed as

$$U = V_{\alpha} \ (1 - a)$$
(3.1.9)

Considering the wind shear, wind shift and tilting, it may be rewritten as

$$U = V_{\alpha_0} \quad \text{Cos } \alpha_T \text{ Sin } \gamma \ (1 - a)$$
(4.1.2)

Equation (3.1.10) is expressed as

$$V_{\alpha} - V = 2 \ a \ V_{\alpha}$$
(3.1.10)

With the addition of wind shear, yawing and tilting, this equation becomes

$$V_\alpha - V = 2 a V_{\alpha_o} \; \text{Cos} \; \alpha_T \; \text{Sin} \; \gamma \qquad\qquad (4.1.3)$$

Now for a coned blade the expression for differential area dA can be written as

$$dA = r \; \text{Cos} \; \beta \; d\theta \; dr \; \text{Cos} \, \beta \qquad\qquad (4.1.4)$$

and thus the expression for the thrust becomes

$$dT = 2 \, \rho \; r \; \text{Cos}^2 \beta \; \text{Cos}^2 \, \alpha_T \; \text{Sin}^2 \gamma \; V_{\alpha_o}^2 \quad a(1 - a) \; dr \; d\theta$$

$$\overline{} \qquad\qquad (4.1.5)$$

By changing the momentum in the air in tangential direction tangential force acting upon the element is given by

$$dF_t = dm \; \omega \; r \; \text{Cos} \beta$$

$$\text{or,} \; dF_t = \rho U \; dA \; r \; \omega \; \text{Cos} \beta \qquad\qquad (4.1.6)$$

Considering the equations (3.1.16), (4.1.2) and (4.1.4) the tangential force is expressed as

$$dF_t = 2 \rho \; a' \; \Omega \; r^2 \; Cos^3\beta \quad (1 - a) \; V_{\alpha_0} \quad Cos \; \alpha_T \; Sin\gamma \quad dr \; d\theta$$

$$-- \qquad ----- \qquad (4.1.7)$$

The torque equation can be written as

$$dQ = dF_t \; r \; Cos\beta$$

Putting the value of dF_t from equation (4.1.7), one finds

$$dQ = 2 \; \rho \; r^3 \; a' \; (1 - a) \; V_{\alpha_0} \quad Cos \; \alpha_T \; Sin\gamma \; Cos^4\beta \qquad \Omega \; dr \; d\theta$$

$$. \; ------ \qquad (4.1.8$$

4.1.2 Blade Element Theory

The velocity components acting on a blade element rotating at a radius r are shown in Figure 4.1.2.

With the effect of wind shear the components of the re relative velocity W can be expressed as (19)

$$W_X = V_{\alpha_0 \; 0} \; Cos\gamma \; Cos\theta_K + V_{\alpha_0 \; 0} \; Sin \; \gamma \; Sin\theta_K \; Sin \; \alpha_T - \Omega \; r \; Cos \; \beta$$
$$(1 + a') \qquad\qquad (4.1.9)$$

$$W_y = V_{\alpha_0 \; 0} \; (Sin \; \gamma \; Cos \; \alpha_T \; Cos \; \beta \; (1 - a) + Sin \; \beta \; Sin\theta_K \; Cos\gamma$$

$$- Sin\gamma \quad Sin \; \beta \quad Sin \; \alpha_T \; Cos\theta_K) \qquad\qquad (4.1.10)$$

The local angle of attack α is defined as

$$\alpha = \phi - \beta_T = \tan^{-1} \frac{W_y}{W_x} - \beta_T \qquad (4.1.11)$$

and the relative velocity, $W = \sqrt{W_x^2 + W_y^2}$ $\qquad (4.1.12)$

The aerodynamic force components acting on the blade element are the lift force dL perpendicular to the resulting velocity vector and drag force dD acting in the direction of the resulting velocity vector. The following expressions are used for the sectional lift and drag forces:

$$dL = C_L \; \tfrac{1}{2} \; \rho \, W^2 \, dA \qquad (4.1.13)$$

$$dD = C_D \; \tfrac{1}{2} \; \rho \, W^2 \, dA \qquad (4.1.14)$$

Because we are assuming an infinite number of blades the differential area dA is given by (3.3)

$$dA = \frac{B \; C \; d\theta \; dr}{2 \pi} \qquad (4.1.15)$$

So the elemental lift and drag forces can be written as

$$dL = C_L \; \tfrac{1}{2} \; \rho \, W^2 \; \frac{B \; C \; dr \; d\theta}{2 \pi} \qquad (4.1.16)$$

$$dD = C_D \; \tfrac{1}{2} \; \rho \; W^2 \; \frac{B \; C \; dr \; d\theta}{2\pi} \qquad\qquad (4.1.17)$$

The thrust and torque experienced by the blade element are:

$$dT = dL \; \text{Cos} \; \phi \; + \; dD \; \text{Sin} \; \phi$$

$$\text{or, } dT = \text{Cos} \; \phi \; (dL + dD \; \tan \phi \;) \qquad\qquad (4.1.18)$$

$$\text{and } \; dQ = (dL \; \text{Sin} \; \phi \; - \; dD \; \text{Cos} \phi \;) \; r$$

$$\text{or, } dQ = \text{Sin} \phi \; (dL - dD \; \frac{1}{\tan \phi}) \; r \qquad\qquad (4.1.19)$$

With equations (4.1.16) and (4.1.17) the expressions for thrust and torque become:

$$dT = \tfrac{1}{2} \; \rho \; W^2 \; \text{Cos} \; \phi \; (C_L + C_D \; \tan \phi \;) \; \frac{BC \; \text{Cos} \; \beta \; \; dr \; d\theta}{2\pi} \qquad (4.1.20)$$

$$dQ = \tfrac{1}{2} \rho \; W^2 \; \text{Sin} \; \phi \; (C_L - C_D \; \frac{1}{\tan \phi}) \; \frac{BC \; r \; \text{Cos} \beta \; \; dr \; d\theta}{2\pi} \qquad (4.1.21)$$

Expressions for the elemental thrust and torque coefficients can be written as

$$dC_T = \frac{dT}{\tfrac{1}{2} \; \rho \; A \; V_\infty^2} = (W/V_\infty)^2 \; \frac{\sigma \; r}{\pi \; R^2} \; \text{Cos} \; \phi \; (C_L + C_D \; \tan \phi \;) \text{Cos} \; \beta \; \; dr \; d\theta$$

$$\text{or, } dC_T = (W/V_\infty)^2 \frac{\sigma C_L \text{Cos} \; \phi}{\pi \; R^2} (1 + \frac{C_D}{C_L} \; \tan \phi) \; \text{Cos} \; \beta \; \; r \; dr \; d\theta$$

$$\dots \qquad (4.1.22)$$

and $dC_Q = \dfrac{dQ}{\frac{1}{2}\,\rho\,A\,V_\infty^2\,R} = (W/V_\infty)^2\,\dfrac{\sigma\,r^2}{\pi\,R^3}\,Sin\,\phi\,(C_L - C_D\,\dfrac{1}{tan\phi})\,Cos\,\beta\;dr\;d\theta$

or, $dC_Q = (W/V_\infty)^2\,\dfrac{\sigma\,C_L\,Sin\,\phi}{\pi\,R^3}\,(1 - \dfrac{C_D}{C_L}\,\dfrac{1}{tan\,\phi})\,Cos\,\beta\;r^2\;dr\;d\theta$

$$\cdots\cdots \qquad (4.1.23)$$

Elemental power coefficient can be obtained as follows:

$$dC_P = \dfrac{dP}{\frac{1}{2}\,\rho\,A\,V_\infty^3} = \dfrac{dQ\;\Omega}{\frac{1}{2}\,\rho\,A\,V_\infty^3}$$

or, $dC_P = \dfrac{dQ\;\Omega\;R}{\frac{1}{2}\,\rho\,A\,V_\infty^3\,R} = dC_Q\,\lambda \qquad\qquad (4.1.24)$

4.1.3 Strip Theory

To calculate the interference factors a and a' the expressions for the thrust and torque from the momentum theory and blade element theory are to be equated.

$$dT_{blade\ element} = dT_{momentum}$$

$$dQ_{blade\ element} = dQ_{momentum}$$

By equating the equations (4.1.5) and (4.1.20) and considering the tip loss factor F, one obtains

$$a(1 - a\ F) = \frac{1}{8} \frac{\sigma\ W^2\ \cos\psi\ (C_L + C_D\ \tan\phi\ )}{\cos\beta\ \cos^2\alpha\ \sin^2\gamma\ V_{\infty O}^2\ F} \quad (4.1.25)$$

From equations (4.1.8) and (4.1.21) and with tip loss factor F, the following expression may be derived :

$$a'(1 - a\ F) = \frac{1}{8} \frac{\sigma W^2\ \sin\phi\ (C_L - C_D\ \frac{1}{\tan\phi})}{r\ \cos\alpha_T\ \sin\gamma\ \cos^3\beta\ \Omega\ V_{\infty O}\ F} \quad (4.1.26)$$

According to reference (45), the drag terms should be omitted in the calculations of a and a' on the basis that the retarded air due to drag is confined to thin helical sheets in the wake and have little effects on the induced flows. Omitting the drag terms, the interference factors a and a' are then calculated as:

$$a(1 - aF) = \frac{1}{8} \frac{\sigma W^2 \cos\phi \ C_L}{\cos\beta \ \cos^2\alpha_T \ \sin^2\gamma \ V_{\infty_O}^2 \ F} \qquad (4.1.27)$$

$$a'(1 - aF) = \frac{1}{8} \frac{\sigma W^2 \sin\phi \ C_L}{r \cos\alpha_T \ \sin\gamma \ \cos^3\beta \ \Omega \ V_{\infty_O} \ F} \qquad (4.1.28)$$

4.1.4 Equations for Thrust, Torque and Power coefficients

Considering the equations (4.1.22) and (4.1.27), the elemental thrust coefficient can be written as

$$dC_T = \frac{8}{\pi R^2}(V_{\infty_O}/V_\infty)^2 \ a \ F(1 - aF) \ \cos^2\beta \ \cos^2\alpha_T \ \sin^2\gamma$$

$$X \left(1 + \frac{C_D}{C_L} \tan\phi \right) r \ dr \ d\theta \qquad (4.1.29)$$

So the overall thrust coefficient can be expressed by

$$C_T = \frac{8}{\pi R^2} \cos^2\beta \ \cos^2\alpha_T \ \sin^2\gamma \int\limits_0^{2\pi} \int\limits_0^R (V_{\infty_O}/V_\infty)^2 \ a \ F(1 - aF)^*$$

$$\left(1 + \frac{C_D}{C_L} \tan\phi \right) r \ dr \ d\theta \qquad (4.1.30)$$

From equations (4.1.23) and (4.1.28), the following expression may be derived for elemental torque coefficient

$$dC_Q = \frac{8}{\pi R^3} \frac{V_{\infty O} \, r^3}{V_\infty^2} \, a' \, F \, (1-a \, F) \, Cos \, \alpha_T \, Sin \, \gamma \, Cos^4 \beta \quad *$$

$$(1 - \frac{CD}{C_L} \frac{1}{\tan \phi}) \, \Omega \, dr \, d\theta \qquad (4.1.31)$$

Total torque coefficient can be written as

$$C_Q = \frac{8 \, \Omega}{\pi R^3 V_\infty^2} \, Cos \, \alpha_T \, Sin \, \gamma \, Cos^4 \beta \int_0^{2\pi} \int_0^R V_{\infty O} \, r^3 \, a' \, F \, (1 - a \, F) \quad *$$

$$(1 - \frac{C_D}{C_L} \frac{1}{\tan \phi}) \, dr \, d\theta \qquad (4.1.32)$$

From equation (4.1.24) elemental power coefficient is given by

$$dC_P = dC_Q \, \lambda \qquad (4.1.24)$$

So the total power coefficient can be obtained as

$$C_P = \frac{8 \, \Omega^2}{\pi R^2 V_\infty^3} \, Cos \, \alpha_T \, Sin \, \gamma \, Cos^4 \beta \int_0^{2\pi} \int_0^R V_{\infty O} \, r^3 \, a' \, F(1-a \, F) *$$

$$(1 - \frac{C_D}{C_L} \frac{1}{\tan \phi}) \, dr \, d\theta \qquad (4.1.33)$$

4.2   DESIGN OF WINDMILL

This section discusses the design of a horizontal axis wind turbine, in which lift forces on airfoils are the driving forces. The design of a wind rotor consists of two steps:

1.   The choice of basic parameters such as the number of blades, the radius of the rotor, the type of airfoil and the design tip speed ratio.

2.   The calculations of the blade twist angle β_T and the chord C at a number of positions along the blade, in order to produce maximum power at a given tip speed ratio by every section of the blade.

The design procedure is described in the following subsections:

4.2.1   Selection of Design Tip Speed Ratio and Number of Blades

In considering a wind turbine design, the question arises as to how number blades should be used. In general, as the number of blades increases so does the cost. The advantages of increasing the number of blades are improved performance and lower torque variations due to wind shear. Furthermore, the choice of λ_d and B is more or less related. For the lower design tip speed ratios a higher number of blades is chosen. This is done because the influence of B on C_p is larger at lower tip speed ratio. For higher design tip speed ratio lower number

of blades is chosen. Choice of high number blades B for high
design tip speed ratio will lead to very small and thinn
blades which results in manufacturing problems. Two other
factors, however limit the choice of design tip speed ratio
one is the charactor of load. If it is a piston pump or some
other slow running load, that in most cases will require a
high starting torque, the design speed of the rotor will
usually be chosen low. If the load is running fast like a
generator or a centrifugal pump, then a high design speed
will be selected. The following table can be considered as
the guidelines for the choice of the design tip speed ratio
and the number of blades (20). To obtain the optimum confi-
guration the blade is divided into a number of radial stations.
Four formulas (19) will be used to describe the information
about β_T and C:

Local design speed : $\lambda_r = \lambda_d \frac{r}{R}$ (3.1.22)

Relation for flow angle: $\lambda_r = \frac{\sin \phi \ (2 \cos \phi - 1)}{(1 - \cos \phi) \ (2 \cos \phi + 1)}$

$$\text{or, } \phi = \tfrac{2}{3} \tan^{-1} \frac{1}{\lambda_r} \tag{3.6.6}$$

Twist angle $\qquad\qquad : \beta_T = \phi - \alpha$

Chord $\qquad\qquad : C = \dfrac{8 \ \pi \ r \ (1 - \cos\phi \ )}{B \ C_{L_d}} \qquad\qquad$ (3.2.9)

The blade starting torque can be calculated by (26)

$$Q_{S_t} = \tfrac{1}{2} \ \rho \ V_\infty^2 \quad B \ \int_r^R \ C(r) \ C_L \ (90 - \beta_T(r)) \ r \ dr \tag{4.2.1}$$

The rotor configuration is determined using the assumption of zero drag and without any tip loss. Each radial element is optimised independently by continuously varying the chord and twist angle to obtain a maximum energy extraction.

4.2.2 Selection of Airfoil Data

Power coefficient of the wind turbine is affected by C_D and C_L values of the airfoil sections. For a fast running load a high design tip speed ratio will be selected and airfoils with a low C_D/C_L ratio will be preferred. But for wind turbines having lower design tip speed ratios the use of more blades compensates the power loss due to drag. So airfoils h having higher C_D/C_L ratio are selected to reduce the manufacturing costs.

For the design and performance calculations of the wind turbines two-dimensional airfoil data are to be used in terms of lift and drag coefficients which can be found in references (1), (3) and (8). The available data are normally limited to a range of angles of attack up to maximum lift and the behaviour above this is not well known. The data are suitable for big wind turbines covering Reynolds Number 3.10^6 to 9.10^6. For smaller wind turbines when the Reynolds Number is less than 1.10^6 reliable airfoil data are rarely available. Surface roughness effects on airfoil data are not very well known. For different types of airfoils the sensitivity for surface roughness are also different. Using airfoil data for NACA standard roughness in wind turbine performance calculations results in losses in peak performance of the order of 10-15% (17) in comparison with usual airfoil data for a smooth surface.

4.2.3 Calculation Scheme for Blade Configurations

For calculating the blade geometry the following data must be available beforehand :

Design tip speed ratio, λ_d.

Amount of power to be extracted, P .

Design wind velocity, V_d.

Type of airfoil section.

The following steps are to be carried out for getting the blade configurations:

1. Assume a certain number of radial stations for which the chord and blade twist are to be found out.

2. Draw a tangent from the origin to C_L- C_D graph of airfoil section to locate the minimum value of C_D/C_L. Corresponding to this value find the design angle of attack α_d and design lift coefficient C_{L_d}. This is explained in Appendix B.

3. Select the number of blades B corresponding to the design tip speed ratio λ_d.

4. Assume a reasonable value of C_p. Estimation of the value of C_p has been explained in Appendix B.

5. Calculate the blade radius from the equation

$$C_P = \frac{P}{\frac{1}{2}\,\rho\,\pi R^2\,V_\infty^3}$$

6.   Choose a fixed value of hub and tip radius ratio, r_{hub}/R.

7.   Calculate the value of λ_r for each radial station using the equation $\lambda_r = \lambda_d \, r/R$.

8.   Determine the value of ϕ by using the equation

$$\phi = \frac{2}{3} \tan^{-1} \frac{1}{\lambda_r}$$

9.   Find the value of chord for each radial station using the equation $C = \dfrac{8 \, \pi \, r}{B \, C_{L_d}} \, (1 - \cos \phi)$

10. Calculate the value of blade twist using the following relation $\beta_T = \phi - \alpha_d$.

11. Consider a fixed value of coning or tilt angle.

12. After getting the blade geometry find the value of actual C_P by the following iterations procedures:

a) Assume initial values of a and a'.

b) Considering the wind shear and no yawing calculate the components of relative velocity W from the equations

$W_X = V_{\infty_0} \, Sin\theta_K \, Sin \, \alpha_T - \Omega r \, Cos \, \beta \, (1 + a')$

in the present case, $\alpha_T = 0$, and $\beta = 0$

and $W_Y = V_{\infty_0} \, (Cos\alpha_T \, Cos \, \beta \, (1-a) - Sin \, \beta \, Sin \, \alpha_T \, Cos\theta_K)$

c) Determine ϕ using the equation, $\phi = \tan^{-1} \dfrac{W_Y}{W_X}$

d) Calculate the local angle of attack α by substrac-

e) Find the values of lift and drag coefficients from a given table or polynomial.

f) Determine the correction factor F for tip and hub losses.

g) Calculate a with $a(1 - aF) = \dfrac{1}{8} \dfrac{\sigma W^2 \cos\phi \; C_L}{\cos\beta \; \cos^2 \alpha_T \; V_{\alpha_0}^2 \; {}_0F}$

h) Calculate a' with $a'(1 - aF) = \dfrac{1}{8} \dfrac{\sigma W^2 \sin\phi \; C_L}{r \cos \alpha_T \; \cos^3\beta \; \Omega \; V_{\alpha_0} \; {}_0F}$

i) Compare the values of a and a' with the original assumed values and continue the iteration procedures until the new values are within desired limit.

j) The values of α, ϕ, C_L and C_D from the final iteration step are used to calculate local force components. The local power for the blade element is calculated from the equation

$$dP = \frac{1}{2} \rho W^2 \sin\phi \; (C_L - C_D \frac{1}{\tan\phi}) \; \sigma \cos\beta \; r^2 \; \Omega \; dr \; d\theta$$

and the elemental power coefficient is obtained from the equation

$$dC_p = \frac{dP}{\frac{1}{2} \rho A V_\alpha^3} = (W/V_\alpha)^2 \frac{r^2}{R^3} \sin\phi \; (C_L - C_D \frac{1}{\tan\phi})$$

$$\sigma \; \lambda \; \cos\beta \; dr \; d\theta \; .$$

k) Calculate the total power coefficient by integrating the elemental power coefficients using the Simpson's rule.

13. Compare the calculated power coefficient with the earlier assumed value. If it is not within certain desired a accuracy repeat all the procedures starting from step 4.

14. Find the starting torque from the equation

$$Q_{S_t} = \tfrac{1}{2} \rho \, V_\infty^2 \quad B \quad \int_r^R C(r) \, C_L \, (90 - \beta_T(r)) \, r \, dr$$

15. If the starting torque is less than the desired load torque, increase number of blades and repeat all the procedures from step 4.

4.2.4 Deviations from the ideal Blade Form

In the last paragraph it has been discussed how to cala-
late the ideal blade form. The chord as well as the blade
twist vary in a non-linear manner along the blade. Such blades
are usually difficult to manufacture and may not have structural
integerity. In order to reduce these problems it is possible
to linearize the chords and the twist angles. This results
in a small loss of power. If the linearization is done is a
sensible way the loss is only a few percent. In considering
such linearizations it must be realized that about 75% of the
power that is extracted by the rator from the wind is extracted
by the outer half of the blades. This is because the blade
swept area varies with the square of the radius and the effi-
ciency of the blades is less at smaller radii, where the tip
speed ratio λ_r is small on the other hand, at the tip of the
blade the efficiency is low due to the tip losses. For the
reasons mentioned above it is advised to linearize the chord C
and the blade angles β_T between r = 0.5R and r=0.9 R (20). The
equation for linearized chord and twist can be written in
following way:

$$C = a_1 r + a_2$$

$$\beta_T = a_3 r + a_4$$

where a_1, a_2, a_3 and a_4 are constants. With the values of, a
and BT at 0.5R and 0.9R from the ideal blade form the values
of a_1, a_2, a_3 and a_4 can be find out. The ultimate expressions
for chord & twist of linearized blade can be written as:

$$C = 2.5(C_{90} - C_{50}) \ r/R + 2.25 \ C50 - 1.25C_{90} \qquad (4.2.2)$$

$$\beta_T = 2.25 \ (\ \beta_{90} - \beta_{50}) + 2.25 \ \beta_{50} - 1.25 \ \beta_{90} \qquad (4.2.3)$$

(In appendix-D)

where ρ

C_{50} = Chord of the ideal blade form at 0.5R

C_{90} = Chord of the ideal blade form at 0.9R

β_{50} = twist angle of the ideal blade form at 0.5R

β_{90} = twist angle of the ideal blade form at 0.9R

A further simplification of the blade shape consists of omitting
the twist altogether. Introduction of a rotor blade without
twist results in a power loss penalty of about 6 to 10% (40).
This might be acceptable for a single production. When the
main purpose is the design of a cheap wind turbine an untwisted
blade with a content chord seems to be a good choice with only
limited power losses.

4.3   CALCULATION PROCEDURE FOR PERFORMANCE ANALYSIS

After designing the rotor configurations according to the formulas in the previous sections, the characteristics of the rotor can now be calculated. The following data are assumed to be available beforehand.

Rotor radius, R.

Chord (C) and twist ($^\beta$r) distribution along the radius.

Tip speed ratio, λ •.

Number of blades, B.

Lift and drag characteristics of the blade profile section. Now for a number of radial positions the fvalues of axial and tangential interference factors will be found out. As there is no analytical expression for the interference factors, the following iteration procedures are to be performed for each radial station,

1.   Assume resonable values of a and a'

2.   Find the values of W_x and W_y from the following equations

$$W_x = V_{\infty_0} \cos \gamma \cos \phi_k + V_{\infty_0} \sin \gamma' \sin \phi_k \sin \alpha_T - \Omega r \cos \beta (1+a')$$

$$W_y = V_{\infty_0} (\sin \gamma \cos \alpha_T \cos \beta (1-a) - \sin \beta \sin \gamma \sin \alpha_T \cos \theta_k$$

$$+ \sin \beta \sin \theta_k \cos \gamma)$$

3.   Calculate ϕ by using the equation, $\tan \phi = \dfrac{W_y}{W_x}$

4. Determine angle of attack α by using the equation,

$\alpha = \phi - \beta_T$

5. Calculate C_L with $C_L(\alpha)$ graph or table.

6. Determine the total correction factor F for tip and hub losses.

7. Calculate a with $a(1-aF) = 1/8 \dfrac{\sigma w^2 \cos\phi \, C_L}{r \cos\beta \, \cos\alpha_T \, \sin^2\gamma \, V_{\infty_o}^2 \, F}$

and a' with $a'(1-aF) = 1/8 \dfrac{\sigma w^2 \sin \, C_L}{r \cos\alpha_T \, \sin\gamma \cos^3\beta \, V_{\infty_o} \, \Omega \, F}$

8. The new values of a and a' are compared with those from step 1 and the iteration procedure is continued until the desired accuracy is reached.

9. The values of α, ϕ, C_L and C_D from the final iteration step are used to calculate local force components.

10. The local configurations to thrust, torque and power co-efficients are calculated from the following equations.

$$dC_T = \frac{8}{\pi R^2} \left(\frac{V_{\infty_o}}{V_\infty}\right)^2 aF(1-aF)\cos^2\beta \, \cos^2\alpha_T \, \sin^2\gamma$$

$$(1 + C_D/C_L \, \tan\phi) \, r \, dr \, d\theta$$

$$dC_Q = \frac{8}{\pi R^3} \frac{V_{\infty_o} \, r^2}{V_\infty^2} a'F(1-aF)\cos\alpha_T \, \sin\gamma\cos^4\beta$$

$$(1 - \frac{C_D}{C_L} \frac{1}{\tan\phi}) \, \Omega \, dr \, d\theta$$

when the iteration procedure is finished for all blade elements,
the local contributions for torque, thrust and power are integra-
ted by using Simpson's rule to determine the performance of the
rotor.

4.4   DISCUSSIONS OF VARIOUS WIND CONDITIONS

In case of horizontal axis wind turbine, one of the
decisions that must be made in the design of a wind turbine is
whether the blades will be placed upwind of the tower support
structure or down wind of the support structure. There are
advantages and disadvantages to each arrangement. With blade
upwind of the tower the blade themselves receive the undisturbed
wind, but the configuration is not conductive to self orientation
with changes in wind direction. With a downwind rotor system,
the blades can be mounted closer to the tower, because blade
deflections will be away from the tower. Also the configurations
tends to be self orienting with changes in wind direction.

4.4.1   Effect of wind conditions

In reality, the wind velocity will be neither uniform,
steady or uni-directional. Vertical wind gradient, gustiness
and wind turning with elevation all present various difficul-
ties to the design and operation of wind turbines. The local
flow conditions and the techniques to predict the magnitude
of the effects of the flow variations must be known beforehand.

The different wind conditions include the effects of wind shear, wind shift & tower shadow. In the following sub sections the effects of these condition have been discussed.

4..4.2   Effect of wind shear

Near the surface of the earth the wind flow is seriously retarded by friction with the surface. Due to this friction a boundary layer is produced which creates a gradient in wind velocity with altitude. The wind shear depends on the wind direction, the wind velocity and the stability condition of atmosphere.

Since surface roughness can vary from relatively smooth (at coasts) to very rough (Citycentres) it is obvious that the velocity profile depend upon the nature of the terrain. In the new Belgium wind code draft (32) several classes of terrain are defined.

I. Sea coast.

II. Open terrain with few obstacles

III. terrain with low buildings, trees, etc.

IV. Suburban terrainor industrial terrain

V. City centers

In the atmosphere the nature of the boundary layer is three dimensional and is complicated by rotational effects and temperature gradient which affect the vertical mobility of the

turbulent eddies and thus the characterestics of the shear
layer flow. However, in the present work three dimensional
effect is neglected and the atmospheric boundary layer is
assumed to be two dimensional. The velocity of wind increases
with the height upto a level where the friction can be neglected.
This level is called gradient height Zg and the velocity at
this point, which is determined by the large weather system is
called the gradient velocity Vg. The distance between the surface
of the earth and the gradient height is the thickness of the
boundary layer.

The variation of the wind velocity with the height can
be presented analytically by both a power low & a lograrithmic
law. The logarithmic law can be presented as (33).

$$\frac{V}{V_{ref}} = k^* \ \ln(\frac{z-d}{z_1})$$

where, k^* = constant depending upon surface roughness

z_1 = surface roughness

d = zero plane displacement

z = height above ground

v = wind velocity at height z

V_{ref} = reference wind velocity

The power law formulation can be presented as

$$\frac{V_{\infty_0}}{V_{ref}} = (\frac{z}{z_{ref}})^n$$

Or $V_{...} = V_{ref}(\dfrac{z}{z_{ref}})^n$

where z_{ref} = reference height

n = power low exponent

The influence of wind shear on the power output and the blade loading of a horizontal axis wind turbine is complicated, because each blade element is subjected to a varying wind velocity during a revolution of the motor: There is some arbitrariness in the choice of the reference wind velocity at half the rotor height. The theoretical results are presented for a wind power law exponent of 1/6 and for the present analysis the hub height is considered as the reference height.

4.4.3   Effect of Wind Shift

The aerodynamic forces on a blade will vary during a revolution in the case where the rotor axis is not parallel to the wind direction, even though wind speed is constant. This results from changes in both magnitude and direction of the resulting loaal wind speed for the profiles which alters with the varying moment of the blade with and against the wind direction.

In non-axial flow, the cyclic variations in the aerodynamic forces at the blade root could lead to resonance in either

the blade, or the supporting structures and possibly reduce the life time of the turbine. The effects of non-axial flow, therefore need to be considered in the design of horizontal axis wind turbine.

4.4.4   Effect of Tower Shadow

The aerodynamic interference created by the tower is an important source of periodic wind load. The projected area of the tower structural element, their average drag coefficient, and the sector of the rotor area affected by the wake area are necessary for determining this periodic loads. An evaluation has been conducted for the effects of tower shadow on the forces, power, thrust, moment and stresses for a downwind mounted   wind turbine blade. The large and abrupt changes that occurs as the blade passes through the tower shadow will obviously cause significant changes in blade. The magnitude of these changes will depend on the amount of flow blockage occuring and duration of the blade remains is the tower shadow. For the present analysis, the blades area assumed to be in the tower wake at azimuths from 165 degree to 195 degree and value of the wind power low exponent is taken as 1/6. For a wide range of tip speed ratio the power deficit remains almost constant. However, power deficit only due to wind shear is very small. About 7% decrease of power may take place due to wind shear & tower shadow (25).

4.4.5. EFFECT OF ROTOR TILT

If rotor blades are coned it follows that the blade tip at its lowest point is moved nearer the support tower for an upwind rotor. To reduce the overhang require at the hub axis of the drive shaft is frequently tilted. If the tilt angle equals the cone angle the blade becomes vertical when pointing downwards. There will be change in both magnitude & direction of the local wind speed for the blade profile due to the tilting of the rotor.

For a blade in the lower half of the rotor disc the blade will move towards the wind and for the upper half of the disc it will be further away from the wind. Also due to wind shear the blade will receive higher wind velocity when it will be at the uppor half of the circle.

4.4.6 EFFECT OF BLADE CONING

Since stress induced by flapwise loads are greatest in magnitude, blades are freqently coned so that bending stresses that are induced by centrifugal forces, cancelling those due to aerodynamic loads. Exact cancellation is only possible at one aerodynamic loading condition and equilization of stresses along the entire blade requires a complex blade curvature. The coning angle, as expected, is inversely proportional to the mass of the blade. (In Appendix-G). Due to coning there is change in both magnitude & direction of the resulting wind speed for the profile which alters with azimuth (17).

Increasing the coning angle reduces the aerodynamic forces due to the reduction of the swept area of the wind turbine. Also increasing the coning angle results in better balance between centrifugal forces & the thrust, which reduces the flapping moment.

4.4.7   EFFECT OF BLADE SHAPES

The normal procedure for determing the blade shape of a horizontal axis wind turbine is to optimize independently each radial element by continuously varying the chord and twist angle to obtain maximum energy extraction. This method results in complex blade shapes which can be expensive to manufacture and may not have structural integrity. In order to reduce these problems it is possible to linearize the chord & twist angles. This results in a small loss of power. However, if the linearization is done in a sensible way the loss is only a few percent.

In the present analysis, three types of blade shapes have been considered: optimum-chord optimum twist, linear chord linear twist and linear chord zero twist. The linearization of the chords and twist angles have been done by taking the values from the optimum blade configuration at $r = 0.5 \, R$ and $r = 0.9 \, R$.

Fig. 4.4.5 & Fig. 4.4.6 show the distribution of chord & blade setting angles for these three types of blades. From these figures it is found that the changes in chords and twist

angles are very small at outer half of the blade large variations with the linear chord and twist distributions are found only at the lower part of the blade. It must be realized that about 75% of the power that is extracted by the rotor from the wind, is extracted by the outer half of the rotor. This is because of the fact that the blade swept area varies as the square of the radius. So this will not lead for any significant power loss but the starting torque will be less and in cases where the starting is an important factors this effect must be considered. Variation of starting torque for different blade configurations is shown in figure (4.4.7) where approximately 31% differences may occur between the optimum blade and zero twist blade (17) '. The effect of blade twist is to maintain the aerodynamic angle of attack at maximum lift to drag ratio. Considering both aerodynamic and structural performances, it has been observed that a linear-chord linear blade is comparable to the optimum designed blade, while offering a considerable reduction in manufacturing time & costs. However, when the main aim is the design of a cheap wind turbine an untwisted blade seems to be a good choice. But for a small scale turbine might behave badly due to the premature stall near the hub even at rather high tip speed ratios.

4.4.8   EFFECT OF NUMBER OF BLADE

As the number of blades increases so does the cost. The advantage of increasing the number of blades are improved performance and lower torque variations due to wind shear. The maximum power co-efficient is also affected by the number of blades. This is caused by the so-called tip losses that occur at the tips of the blades. These losses depend on the number of blades and tip speed ratios. For the lower design tip speed ratios, in general, a high number of blades is chosen. This is done because the influence of number of blades on power co-efficient is larger at lower tip speed ratios. For a high design tip speed ratio, a high number of blade will lead to vary small and thin blades which results is manufacturing & negative influence in the lift & drag properties of blades.

4.5   DESIGN OF A 30 KW WIND TURBINE

The configuration studied is a two-bladed 30 kw down-
wind wind turbine with a tip speed ratio of 8 and variable
pitch. The value of $r_{hub}/R = 0.10$ is chosen rather arbitrarily.
From a structural and costs point of view, it might be favou-
rable to increase r_{hub}/R because the largest part of the blade
area and also the largest part of twist variation is concentra-
ted near the hub. Throughout the theoretical studies NACA
4418 airfoil and prandtl's tip loss correction were used to
develope the curves. The blade characteristics were found
out by considering average wind velocity and without any
coning or tilt angles. The blade geometry was optimised to
give peak performance at 4 m/sec. The blade radius has been
divided into a number of radial stations. Each station has a
distance r from the rotor centre and has a local tip speed
ratio $_r$. The wind flow velocity angle at each station was
found out by the equation (3.6.6). The chord & twist angle for
each station were found out by equations (3.6.2) and (3.2.9).
In finding the blade geometry each radial station is optimised
independently by continuously varying the chord and twist angle
to obtain a maximum energy extraction. This is done when every
element of the blade is operating at the maximum lift to drag
ratio of the profile. Figures 4.5.1 & 4.5.2 show the distri-
bution of chord & twist angle of the optimum designed wind
turbine for the given conditions.

CHAPTER 5: RESULTS AND DISCUSSIONS

5.1   THEORETICAL RESULTS OF 30 KW WIND TURBINE

The effect of Pitch angle on Calculated power thrust and torque coefficients can be seen in figures 5.1.1 to 5.1.9 at SH=1,SH=2, SH=3, respectively.

Increased pitch angle reduces the maximum power but can increase the power available at low tip speed ratios. At low speed ratios, the power co-efficient versus tip speed ratio in figures 5.1.1, 5.1.4 & 5.1.7 can be used to illustrate some generalizations concerning wind machines. At low tip speed ratios the power co-efficient is strongly influenced by the maximum lift co-efficient. The angle ϕ is large at low tip speed ratios and much of the rotor, particularly the inboard stations, can be stalled when operating below the design speed. At tip speed ratios above the peak power co-efficient, will result in a rapid decrease in power and at some large tip speed ratio the net power output will become zero. The power curve is sensitive mainly to blade pitch angle in the stalling region. To avoid too much drop off of the power after the stalling point a blade pitch angle of 2° and 4° are seem to be more convenient than the performance at 0° pitch angle.

From figure 5.1.2 it is found that the rotor thrust co-efficient increases continuously with tip speed ratio and that the values greater than unity can be achieved. The variation of torque co-efficient with tip speed ratio is

shown in figure 5.1.3. With the increase of pitch angle, the maximum value of torque co-efficient moves towards the lower values of tip speed ratio. By changing the blade angle means that the resulting angle of attack is reduced and lift co-efficient is shifted from the stalling region. The pitching of the blade provides higher torque co-efficient at lower tip speed ratios.

When any part of the turbine blade operates with a resulting angle of attack that is higher than the value corresponding to maximum lift for the local blade section flow separation is encountered. This implies three dimensional effects which violates the basic assumption of the blade element theory and the solutions obtained are then not fully reliable. Such conditions occur for high wind speeds. The flow angle ϕ & hence α will then increase with increasing wind speed keeping other parameters constant. Flow separation will first occur in the hub region where ϕ has its largest values. Increasing the blade pitch angle means that the resulting angle of attack is 'lowered and more reliable solutions are obtained. Radial distribution of power, thrust, torque and moment are shown in figures 5.1.10 to 5.1.14. It is to be noted that about 75% of the power, thrust and torque are produced by the outer 50% radius. This is because the blade swept area varies with the square of the radius and also the efficiency of the

blades is less at small radii where the speed ratio λ_r is small.
On the other hand due to the tip losses there is decrease of
power and moment near the tip of the blades.

The dependence of the torque at Ω =o on pitch angle is
shown is fig. 5.1.15. . The strong increase in starting torque
with increasing pitch angle can take advantage of, if the
starting torque at the pitch angle desired at operating angular
velocity is sufficient, and if the overall pitch angle can be
changed. In that case, a high overall pitch angle is chosen
to start the rotor from Ω =o, where the internal resistance
is large. Usually, the internal resistance diminishes as
soon as the angular velocity is non-zero. So when a certain
angular velocity is reached, the pitch angle is diminished
for a value close to the optimum one.

5.2   COMPARISON OF THEORETICAL RESULTS WITH EXPERIMENTAL
       DATA.___   ____ .___

The variations of power co-efficient with tip speed
ratio at different pitch angles of HMZ windmaster windmill is
shown in Figure 5.2.1. . This turbine is an upwind machine and
it utilizes a NACA 44XX series airfoil with thickness ratio
varying from root to tip. The rotor axis tilted 5$^{\text{O}}$ to keep the
blade away from the tower during gust.

The present calculations were done by using NACA 4418
airfoil sections. The variation of thrust coefficient with

top speed ratios at different pitch angles is shown in Figure

5.2.2 . The variation of torque co-efficient with tip speed

ratio at diferent pitch angle is shown in figure 5.2.3 .

The stork WPX -8 is a 8m diameter horizontal axis wind

turbine which uses a NACA 4418 profile for its blade. Its rated

power is 23 Kw and number of blade may be 2 or 3. Figures

5.2.4 to 5.2.6 show the power coefficient.,

thrust co-efficient & torque co-efficients of stork WPX -8

wind turbine at different pitch angles. These graphs are

plotted by considering two blades only. For large positive

pitching angles the important region of power co-efficient

moves to smaller λ values. Increasing the pitch angle results

in a decrease of angle of attack. As a result lift co-efficient

is shifted from the stall region and it moves towards the higher

value at low top speed ratios.

CHAPTER 6 : STUDY OF PUMPS

6.1   GENERAL :

There exists a large variety of water lifting devices.
The scope of this study is confined to pumps that can be driven
by wind rotors with a focus on the reciprocatory piston pump.

Broadly pumps can be divided into three types : displace-
ment, impulse and other pumps each with a number of designs $\sqrt{27}$.

6.2   PISTON PUMPS

A reciprocating piston pump basically consists of a
piston, two valves, a suction pipe and a delivery pipe. Some-
times airchambers are utilized to smooth the flow and to reduce
shock forces.

The operation principle of the reciprocating piston pump
is simple : if the piston moves downward the upper valve
opens, the foot valve closes; i.e. the flow is zero, and the
piston moves freely through the watercolumn. As soon as the
piston moves upward the upper valve will close, the foot valve
opens and water is being lifted (above the piston) and sucked
(below the piston, if the pump is above the water level) until
the piston moves downward again. The result is a pulsating
sinusolidal water flow, like an alternating current after
passing a rectifier (fig. 6.1)

6.2.1 Behaviour of ideal Piston Pump

The behaviour of the ideal pump at low speed, i.e. with accelerations small compared to the acceleration of gravity and neglecting friction forces and dynamic forces are discussed here.

The force on the piston is equal to the weight of the water column acting upon it.

$$F_p = \rho_w g \, H \, \frac{\pi}{4} D_p^2 \tag{6.1}$$

We assume H to be the static head, but later on the extra head required to cover the losses has to be added.

The ideal torque which is sinusoidal during the upward storke and zero during the downward storke. In formula :

$$Q_{id} = \rho_w g \, H \, \frac{\pi}{4} D_p^2 \, \tfrac{1}{2}s \, \sin \Omega t \quad \text{for} \quad 0 < \Omega t < \pi \tag{6.2}$$

Integrating this instantaneous torque over a full circle, gives,

$$\frac{1}{2\pi} \int_0^{2\pi} \sin \Omega t \; d \Omega t = \frac{1}{\pi} \tag{6.3}$$

the expression for the average torque:

$$\bar{Q}_{id} = \frac{1}{\pi} \rho_w gH \frac{\pi}{4} D_p^2 \frac{1}{2}s \qquad (6.4)$$

or $\qquad \bar{Q}_{id} = \frac{1}{2\pi} \rho_w gHV_s$

with V_s being the stroke volume $\frac{\pi}{4}D_p^2 s$

The average ideal power required is equal to:

$$\bar{P}_{id} = \bar{Q}_{id} \quad * \quad \Omega = \frac{\Omega}{2\pi}\rho_w gHV_s \qquad (6.5)$$

or $\qquad \bar{P}_{id} = \rho_w gH$

where $\quad q = V_s \frac{\Omega}{2\pi}$

6.2.2 Practical behaviour of Piston Pumps

The ideal piston pump of section 6.2.1 required a mechanical power equal to the net power to lift the water, i.e. an efficiency of 100%. In reality the mechanical power required is higher than the net water lifting power because of mechanical losses, due to friction between piston and cylinder, and hydraulic losses, due to flow friction losses in the valves mainly.

The mechanical efficiency is defined as :

$$\eta_{mech} = \frac{P_{hydr}}{P_{mech}}$$ (6.6)

in which P_{hydr} : net power to lift the water ($\rho_w gH$)

P_{mech} : mechnical power driving the pump (in our case the power from the rotor)

The volumetric efficiency arises because the actual output is usually less than the product of stroke volume and speed. Its definition is :

$$\eta_{vol} = \frac{q}{V_s \frac{\Omega}{2\pi}}$$ (6.7)

$$\eta_{mech} = \frac{\rho_w gH}{\overline{Q}_{mech} \, \Omega} = \frac{\eta_{vol} \quad V_s \frac{\Omega}{2\pi} \rho_w gH}{\overline{Q}_{mech} \, \Omega}$$ (6.8a)

With the equation (6.4) for the ideal torque this becomes :

$$\eta_{mech} = \frac{\eta_{vol} \quad \overline{Q}_{id}}{\overline{Q}_{mech}}$$ (6.8b)

6.3 ACCELERATION EFFECTS

The behaviour of the reciprocating piston pump, represents the low-speed behaviour of the pump. At higher speeds, say 1 to 2 strokes per second and above, acceleration effects cannot be neglected anymore.

A piston pump, directly driven via a crank, exhibits a nearly sinusoidal displacement of the piston as a function of the angular rotation of the driving shaft (fig. 6.2). Taking the displacement z and the time t as zero when the piston is at its bottom position, the position of the z_p as a function of angular rotation is given by :

$$z_p = \tfrac{1}{2}s - \tfrac{1}{2}s \cos \Omega t \qquad (6.9)$$

Two subsequent differentiations give us velocity and acceleration (is constant):

$$V_p = \frac{dzp}{dt} = \tfrac{1}{2} \Omega s \quad \sin \quad \Omega t \qquad (6.10)$$

$$a_p = \frac{dvp}{dt} = \frac{dzp}{dt^2} = \tfrac{1}{2} \Omega^2 s \cos \Omega t \qquad (6.11)$$

$$C_a = \frac{a_{p_{max}}}{g} = \frac{\tfrac{1}{2} \Omega^2 s}{g} \qquad (6.12)$$

were C_a is known as acceleration co-efficient which is the ratio between the actual max/min. acceleration and acceleration due to gravity.

The behaviour of the two idealised pumps given Fig. 6.2 and Fig. 6.3, in order to predict the cavitation are described. The acceleration of the water column can be calculated s_w by calculating force and mass, assuming that its diameter is equal to the diameter of the piston D_p .

$$\text{Force} = P_{atm} * \frac{\rho}{4} D_p^2 - \rho H * \frac{\pi}{4} D_p^2 \qquad (6.13)$$

$$\text{or Force} = \rho g(10-H) * \frac{\pi}{4} D_p^2 \quad \text{(at sea level)} \qquad (6.14)$$

$$\text{and Mass} = \rho L * \frac{\pi}{4} D_p^2 \qquad (6.15)$$

So the acceleration a_w becomes :

$$a_w = \frac{10 - H}{L} * g \qquad (6.16)$$

In order to avoid cavitation.

$$\frac{10 - H}{L} g > \frac{1}{2} \Omega^2 s \qquad (6.17)$$

The best way of avoiding cavitation is the avoid high suction heads, or, if this is not possible, to reduce the lenght L of the water column concerned, by introducing an air chamber (fig. 6.4).

With air chorbon the acceleration becomes.

$$a_w = \frac{10-H}{1} * g \qquad (6.18)$$

Acceleration can be increased by reducing L to fulfil the non-cavitation condition (.6.17).

When the decleration of the piston exceeds g during the last part of the upward stroke, the water column will continue to move upward on its own, now decelerated by g only. This means that the piston valve has to open and that an extra amount of water passes the piston valve. In other words, the pump will displace more water than its stroke volume and its volumetric "efficiency" can become higher than 100%. This is illustrated in Fig. 6.5.

The position angle Ωt_1 at which an acceleration of $- g$ is reached is found with :

$$- g = \Omega^2 \tfrac{1}{2}s \cos \Omega t_1 \qquad (6.19)$$

$$\text{so } \cos \Omega t_1 = \frac{- g}{\tfrac{1}{2} \Omega^2 s} = - \frac{1}{C_a} \qquad (6.20)$$

In the example of Fig. 6.5 with $\Omega^* = 12.3786$ rad/s and

$s = .425$ m, the acceleration coefficient becomes $c_a = 3.319$

and the position angle becomes $\Omega t_1 = 1.8768$ rad $= 107.53°$.

From this moment on the water column above the position is

"launched" and moves upward, although its velocity is

linearly decreasing with a velocity $-g(t-t_1)$. When the

velocity decreases to zero the foot valve will close.

The position angle Ωt_2 at which the water speed becomes

zero, is found by realizing that the speed at t_1, when the

piston valve opens, can be calculated with equations (6.10),

(6.20) and $\sin \Omega t = \sqrt{(1 - \cos^2 \Omega t)}$:

$$V_w(t_1) = V_p(t_1) = \tfrac{1}{2}\Omega s \quad \sqrt{\left(1- \frac{1}{c_a^2}\right)} \qquad (6.21)$$

Now the linearly decreasing speed is given by

$$V_w = V_w(t_1) - g(t - t_1)$$

or
$$V_w = V_w(t_1) - \frac{g}{\Omega}(\Omega t - \Omega t_1) \qquad (6.22)$$

and with equation (4.21) and (4.20) this becomes:

$$V_w = \tfrac{1}{2}\Omega s \quad \sqrt{\left(1 - \frac{1}{c_a^2}\right)} - \frac{g}{\Omega}\left(\Omega t - \cos^{-1}\left(-\frac{1}{c_a}\right)\right) \quad (6.23)$$

Zero water speed is reached at the position Ωt_2, which can

be found by substituting $V_w = 0$ in (4.23):

$$\Omega t_2 = \sqrt{(c_a^2 - 1)} + \cos^{-1}\left(-\frac{1}{c_a}\right) \qquad (6.24)$$

This expression is valid for $\Omega t_2 < 2\Pi$, otherwise a new stroke has already begun.

In example $V_w(t_1) = 2.508$ m/sec. and $\Omega t_2 = 5.041$ rad $= 288.86$. for $\Omega = 12.375$ and $S = 0.425$m (appendix G)

The extra amount of water displaced can be found by calculating the extra displacement $z_w - s$ (fig.**6**.5) of the water column at the moment $t = t_2$. The position of the water column at $t = t_2$ is given by:

$$z_w(t_2) = z_w(t_1) + V_w(t_1) * (t_2 - t_1) - \tfrac{1}{2}g(t_2 - t_1)^2 \qquad (6.25)$$

Substitution of equations (**6**.20) and (**6**.21) in equation(**6**.25)yel

$$z_w(t_2)-s = \tfrac{1}{2}s(1-\cos \Omega t_1) + \tfrac{1}{2}s \; \sqrt{(1- \tfrac{1}{c_a^2})} * \tfrac{1}{\Omega}\sqrt{(c_a^2 - 1)} - g \; \frac{c_a^2 - 1}{\Omega^2} - s$$

$$z_w(t_2)-s = \tfrac{1}{2}s(1+ \tfrac{1}{c_a}) + \tfrac{1}{2}s \; \frac{c_a^2 - 1}{c_a} - \tfrac{1}{4} \; s \; \frac{c_a^2 - 1}{c_a}$$

$$z_w(t_2)-s = s \left[- \tfrac{1}{2} + \frac{1}{4c_a} + \frac{c_a}{4} \right] \text{ for } \Omega t_2 < 2\pi \qquad (6.26)$$

Substitution of $c_a = 3.319$ of example leads to $z_w(t_2) - s = s * .405$, so in the ideal case the volumetric efficiency is increased to $(1 + .405) * 100\% = 140\%$.

6.4 Valve behaviour

The two acceleration effects of section 6.3 were described for an ideal pump, i.e. with a perfectly fitting piston and with valves closing immediately when the flow velocity becomes zero. In practice this is not the case and and at higher speeds the valves tend to close later than they should do, because of their inertia.

The behaviour of disk-shaped free-floating valves in reciprocating piston pumps are discussed here (27).

There are a number of forces acting on the valve, acting downward (-ve sign) or upward.

weight of the valve	$-m_v g$	(m_v: mass of valve)
buoyancy force	$\rho_w g\ \nabla_v$	(V_v : volume of valve)
Stationary drag force	F_{st}	
instationary drag force	F_{inst}	
static force(when closed)	$-F_{cl}$	

Newton's law now can be written as:

$$m_v a_v = -m_v g + \rho_w g V_v + F_{st} + F_{inst} - F_{cl} \qquad (6.28)$$

Conservation of mass requires that the mass flow below the piston is equal to the mass entering the valve:

mass flow below piston $\qquad \rho_w A_p V_p$

mass flow in gap below valve $\qquad \rho_w \pi D_v z_v V_g$ (D_v: diameter valve)

mass flow below moving valve $\qquad \rho_w A_v V_v$ (A_v: area valve)

mass flow due to expanding pump cylinder with closed valves $\qquad \rho_w \dfrac{V_{cyl}}{E} \dfrac{dp}{dt}$

The last term is the result of Hooke's law for fluids, with compressibility modulus E, pump cylinder volume V_{cyl} and pressure difference p. This term plays a role only for very small values of z_v and is important in opening the valve. The total conservation law now is given by:

$$A_p V_p + \frac{V_{cyl}}{E} \frac{dp}{dt} = \pi D_v z_v V_g + A_v V_v \qquad (6.29)$$

The term F_{st} known as static drag force on a flat valve is discribed with :

$$F_{st} = \frac{1}{2} \rho_w \left(\frac{V_g}{\mu}\right)^2 A_v \qquad (6.30)$$

With μ being a constant of which the value depends on the type of valve and the ratio between the gap area and the valve entrance area. Often μ is taken to be equal to 0.8. /27 /

The expression for instationary force on valve is

$$F_{inst} = \rho_w V_{added} \left(\frac{A_p}{A_v} a_p - a_v\right) \qquad (6.31)$$

$$V_{added} = \frac{\pi}{12} D_v^3 \qquad (6.32)$$

In the situation of a perfectly closed valve the pressure P_{av} above the valve acts on area A_v, but the pressure P_{bv} below the valve acts only on the area A_{vo} of the valve opening :

$$F_{cl} = -P_{bv} A_{vo} + P_{av} A_v \qquad (6.33)$$

The equilibrium of forces for the closed valve just before opening becomes :

$$-P_{bv} A_{vo} + P_{av} A_v - mg + \rho_w g V_v = 0 \qquad - \quad (6.34)$$

Substitution of the different terms in equation (6.28)

leads to the following non-linear differential equation :

$$m \frac{d^2z}{dt^2} + (m - \rho_w V_v)g - (F_{st}) * \frac{\rho_w A_v (A_p V_P - A_p \frac{dz}{dt} + \frac{V_{cyl}}{E} * \frac{dp}{dt})^2}{2 \mu^2 \rho^2 D_v^2 z^2}$$

$$- \rho_v V_{added} (\frac{A_p}{A_v} a_p - \frac{d^2z}{dt^2}) + F_{cl} = 0 \qquad (6.35)$$

This equation cannot be solved analytically, so numerical

solution is necessary.

6.5 AIR CHAMBER

6.5.1 General

Shock forces experienced by the piston at the moments

the valves close strongly depend on the mass of water above

and under the valves. The installation of air chambers near

the valves softens the influence of mass of water beyond the

air chambers and can greatly reduce the forces on the piston

and consequently reduce the forces on the pump rod and reduce

the acceleration force on the piston have already discussed

in section 6.3.

6.5.2 Volume variations

An ideal air chamber is coupled to a single-acting

piston pump. Ideal in this respect means that the outgoing

flow is perfectly constant (fig. 6.7)

If the pump has a piston area A_p, a stroke s and a

rotational speed , then the incoming flow to the air Chamber

can be described as follows :

$$q_{in} = A_p \Omega \tfrac{1}{2}s \sin \Omega t \quad (m^3/s) \text{ for } 0 < \Omega t < \pi$$

$$q_{in} = 0 \qquad\qquad\qquad \text{for } \pi < \Omega t < 2\pi \qquad (6.36)$$

$$q_{out} = A_p \Omega \tfrac{1}{2}s \frac{1}{2\pi} \int_0^{2\pi} \sin \Omega t \quad d\, \Omega t$$

resulting in :

$$q_{out} = A_p \ \Omega \tfrac{1}{2}s \frac{1}{\pi} \qquad\qquad\qquad (6.37)$$

Comparing equation (6.37) with equation (6.36) the moment

at which $\sin t = \frac{1}{\pi}$ the ingoing and outgoing flows are equal.

$$\Omega t_1 = \sin^{-1} \frac{1}{\pi} \text{ implies } t_1 = 0.324 \text{ rad or } 18.56^\circ \qquad (6.38)$$

$$\Omega t_2 = 2.818 \text{ rad or } 161.44^\circ$$

At t_1 the water volume of the air chamber is at its minimum

and at t_2 the water volume is maximal. In order to find the

volume variations in the ideal air chamber it is integrated

$(q_{in} - q_{out})$ with respect to t (fig. 6.7)

For O $< \Omega t < \pi$ we can write :

$$(q_{in} - q_{out}) \, dt = A_p \tfrac{1}{2} s \quad \int \quad (\sin \Omega t - \tfrac{1}{\pi}) \, d \, \Omega t$$

$$= A_p \tfrac{1}{2} s \, (-\cos \, \Omega t \quad - \tfrac{\Omega t}{\pi} + constant)$$

The boundary condition of zero volume at $\Omega t = O$ leads to :

$$(q_{in} - q_{out}) \, dt = A_p \tfrac{1}{2} s \, (1 - \cos \Omega t - \tfrac{\Omega t}{\pi}) \qquad (6.36)$$

For $\pi < \Omega t < 2 \pi$ one finds :

$$(q_{in} - q_{out}) \, dt = A_p \tfrac{1}{2} s \, (2 - \tfrac{\Omega t}{\pi}) \qquad (6.39)$$

These two parts of the function are shown in fig. 6.8

The difference between the minimum and maximum volume can be found with equations (6.38) and (6.39).

$$V_{max} - V_{min} = \tfrac{1}{2} V_s \, (1 - \cos \Omega t_2 - \tfrac{\Omega t_2}{\pi} - 1 + \cos \Omega t_1 + \tfrac{\Omega t_1}{\pi})$$

$$V_{max} - V_{min} = 0.551 \, Vs \qquad (6.41)$$

CHAPTER : 7 : DESIGN OF A ROTOR COUPLED PUMP

7.1 DESCRIPTION AND DIAMETER CALCULATION OF THE PUMP

If a pump is coupled to a wind rotor at a given wind speed V, the rotor will turn at a speed such that the mechanical power of the rotor is equal to the mechanical power exerted by the pump. This working point can be found by the intersection of the rotor curve and the pump curve (fig. 7.1)

To find the hydraulic output as a function of wind speed, a series of rotor power curves must be drawn (fig. 7.2). As a result the net output curve is found, as well as the over-all efficiency (from wind to water) of the system (fig. 7.2).

It can be seen that the resulting output curve is nearly a linear function of the wind speed (fig. 7.3). The overall efficiency varies strongly with the wind speed. The wind speed at which the overall efficiency reaches a maximum is the design wind speed V_d of the system. In practice, it is the wind speed at which C_p reaches its maximum value C_{pmax}.

The net power supplied by the rotor-pump combination must be equal to the hydraulic power to lift the water:

Total rotor-pump power = hydraulic power

$$\eta_{mech} \, P_{mech} \qquad\qquad = \; P_{hydr} \qquad\qquad (6.6.)$$

$$\eta_{mech} \, C_p \, \tfrac{1}{2} \, \rho \, V^3 \, \pi R^2 \;=\; q \, \rho_w \, g \, H \qquad\qquad (7.1.)$$

$$\text{At } V = V_d : \; \eta_{mech} \, C_{P_{max}} \, \tfrac{1}{2} \, \rho \, V_d^3 \, \pi R^2 = q_d \, \rho_w \, g \, H \qquad (7.2)$$

The flow q is equal to the ideal flow, determined by the stroke volume and the speed, multiplied by the volumetric efficiency of the pump and the number of the pump.

$$q = \eta_{vol} \; s \; \tfrac{\pi}{4} \, D_p^2 \; \frac{\Omega_*}{2\pi} \; T^* \qquad\qquad (7.3.)$$

$$\text{or} \qquad q = \eta_{vol} \; s \; \tfrac{\pi}{4} \, D_p^2 \; \frac{\lambda V}{2 \, \pi R} \; T^*$$

where T^* = number of pumps

Substituting (7.3.) in (7.2) for $V = V_d$ gives an expression for V_d.

$$V_d = \sqrt{\left(\frac{9 \eta_{vol} \; s \cdot D_p^2 \; \lambda_d \rho_w \; g \; H \; T^*}{4 \; C_{Pmax} \; \eta_{mech} \; \rho \; \pi \; R^3} \right)} \qquad\qquad (7.4.)$$

In this study

η_{vol} = 100%

V_d 4 m/sec.

λ_d = 8

ρ_w = 1000kg/m^3

H = Hs + Hd + H losses = 8.5 m.

ρ = 1.225 kg/m^3

C_{Pmax} = 0.45

η_{mech} = 0.82 $\angle$22$\angle$7

R = 23.2668m

T* = 3(The pumps is arranged at a phase difference of 120)

Ω Ω =   rpm of rotor = 1.378 rad/sec.

Ω^* =   rpm of pump = 9   1.375 = 12.375 rad/sec.

= 118.17 rpm

$$4 = \sqrt{\frac{9 \times 1 \times D_p^2 \ s \times 8 \times 1000 \times 9.81 \times 8.5 \times 3}{4 \times .45 \times .82 \times 1.225 \times \pi \times (23.2668)^3}}$$

D_p^2 s   = 0.06355

For Optimum Design.

$$\frac{S}{D_p} = 1.1 \quad \boxed{22}$$

$$1.1 \ D_p^3 = .06355$$

$$D_p = .386 \ m = 15.21"$$

$$S = .425 \ m = 16.74"$$

7.1.1 Torque calculation

$$\overline{Q}_{id} = \frac{1}{2}\pi \rho_w gH \ \nabla_s \qquad\qquad (6.4)$$

where $\nabla_s = \frac{\pi}{4} D_p^2 \ s$

$$\overline{Q}_{id} = \frac{1}{2}\pi \times 1000 \times 9.81 \times 8.5 \times \frac{\pi}{4}(.386)^2 \times .425$$

$$= 660.02 \ (N - m)$$

$$Q_{id(max)} = \pi \overline{Q}_{id}$$

$$= 2073.53 \ (N - m)$$

$$n_{mech} = \frac{n_{vol} \ \overline{Q}_{id}}{Q_{mech_p}} \qquad\qquad (6.8)$$

$$Q_{mech_p} = \frac{n_{vol} \ Q_{id}}{n_{mech}}$$

$$= \frac{2073.53}{.82}$$

$$= 2528.70 \ (N - m)$$

$$P = Q_{id\ R_{max}} * \Omega R = Q_{id\ P_{max}} \times \Omega^*$$

$$Q_{id\ R_{max}} = max^m \text{ torque of the rotor}$$

$$Q_{id\ P_{max}} = " \quad " \quad " \quad " \quad \text{pump}$$

$$\frac{\Omega^*}{\Omega R} = \frac{\text{angular velocity of pump}}{\text{angular velocity of rotor}} = 9.$$

$$Q_{id\ P*(max)} = 9 \times 2528.70$$

$$= 22758.31 \text{ (N - m)}$$

There are three 10 kw pumps. The pumps are placed 120° Crank angle apart (phase difference 120°). From torque analysis maximum torque required 2275(Nm. But available at zero pitch is 21,800(N - m) which is slightly lower than required torque. From torque characterstics for different pitch angles, at 1,2,3 rotor torque is higher and sufficient to overcome the maximum torque of the pump.(fig. 7.4)

7.2   Starting behaviour

The starting behaviour of a water pumping windmill
is the static description in which the starting torque of the
rotor is equal to the maximum torque required by the
pump at the starting wind speed.

$$c_{Q_{st}} \; \tfrac{1}{2} \, \rho \, V_{st}^2 \, A \, R = \tfrac{1}{2} \, s \, \rho_w \, g \, H \, \tfrac{\pi}{4} \, D_p^2 \tag{7.5}$$

Maximum torque of the pump is π times i.e. average torque
and that the average torque is equal to the torque Q_d
produced by the rotor at its design wind speed.

$$c_{Q_{st}} \; \tfrac{1}{2} \, \rho \, V_{st}^2 \; A \, R \; = \; \frac{c_{p_{max}}}{d} \; \tfrac{1}{2} \, \rho \, V_d^2 \; A \, R \tag{7.6}$$

$$V_{st} \; = \; V_d \; \sqrt{\frac{\pi}{\lambda_d} \frac{c_p}{c_{Q_{st}}}}$$

The higher the tip speed ratio λ_0 of a rotor, the lower
the starting torque. As a rough rule of the thumb the starting
torque is given by :

$$c_{Q_{st}} \; = \; \frac{0.6}{\lambda d^2} \qquad\qquad [18]$$

$$= \; \frac{0.6}{8^2} \; = \; 0.009375 \tag{7.7}$$

$$V_{st} = V_d \sqrt{\frac{\sqrt{} X \quad .45}{.00935 \; X \; 8}}$$

$$= 4.34 \; V_d$$

$$= 4.34 \quad X \; 4$$

$$= 17.36 \; m/s$$

Windmills need a quest of wind, with a velocity of 4.4 times the design speed to be able to start. The effect of rotor inertia will reduce this factors somewhat but still the starting wind speed will usually be higher than the design wind speed.

7.3   CALCULATION OF THE DIAMETER OF A LEAKHOLE

A small hole is drilled in the piston in order to improve the starting characteristics of windmill equipped with a reciprocating pump. The effect of this leakhole is that at very low speeds, i.e. at starting, all water that could be pumped is leaking through the hole. This implies that the pressure on the piston is very low and as a result the starting torque required is low. If the speed is high, then the quantity of water leaking through the hole is small compared to the normal output of the pump, and the pump behaves as a normal piston pump (Fig. 7.3)

Assuming that at the design speed the leak flow is only 10% of the design flow, $\underline{/27\underline{/}}$ in otherwords the volumetric efficiency.

$$\eta_{leak, \, vol} = 0.90 \tag{7.8}$$

In Fig. E.1 (appendix E) it can be seen or calculated from equation (4.69) that the value will be read when $\Omega = \Omega_d$.

$$\frac{\Omega_d}{\Omega} =. \; 15.4 \tag{7.9}$$

The design speed Ω_d is found from the expression 7.3) for the design wind speed V_d :

$$\Omega_d = \frac{\lambda_d}{R} * \sqrt{\frac{\lambda_{vol} \; s D_P^2}{4 C_{pmax}} \; \frac{\lambda_d}{\eta_{mech}} \frac{\rho_w \; g \; H}{\rho \pi \; R^3}} \tag{7.10}$$

with the expression Ω_o (detail in appendix E) the speed at which pumping starts equations (7.9) and (7.10) can be written into :

$$\frac{2d^2}{D_P^2 s} * \frac{2 \; gH}{f} = \frac{\lambda_d}{15.4} * \frac{m_{vol} \; sD_P^2}{4 C_{pmax}} \frac{\lambda_d \rho_w \; g \; H}{\eta_{mech,} \; \rho \; \pi \; R^3} \tag{7.11}$$

Rearranging yields an expression for the leakhole diameter.

$$d^2 = \frac{D_p^3}{30.8} \quad \sqrt{\frac{\eta_{vol} \, s^3 \, \lambda^3_d}{C_{p_{max}} \, \eta_{mech,} \, R^5}} \; * \; \rho \frac{w \, f}{8 \, \pi \, \rho} \qquad (7.12)$$

Using formula (7.12), the diameter of leakhole is (appendix E)

$$d = 8.17 \text{ mm.}$$

From appendix E

$$\frac{\Omega^*}{\Omega_o} = 752.83.$$

The discharge starts at angle θ_o

$$\theta_o = \sin^{-1} \frac{\Omega_o}{\Omega^*} = 0.0759^o.$$

7.4 Gear Design

For D pinion (fig. 7.6)

The pitch line speed and transmitted load are $\underline{/}10\underline{/}$

$$V_m = \pi D n = \pi \left(\frac{12}{12}\right) \times 117 = 367.56 \text{ fpm.}$$

$$F_t = \frac{33000 hp}{Vm} = \frac{33000 \times 3609.2}{367.56} =$$

Commercially cut

$$Fd = \frac{600 + Vm}{600} \ Ft \ lb \qquad \text{if } Vm = 200 \text{ fpm.}$$

$$= 5820.2 \text{ lb.}$$

Cast iron may be chosen because it is less expensive material.
Material ASTM 30 whose endurance limit may be taken

as .4 X 30 = 12ksi. Table AT6 gives the typical.

$S'n$ = 14.0, hence 12ksi is conservative. Let $b = \dfrac{10}{P_d}$

Let k_f = 1.48 Y = 0.337 Table AT 24 is suitable for
approximate solution.

With these various assumption :

$$F_s = Fd = 5820.2 = \frac{sbY}{k_f P_d} = \frac{12,000 \times 10 \times 0.34}{1.48 \times P_d^2}.$$

$$P_d = 2.176 \doteq 2$$

$$N_p = Pd \ D_p = 2 \times 12 = 24$$

Y = 0.337 from Table AT 24.

k_f = 1.48 as before.

$$F_s = 5820.2 = \frac{12000 \times b \times .337}{1.48 \times 2}$$

b = 4.26 ≈ 4.375 = $4\frac{3}{8}$"

$P_d b$ = 4.375 X 2 = 8.75 which within the range of

8 to 11.5 and is therefore satisfactory. For m_w = 3.

where m_w is the velocity ratio.

N_g = 3 X ·24 = 72 teeth in the gear.

P_d = 2, b = $4\frac{3}{8}$" , N_p = 24, N_g = 72

For B pinion

$$V_m = \pi D = \pi \times \frac{12}{12} \times 39 = 122.52$$

$$Ft = \frac{33000 \times 402}{122.5} = 10829.39$$

$$F_d = \frac{600 + V_m}{600} Ft \times 10829.388 = 13040.75$$

Material ATSM 60 whose endurance limit may be taken as

60 X .4 = 24 ksi Table AT6 gives typical S n = 24.5 ksi

hence 24 ksiis conservative. Let $b = \frac{10}{P_d}$, let K_f = 1.48

Y = .340   Table AT 24 is suitable for first approximate

solution.

With these various assumption :

$$F_s \; = \; F_d \; = \; 13040.75 \; = \; \frac{sby}{Kf \; Pd} = \frac{24000 \; X \; 10 \; X \; .34}{1.48 \; P_d^2}$$

$$P_d^2 \; = \; 4.2123$$

$$P_d \; = \; 2.05 \; = \; 2.$$

$N_p \; = \; P_d \, D_p \; = \; 2 \; X \; 12 \; = \; 24.$ Y = .337 from Table AT 24.

$$K_f \; = \; 1.48 \; \text{as before.}$$

$$F_s \; = \; 13040.75 \; = \; \frac{sby}{K_f \; P_d} \; = \; \frac{24000 \; X \; 332b}{1.48 \; X \; 2}$$

$$b \; = \; 4.84 \; = \; 4.875$$

$P_d \; = \; 2, \quad b \; = \; 4.875'', \quad N_p \; = \; 24, \quad N_g \; = \; 72.$

CHAPTER 8 : CONCLUSIONS AND RECOMMENDATIONS.

The main purpose of the present work is to obtain a method
for calculationg the performance analysis of a horizontal
axis wind turbine and design of a piston pump and behaviour
of combination.

The following conclusions may be drawn on the basis of this
study.

1) **At a given** λ, a rotor blade must be designed for optimum
C_p. Optimum value of C_p was correspond to the maximum C_L/C_D
ratio which must be kept constant along the entire blade span.
For maximum energy extraction from the wind, it is necessary to
vary the blade chord and twist angle continuously along the
span. This leads to a very complicated rotor blade which will
be expensive to manufacture and may not have structural inte-
grity. It is possible to approach very closely to optimum by
taking a linearly tapered and linearly twist blade.

Introduction of a rotor without twist results power loss
penalty of about 6 to 10%. This might be acceptable for single
production unit but loss its attraction in case of mass pro-
duction. Choosing an untwisted blade design, the constant chord
blade seems rather attractive, because the blade area in the hub
region is reduced where the blade stall starts at relatively
high value of λ.

2) To start a low speed rotor, that has high internal resistance, primarily a high pitch angle is desirable. The internal resistance decreases as soon as device gets started and accelerated. So after attaining certain angular speed, the pitch angle is to be reduced to the optimum value.

3) Power losses due to aerodynamic profile drag can be reduced by increasing the rotor solidity and reducing tip speed, but only at the expense of blade weight and cost. Improvements in airfoil lift to drag ratio will permit reduced solidity and higher tip speeds.

Increased tip speed would be advantageous for reducing capacity of the speed increaser gear box needed to step up the low rotor shaft speed to the electrical generator speed or pump speed. (It is necessary to sacrifice some aerodynamic efficiency to reduce blade size and weight of large wind turbine.)

4) The suction head of the pump should be kept in the safe limit so that the net positive suction head remains above the critical value. With long suction pipes there is risk of cavitation and the high acceleration in the suction line delays the valve opening reducing the efficiency of the pump. This can be overcome by matching valve size with the suction line acceleration head.

5) Values of Ca (acceleration co-efficient) above 1 imply a compressive force on the pump rod during the downstorke (with the danger of buckling) because the pump rod is forced to accelerate faster than the gravity acceleration.

Other problems may also occur when the values of Ca is above 0·5. This is caused by the possibility of cavitation behind the piston which occurs when the local pressure falls below the vapor pressure. The introduction of an airchamber also necessary for more regular flow and reduction of impulse forces. To avoid cavitation it must ensure that $a_w > a_{p_{max.}}$

6) A series of rotor power curves are drawn. From this series of curves the resulting output curve can be drawn which is nearly linear function of the wind speed.

7) The effect of the leakhole is that at very low speed i.e. during starting all water that could be pumped is leaking through the hole. This implies that the pressure on the piston is very low and as a result the starting torque required is low. If the speed is high then quantity

of water leaking through the hole is small compared to
normal output of the pump behaves like a normal piston
pump.

8) The limiting condition for pump discharge is attained
    when the speed of the piston $V_p \gg V_o$ where

$$V_o = \frac{d^2}{D_p^2} \quad \text{x} \quad \frac{2_g H}{f}$$

RECOMMENDATION :

1) The power curve is sensitive mainly to blade pitch angle
    in the stalling region. To avoid too much drop off after
    stalling point, a blade pitch angle between 2^O to 5°
    is seem to be more convenient than at an angle of 0°.

2) Arched steel plate ($^C d/^C L = 0^{\cdot}02$) can be used instead of
    NACA 4418 ($\frac{Cd}{Cl} = 0^{\cdot}008$) in order to minimized the manufactu-
    ring cost. About 15 - 18% - power loss may occur if arched
    steel plate is used.

3) A strip theory approach using local optimization resulting
    in higher calculated performance. Optimized wind turbines
    perform best at low drag to lift ratios is to be expected.
    Knowledge of the optimized configuration will enable design
    changes to be directed as to minimize performance loss.

4) For low speed wind turbine positive displacement pumps are suitable because of simple construction and the shaft speed can be increased to reduce the pump size. For speed step up a suitable gear system is designed.

5) Memberane or Diaphram pump can be used instead of piston pump because of simplicity of design and lower manufacturing cost.

6) Low capacity (up to 10kW) pump is recommended for ease of design and manufacture but coupling of three pumps in the same shaft faces difficulties during starting. So arrangement should be made so that pumps start in sequence one after another.

7) In the present research the theoretical study of characterstics of turbine pump set has been made. This study should be verified with experimental results.

REFERENCES

REFERENCES

[1] ABBORT I.H., VON DOENHOFF A.E.

"Theory of Wind Sections"

Dover Publications, New York, 1959.

[2] ALAM M.M.

"Analysis of Yaw stability of Horizantal
Axis Wind Turbine"
Mechanical Engineering Department,
M.Sc. Engg. Thesis in BUET, 1987.

[3] ALTHAUS D.

"Stuttgarter Profilkatalog I"

Universitat Stuttgart, 1972.

[4] ANDERSON M.B.

"Blade Shapes for Horizontal Axis Wind Turbines"

Proc. of Second BWEA Wind Energy Workshop,

Cranfield, April, 1980.

[5] ANDERSON M.B.

"A Vortex Wake Analysis of a Horizontal Axis Wind

Turbine and a comparison with a Modified Blade

Element Theory"

Proc. of Third International Symposium of Wind

Energy Systems, Copenhagen, August, 1980.

/ 6 / BETZ A.

"Gotinger Nachr", P. 193, 1919.

/ 7 / CRIGLER J.L.

"Application of Theodorsen's Theory to Propeller Design"

NACA Report 924.

/ 8 / DOMMASCH D.O., SHERBY S.S., CONNOLY T.F.

"Airplane Aerodynamics"

Pitman Publishing Corporation, New York, 1961.

/ 9 / ELDRIDGE R.F.

"Wind Machines"

Van Nostrand Reinhold Company, 1980

/ 10 / FAIRES V.M.

"Design of Machine Elements (Fourth Edition)"

/ 11 / GARSTANG M., SNOW J.W., EMMITT G.D.

"Measurement of Wind Shear at the MUD-1 Site,

Boone, N.C."

AIAA/SERI Wind Energy Conference, April 9 - 11,

1980/Boulder, Colorado.

/ 12 / GESSOWA., MYERS G.C. Jr.

"Aerodynamics of the Helicopter"

Frederic Ungar Publishing Co., New York, 1952.

/ 13 / GLASGOW J.C., MILLER D.R., CORRIGAN R.D.

"Comparison of Up Wind and Downwind Rotor Operations

of the DOE/NASA 100-KW MOD-O Wind Turbine"

Second DOE/NASA Wind Turbine Dynamics Workshop,

Cleveland, Ohio.

/ 14 / GLASGOW J.C., MILLER D., SULLIVAN T.

"Rotor Blade Bending Loads for MOD-O Experimental

Wind Turbine"

NASA PIR 163 October 1980.

/ 15 / GLAUERT H.

"The Analysis of Experimental Results in the Windmill

Brake and Vortex Ring States of an Airscrew"

Aeronautical Research Council Reports and Memoranda

No. 1026, February 1926.

/ 16 / GOLDING S.

"On the Vortex Theory of Screw Propellers"

Proc. of Royd Soc. A 123, 440, 1929.

/¯17_7   GUSTAFSON L.A., LUNDGRENS., FRISK B.

          "Application of a Method for Aerodynamics Analysis

          and Design of Horizontal Axis Wind Turbines"

          Technical Note AU-1499 Part 1, The Aeronautical

          Research Institute of Sweden, Stockholm, 1980.

/¯18_7   HENGEVELD., LYSEN, E.H., PAULLISSEW L.M.M.

          "Matching of Wind Rotor to low electric Generator"

/¯19_7   ISLAM M.Q.

          "A Theoretical Investigation of the Design of

          Horizontal Axis Wind Turbine"

          Ph.D. Thesis, Vrije Universiteit, Brussel, 1986.

/¯20_7   JANSEN W.A.M., SMULDERS P.T.

          "Rotor Design for Horizontal Axis Windmills"

          Steering Committee for Wind Energy in Developing

          Countries, P.O. Box 85, Amersfoort, The Netherland,

          May, 1977.

/¯21_7   JANSEN W.A.M.

          "Horizontal Axis Fast running Wind Turbines for

          Developing Countries"

          Steering Committee for Wind Energy in Developing

          Countries, P.O. Box 85, Amersfoort, The Netherland,

          March, 1976.

/_22_/   JOHNSON W.

"Helicopter Theory"

Princeton University Press, 1980, PP. 106.

/_23_/   KARASSIK I.J., KRUTZCHW W.C., FRASER W.H., MISINA J.P.

"Pump Handbook"

McGRAW-HILL Book Company.

/_24_/   LERBS H.W.

"Moderately Loaded Propellers With a Finite Number

of Blades and an Arbitrary Distribution of Circulation"

Trans. Soc. Naval Architects and Marine Engrs.,

60, 73-117. 1957.

/_25_/   LINSCOTT B.S., GLASGOW J., ANDERSON W.D., DONHAM R.E.

"Eperimental Data and Theoretical Analysis of an

operating 100 KW Wind Turbine

/_26_/   LOCK C.N.H.

"Note on the Characteristic Curve for an Airscrew

or Helicopter"

Aeronautical Research Council Reports and Memoranda

No. 2673, June, 1947.

/ 27 /   LYSEN E.H.

          "Introduction to Wind Energy"

          Steering Committee of Wind Energy

          for Developing Countries, P.O. Box 85,

          The Netherland, Amersfoort, May, 1983.

/ 28 /   MONIR S.S., AHMED M., ALAM M.

          "Feasibility of Wing Energy

          Project in Bangladesh"

          Mechanical Engineering Department,

          B.Sc. Engineering Thesis in BUET, 1981.

/ 29 /   LYSEN E.H., BEURSKENS H.J.M., HAGEMAW A.J...K.

          HOSPERS G.D., KRAGTONA.

          "Low Speed Water Pumping Windmills : Rotor

          Test and Overall Performance"

          Eindhoven University of Technology,

          The Netherlands.

/30_7   POWELS S.R.J.

"The Effect of Tower Shadow on the Dynamics of

a Horizontal Axis Wind Turbine"

Journal of Wind Engineering, Vol. 7. No. 1. 1983.

/31_7   ROHRBACH C., WOROBEL R.

"Performance Characteristics of Aerodynamically

optimum Turbines for Wind Energy Generators"

American Helecapter Soc. preprint No. S-996,May 1975.

/32_7   RUDY D.

"Dynamic Cross-Wind Response of Tall Rectangular Towers"

Ph.D. Thesis Vrije Universiteit Brussel, August, 1982.

/33_7   SHARPE D.J.

"A Theoretical and Experimental Study of the Darrieus

Vertical Axis Wind Turbine"

Kingston Polytechnic, October, 1977.

/34_7   SHEPHERD D.G.

"Note on a Simplified Approach to Design Point

Performance Analysis of HAWT Rotors"

Journal of Wind Engineering Vol. 8, No. 2. 1984.

/‾35_7   SPERA D.A., JANETZKE

" Effect of Rotor Location, Coning and Tilt.

on Critical Loads in Large Wind Turbines"

Wind Technology Journal, Vol. 1. No. 2, Summer, 1977.

/‾36_7   THEODORSEN . T.

"The Theory of Propellers, I-Determination of the

Circulation Function and the Mass Coefficient for

Dual-Rotating Propellers"

NACA Report 775, 1944.

/‾37_7   THEODORSEN T.

"The Theory of Propellers, IV-Thrust, Energy and

Efficiency Formulas for Single and Dual-Rotating

Propellers with Ideal Circulation Distribution"

NACA Report 778, 1944.

/‾38_7   THEODORSEN T.

"Theory of Propellers"

Mcgraw-Hill Book Co. Inc., New York, 1948.

/‾39_7   Vollen A.

"Aeroelastic Stability and Dynamic Response

Calculations for Wind Energy Converters.

Gassellschoft fur Technisch-Wissens chaft lliche

Datenverabeitung m.b.h., F.R. Germany.

/40_7   VRIES O. de

         "Fluid Dynamics Aspects of Wind Energy Conversion"

         NATO Advisory Group for Aerospace Research and

         Development, The Netherland, July 1979.

/41_7   WALKER S.N.
         "Performance and Optimum Design Analysis/

         Computational for Propeller Type Wind Turbines"

         Ph.D. Thesis, Oregon State University.

/42_7   WILMSHURST S.M., POWELS S.J.R., WILSON D.M.A.

         "The Problem of Tower Shadow"

         Proc. of the Seventh BWEA Wind Energy Conference,

         Oxford 27-29 March, 1985.

/43_7   WILSON R.E., LISSAMAN P.B.S.

         "Applied Aerodynamics of Wind Power Machines"

         Oregon State University, Corvallis, Oregon 97331,

         USA, July 1974.

/¯44_7   WILSON R.E.

"Aerodynamic Potpouri"

Proc. of the DOE/NASA Wind Turbine Dynamics

Conference, February 1981, NASA CP-2185,

DOE CONF-801226.

/¯45_7   WILSON R.E., LISSAMAN P.B.S., WALKER S.N.

"Aerodynamics Performance of Wind Turbines"

Oregon State University, Corvallis, or,

NTIS, USA, 1976.

/¯46_7   WILSON R.E., WALKER S.N.

"Performance Analysis Program for Propeller Type

Wind Turbines"

Oregon State University, March 1981.

/¯47_7   YAMANE T., TSUTSUI Y., ORITA T.

"The Aerodynamic Performance of a Horizontal Axis

Wind Turbine in Large Induced Velocity States"

Proc. of the Fourth International Symposium on

Wind Energy Systems, Stockholm, September 1984.

FIGURES

Fig. 1.1.2: Darrieus Rotor

TOP VIEW

VERTICAL AXIS

VERTICAL AXIS
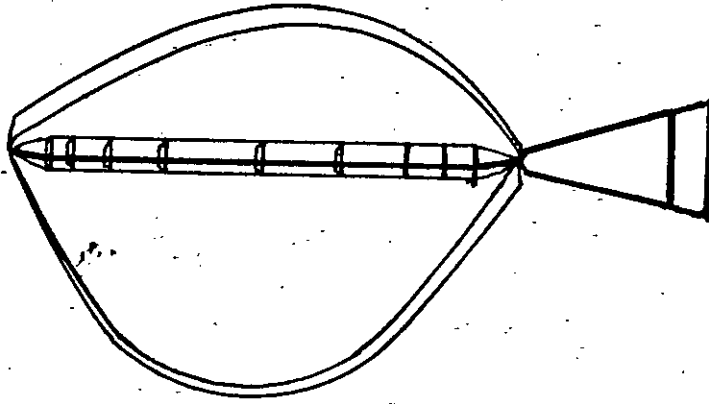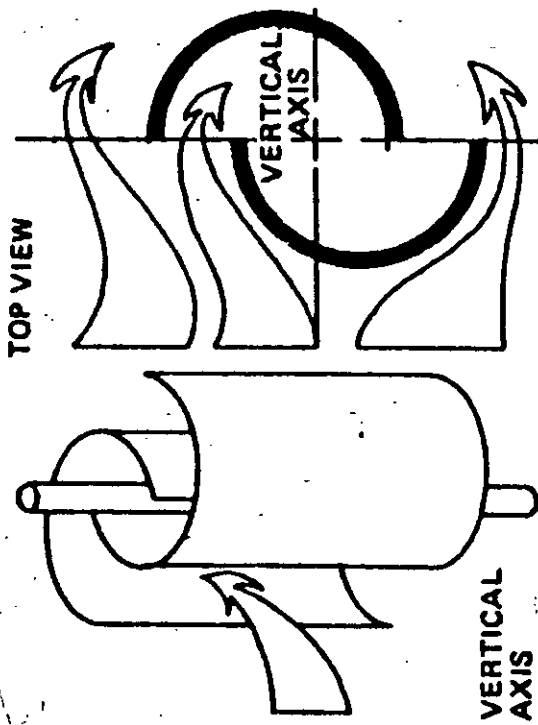
Fig. 1.1.1 : Savonius Rotor
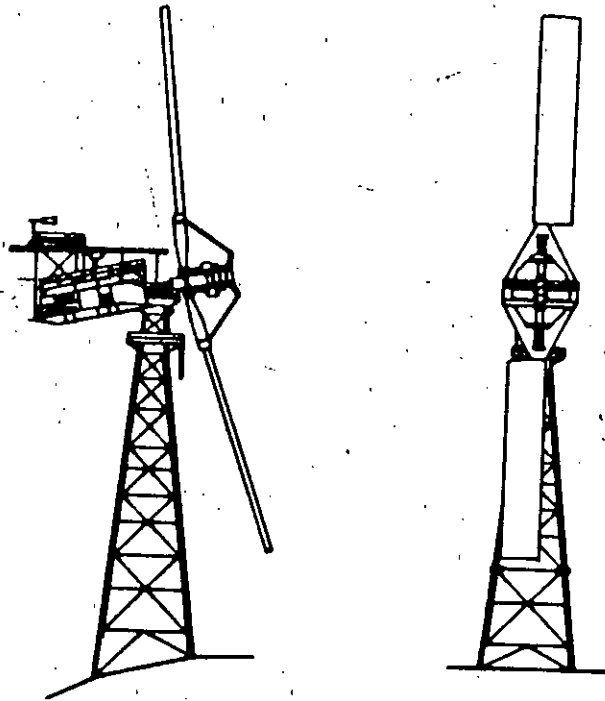
Figure 1.1.3: Smith-Putnam
Wind Turbine.
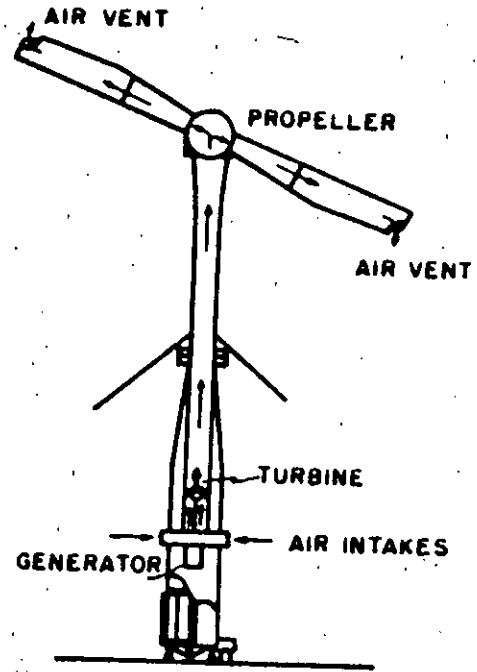
Figure 1.1.4: Enfield-Andreau Ducted Rotor
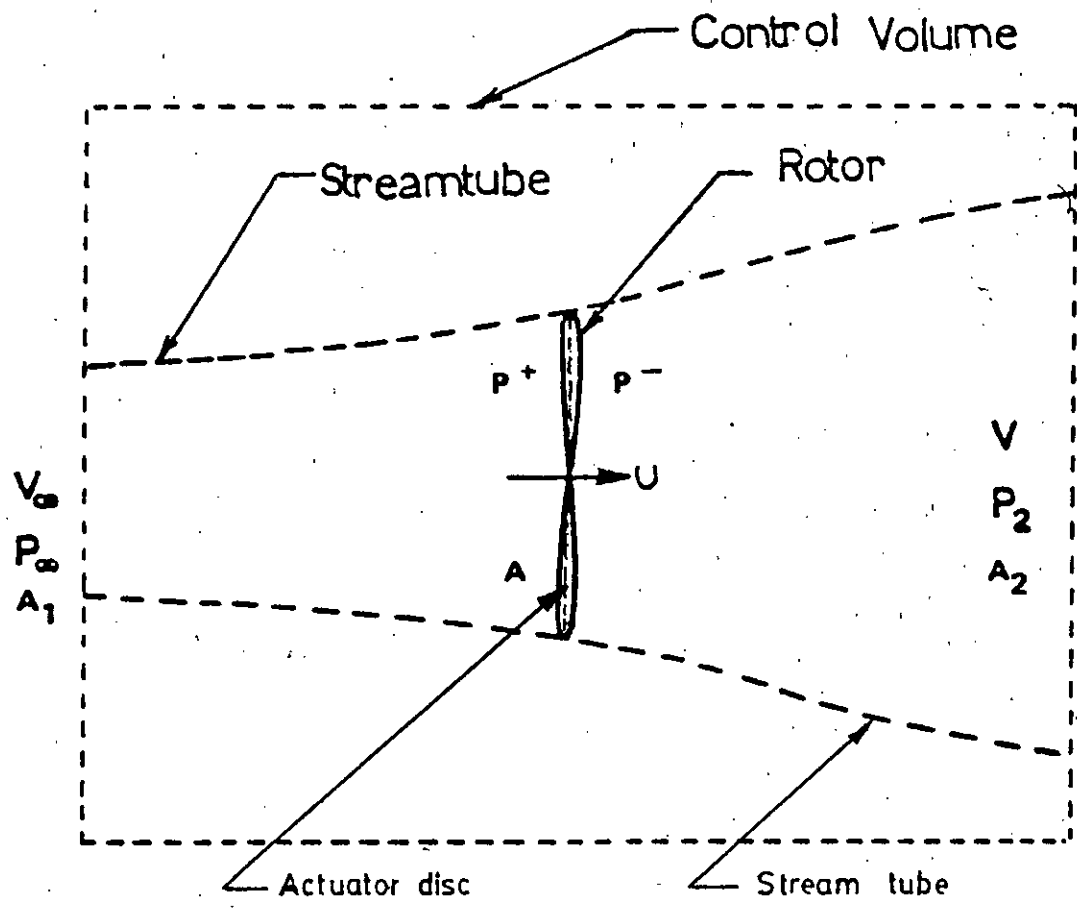
Fig. 3.1.1: Wind Turbine Stream Tube
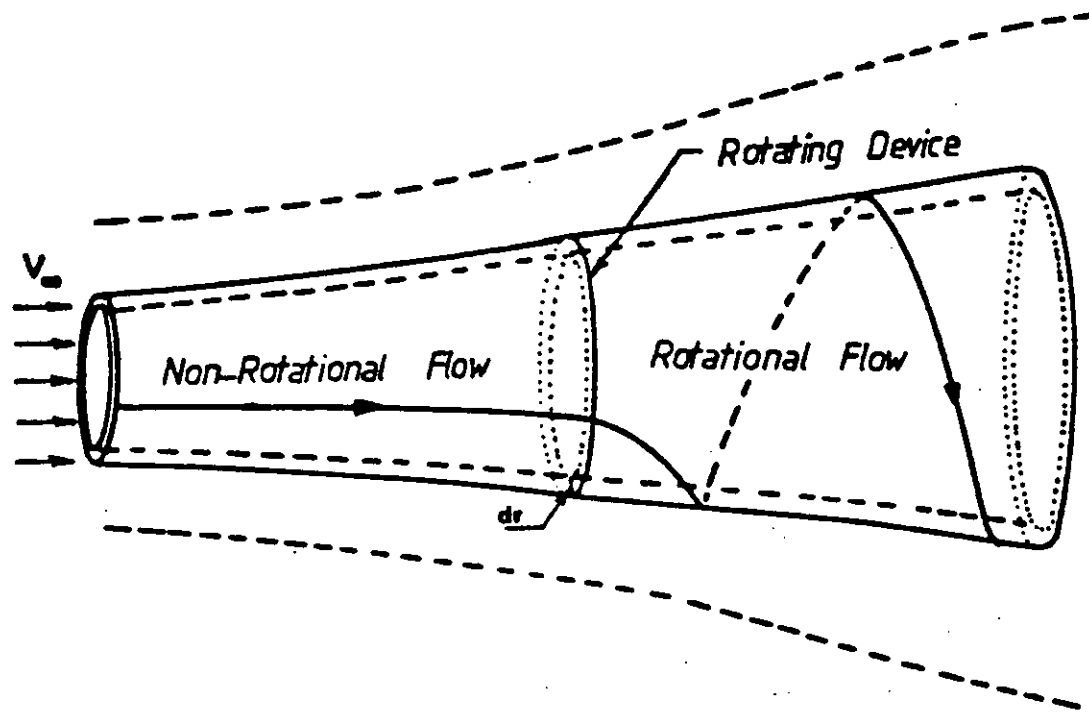
Fig. 3.1.2: Streamtube showing Wake Rotation (27)
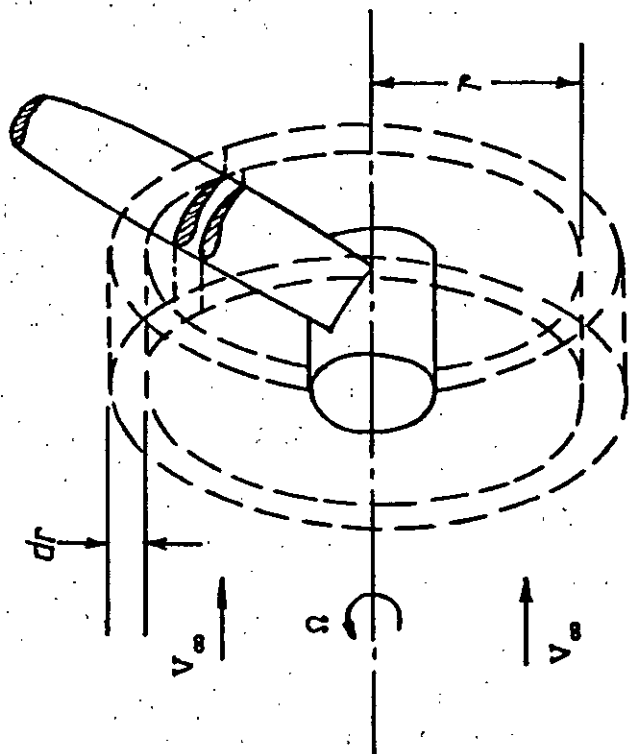
Fig. 3.1.3: Blade Element Annular ring (46)
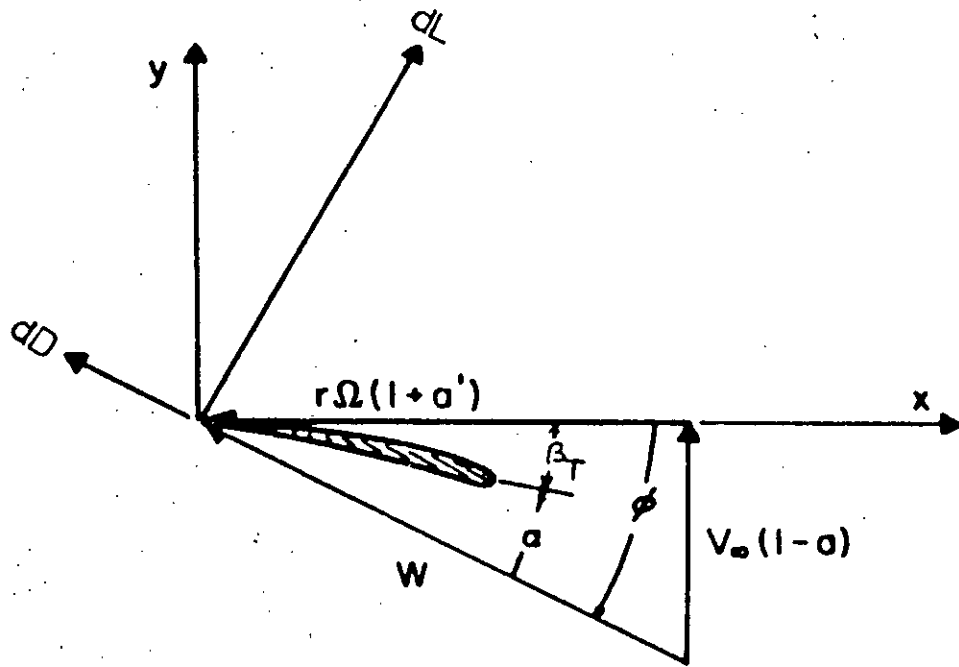
Fig. 3.2.1: Velocity Diagram of a Blade Element (43).
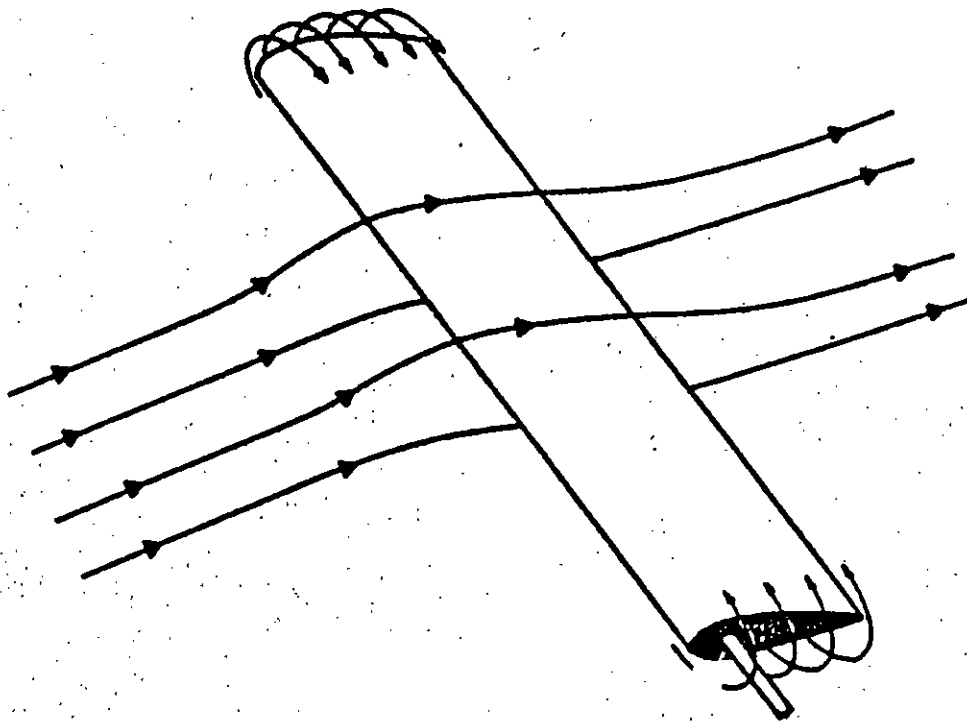
Fig. 3.4.1: Tip and Hub Losses Flow Diagram (45).

Figure 4.1.1: Analytical Model for Momentum Theory (45).

Figure 4.1.2: Velocity Diagram for Rotor Blade Element.

TABLE 4.2.1 [20]

Design Tip Speed Ratio λ_d	Number of Blades B
1	6 – 20
2	4 – 12
3	3 – 6
4	2 – 4
5 – 8	2 – 3
8 – 15	1 – 2
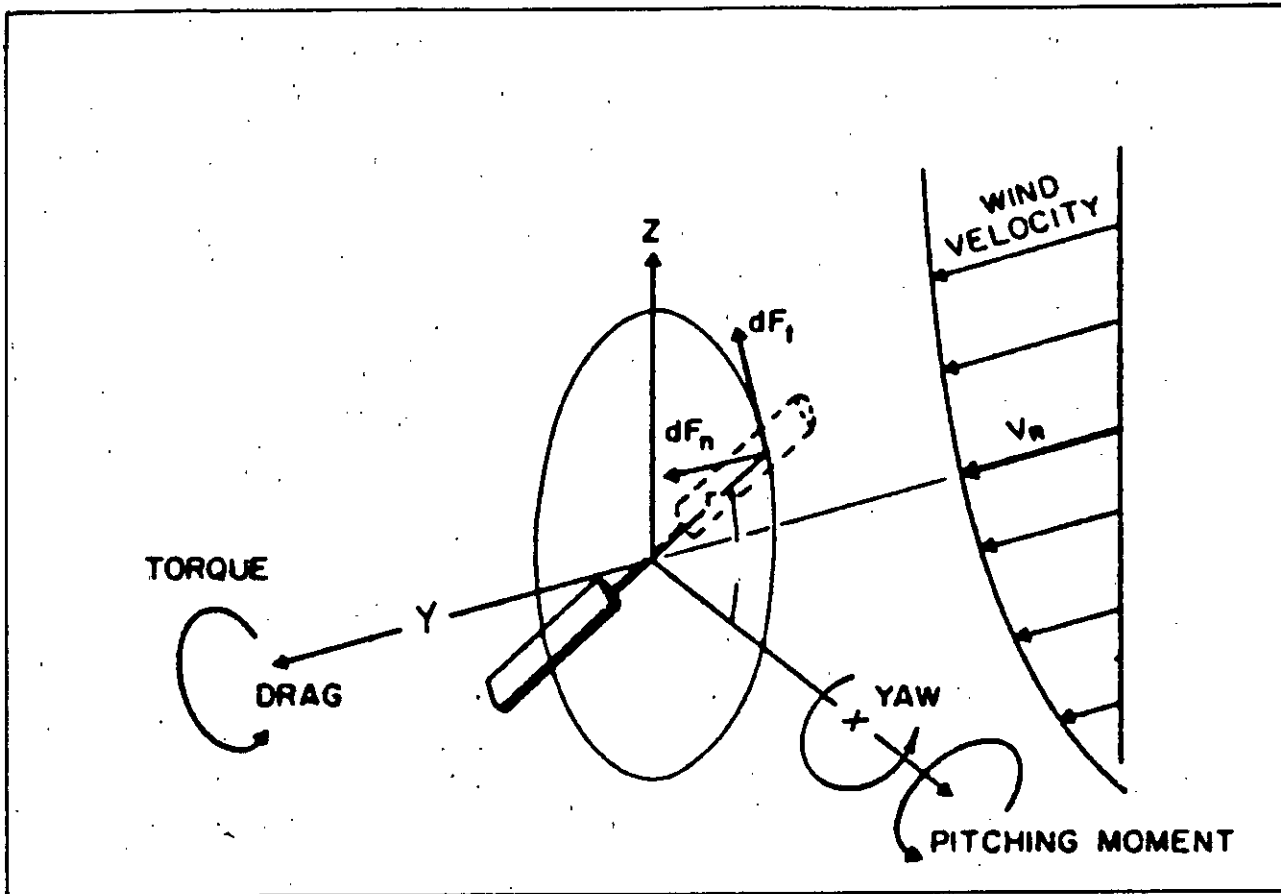
Fig. 4.4.1 .: Effect of Wind Gradient on Rotor
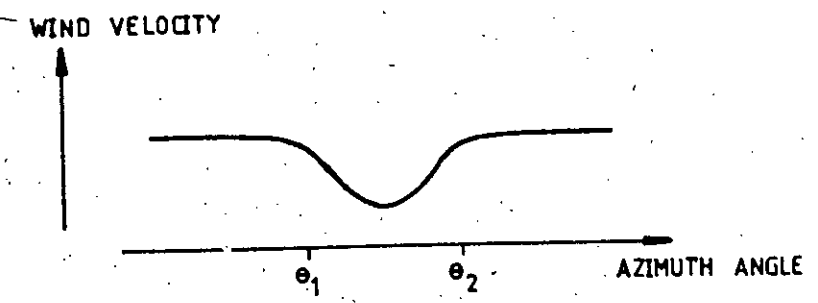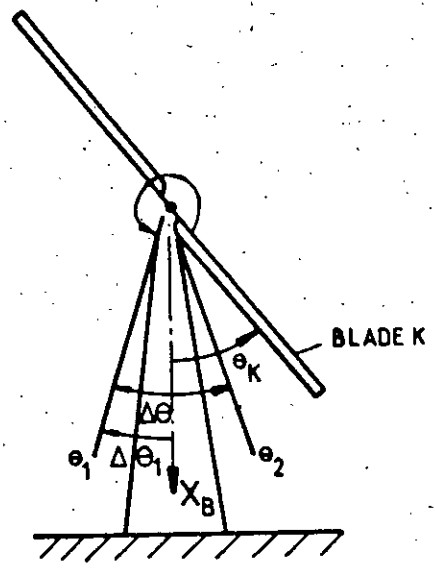
Fig. 4.4.2: Influence of Tower Shadow on Wind Velocity (38)
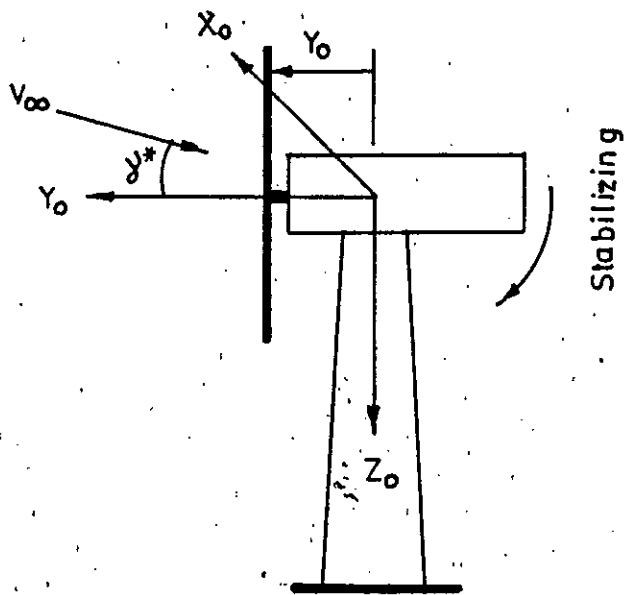
Fig. 4.4.3(a): Upwind Rotor without Coning or

Tilting (2)
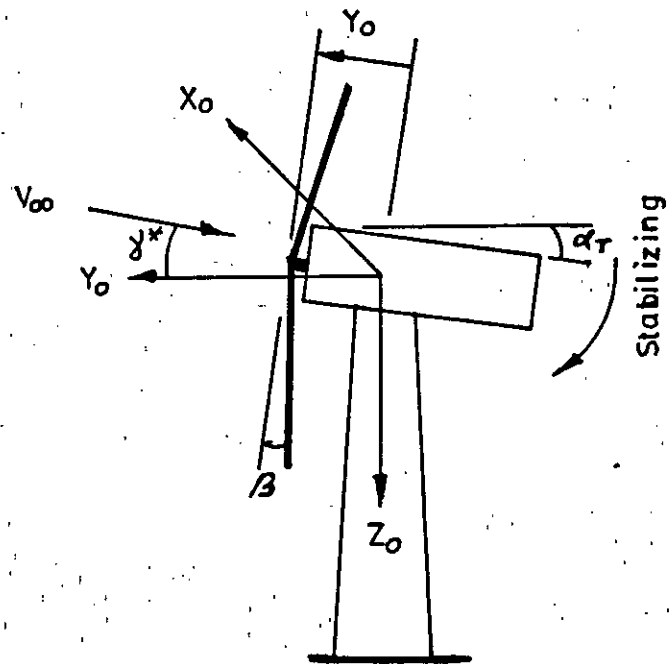
Fig. 4.4.3(b): Upwind Rotor with Coning

& Tilting (2)
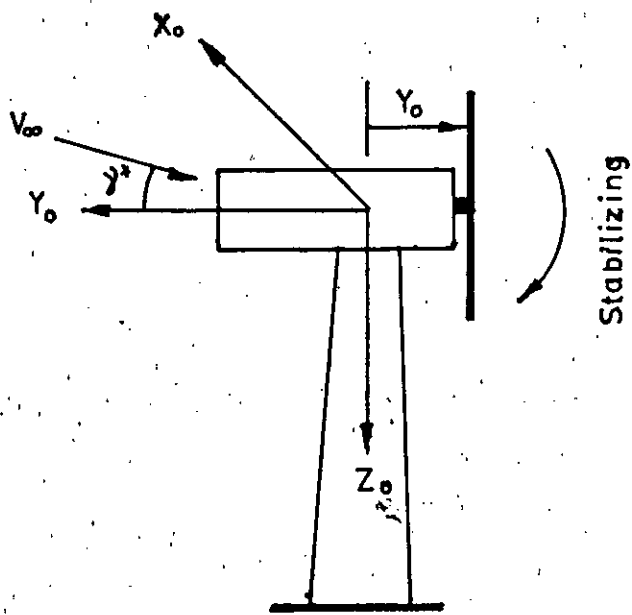
Fig. 4.4.4 (a): Downwind Rotor without
Coning (2)
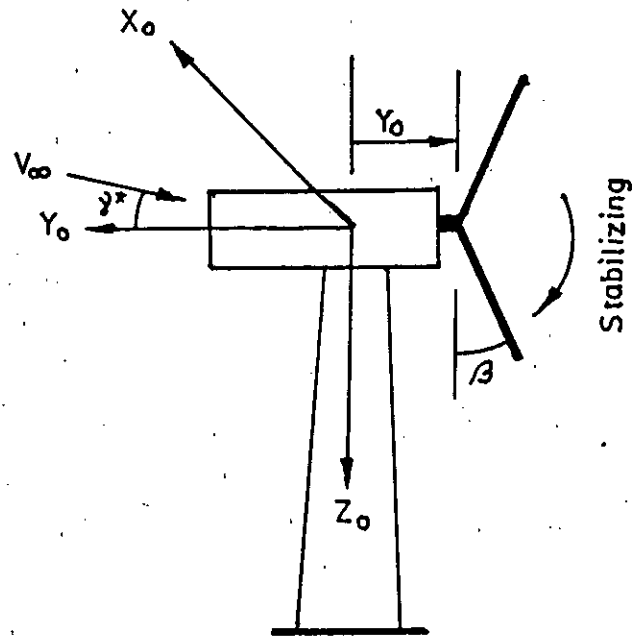
Fig. 4.4.4 (b): Downwind Rotor with
Coning Angle (2)
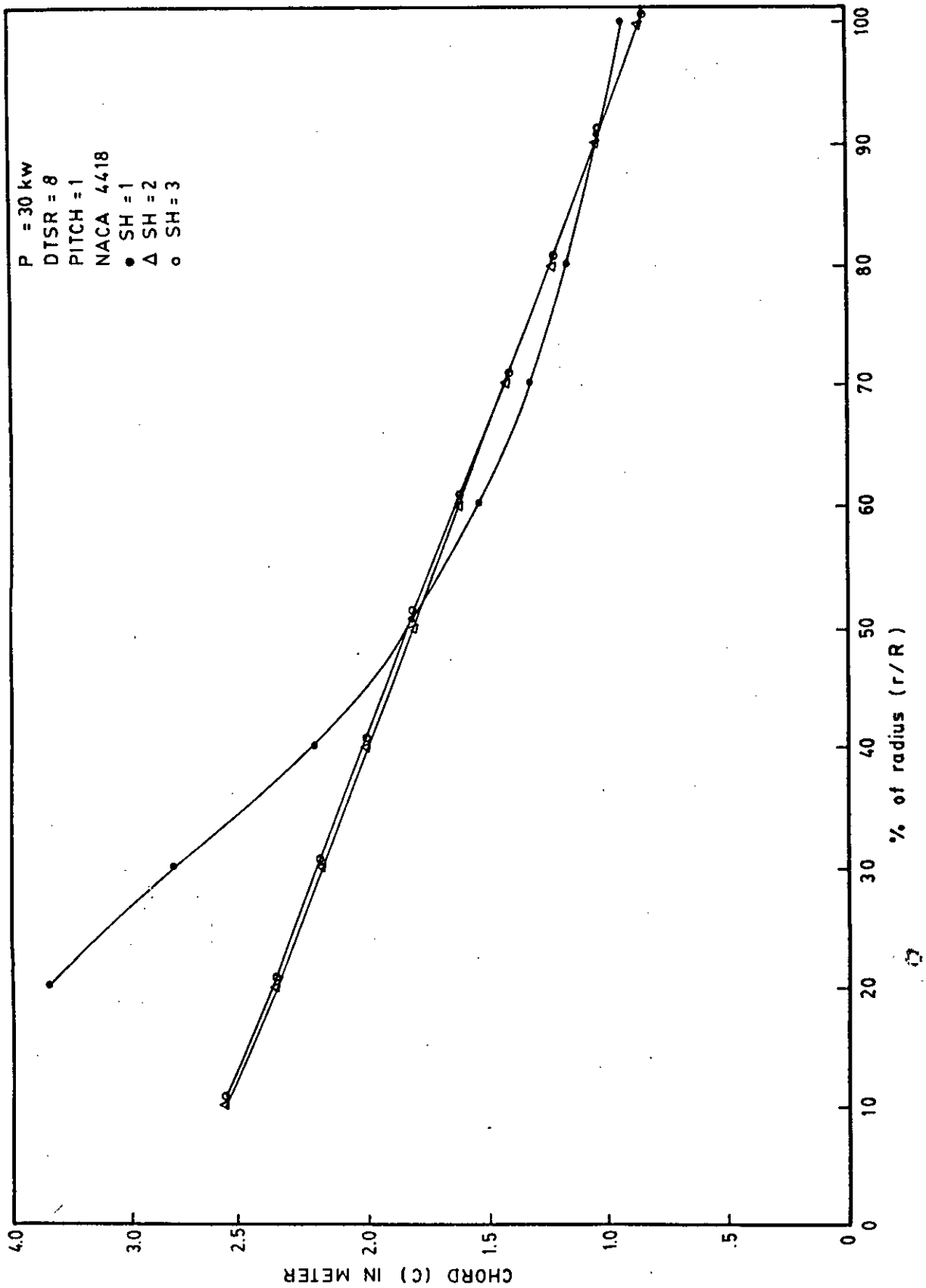
Fig.4.4.5.Optimum and linearized blade chord distribution
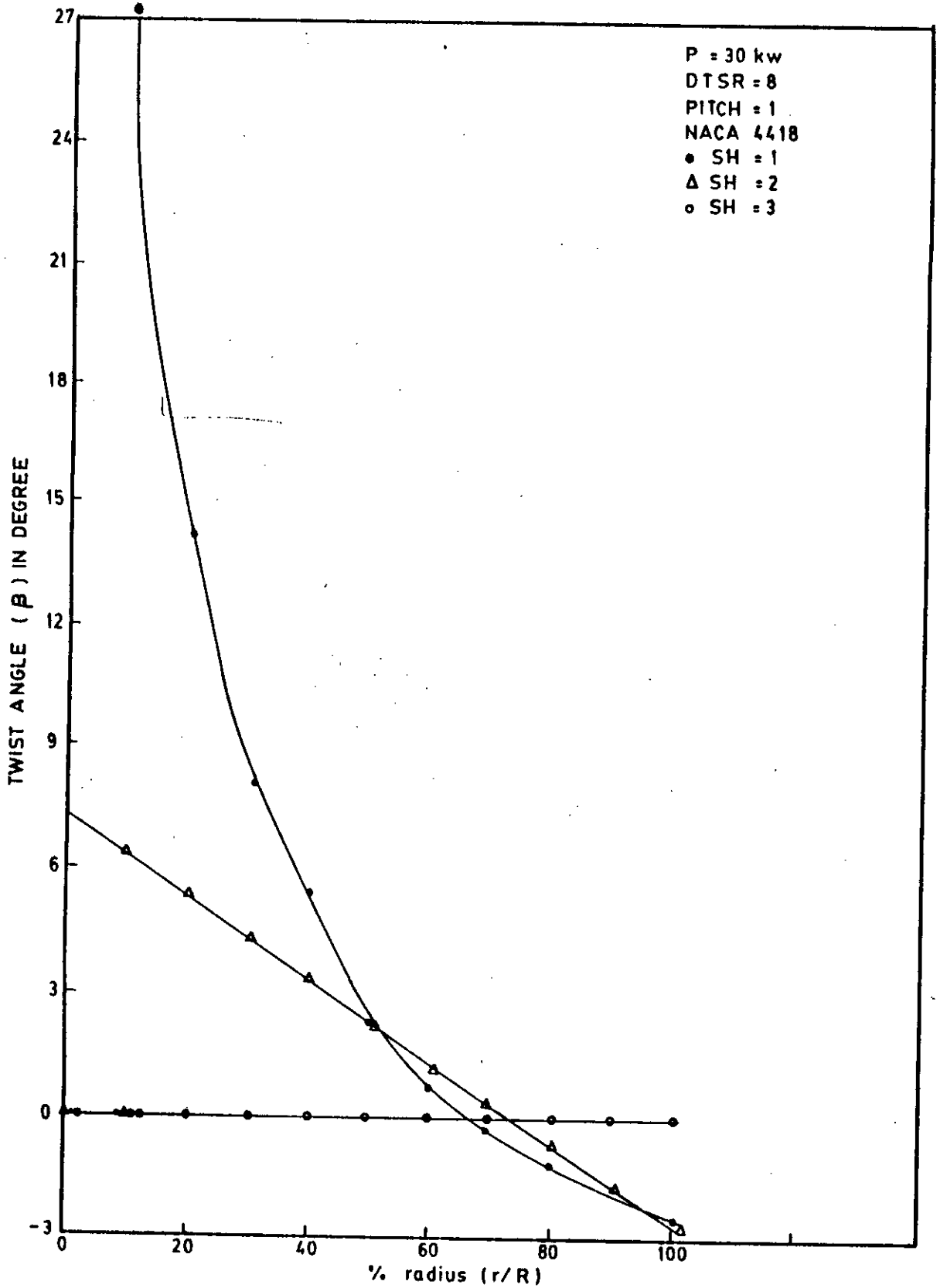
Fig4.4.6 Optimum and linearized blade twist distribution

o Optimum Chord Optimum Twist
△ Linear   „   Linear   „
x   „   „   Zero   „

NACA 4418
R = 23.2668 m
B = 2

PITCHING ANGLE (θp)

STARTING TORQUE CO-EFFICIENT (Cθst)
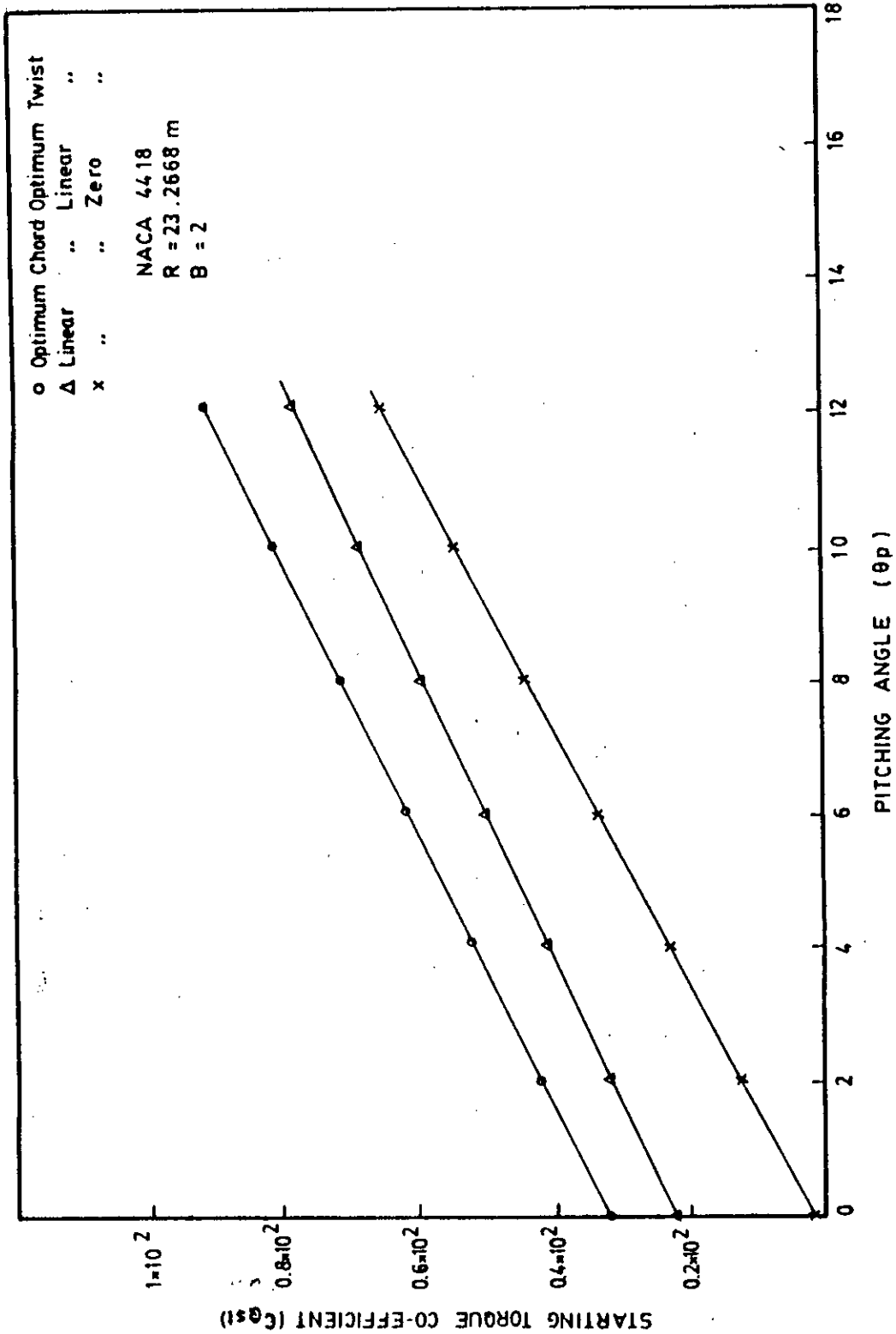
Fig.4.4.7 Comparison of starting torque co-efficient for different blade shapes wind turbine
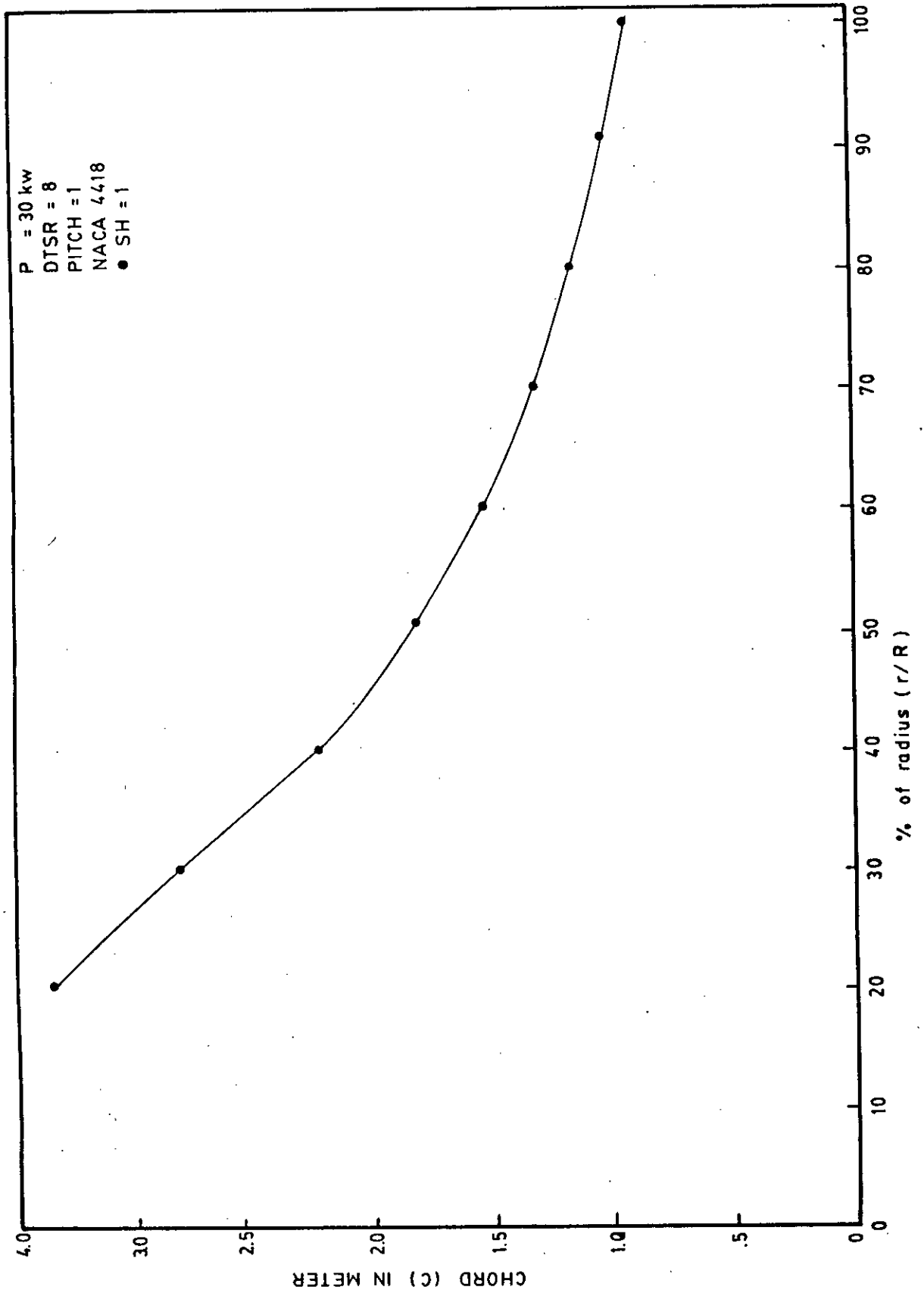
Fig. 4.8.1 Blade chord distribution for optimum performance
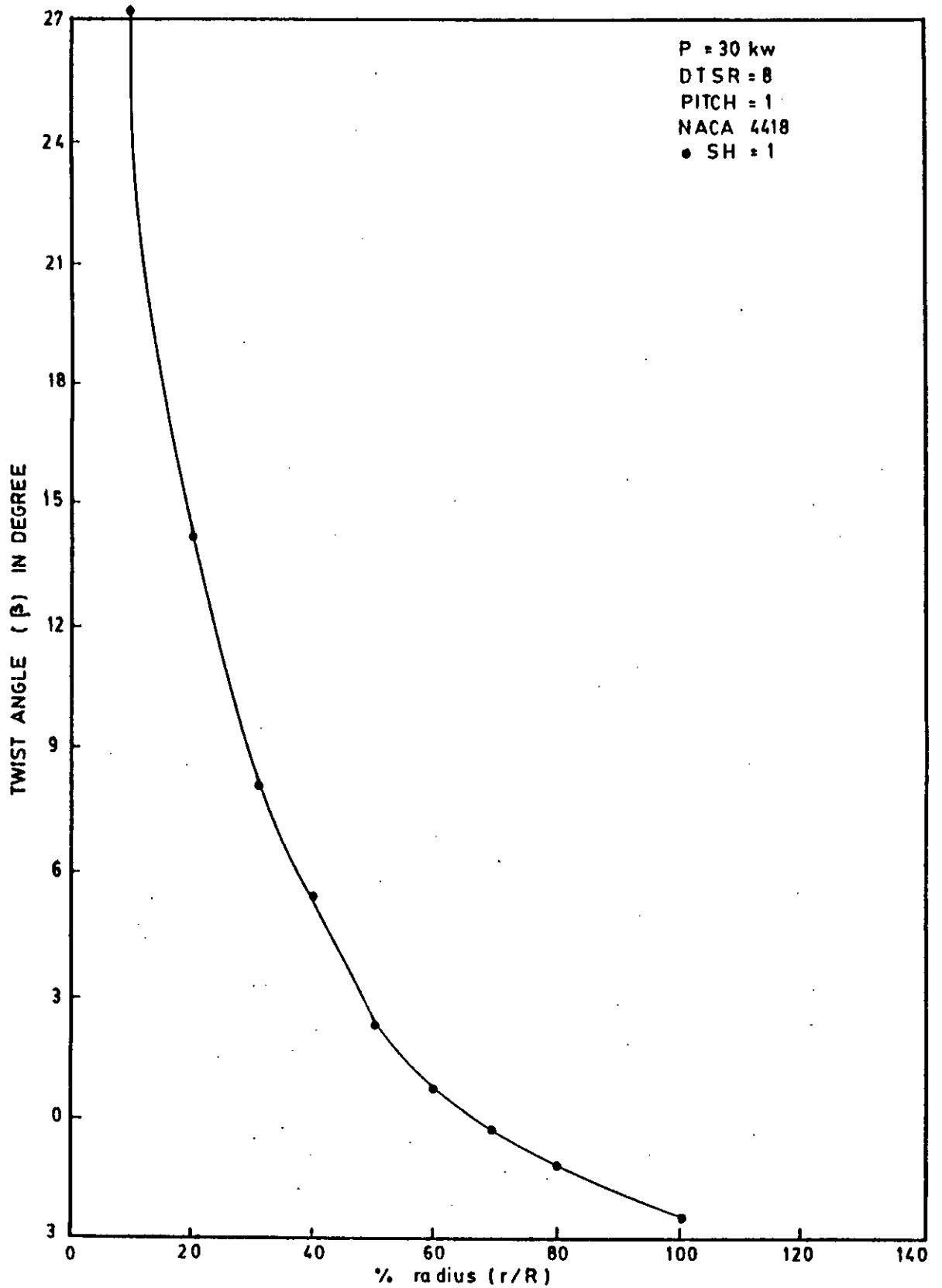
Fig.4.5.2 Blade twist distribution for optimum performance
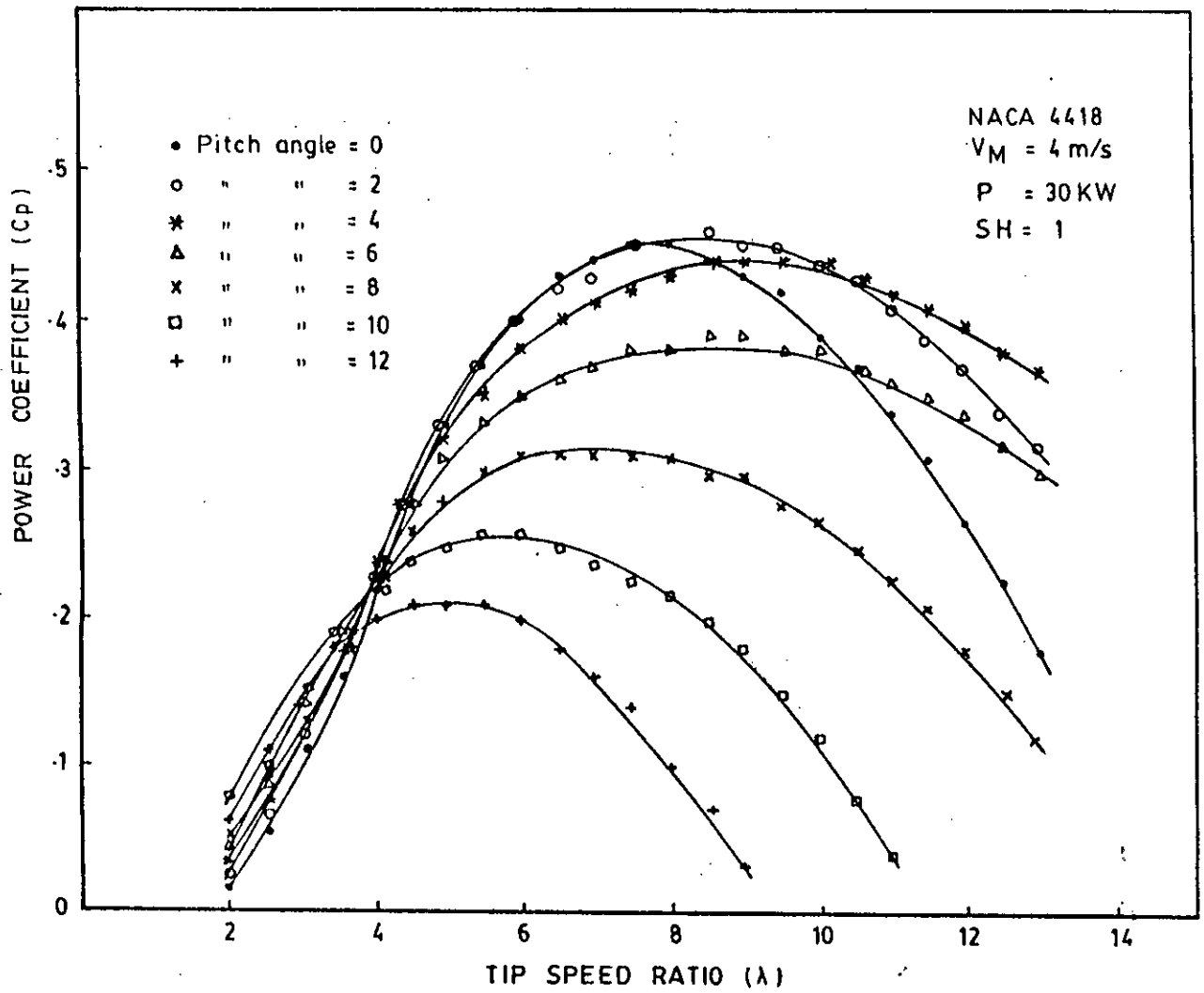
Fig. 5.1.1 Variation of power coefficient with tip speed ratio of ideal case.
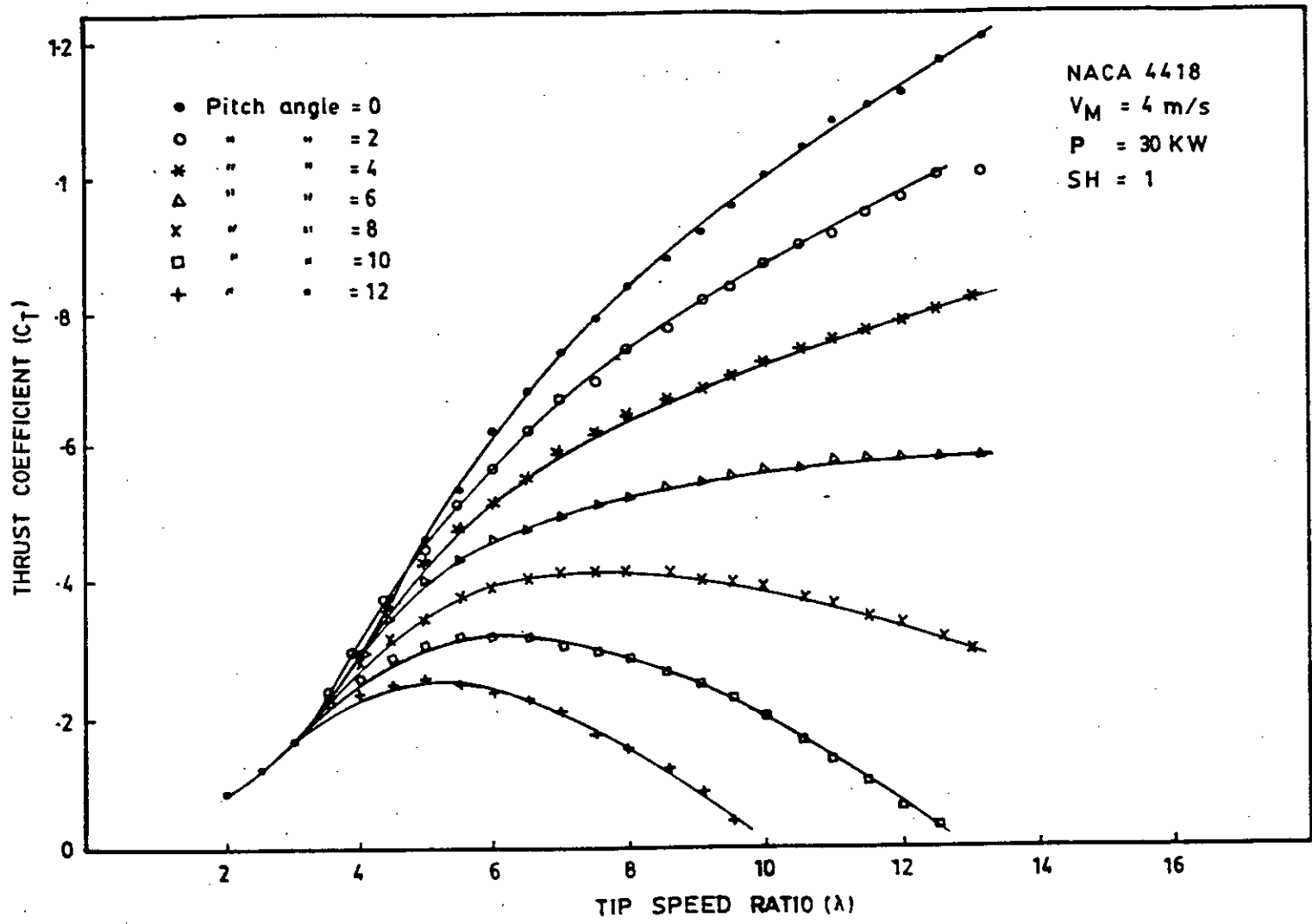
Fig.5.1.2 Effect of pitching on thrust co-efficient at ideal case
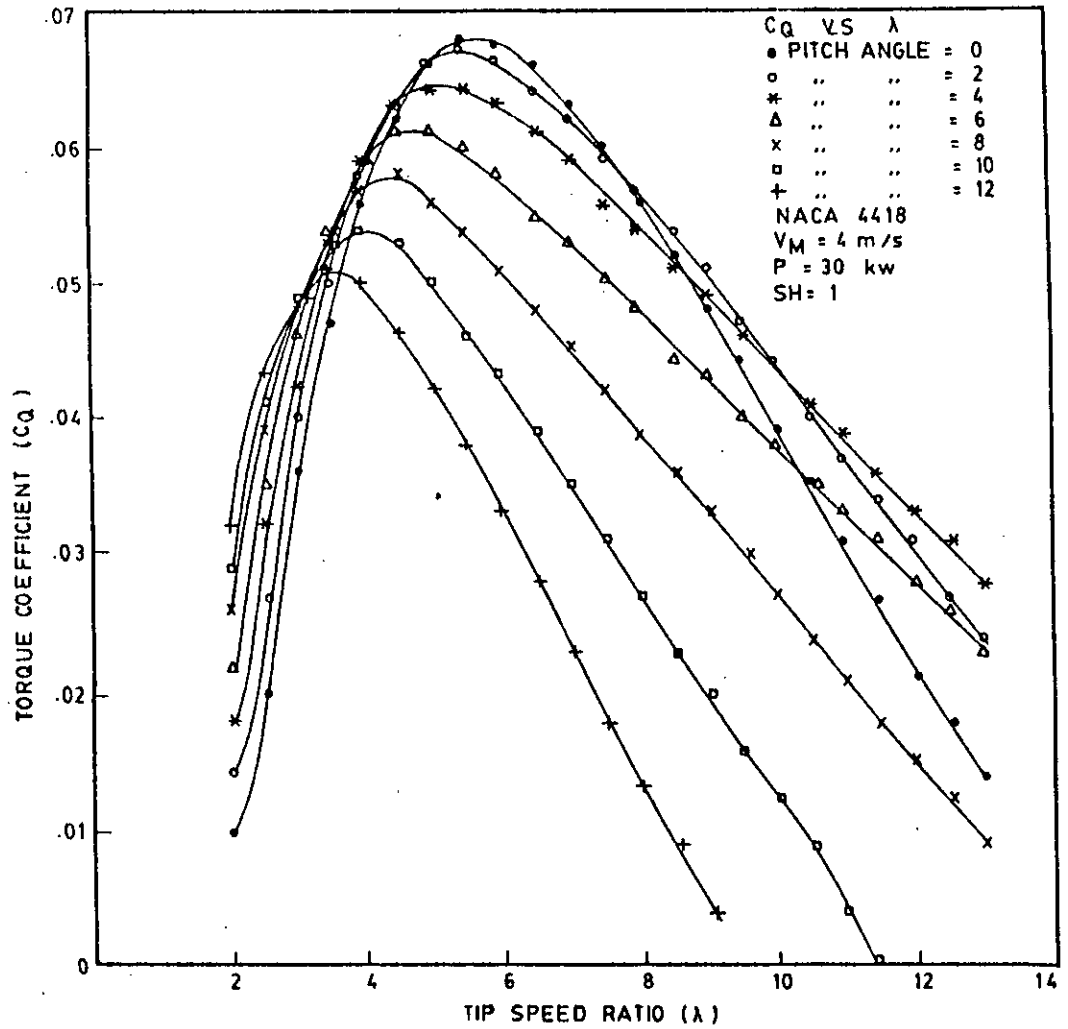
Fig. 5.1.3. Variation of Torque Co-efficient with tip speed ratio of ideal case
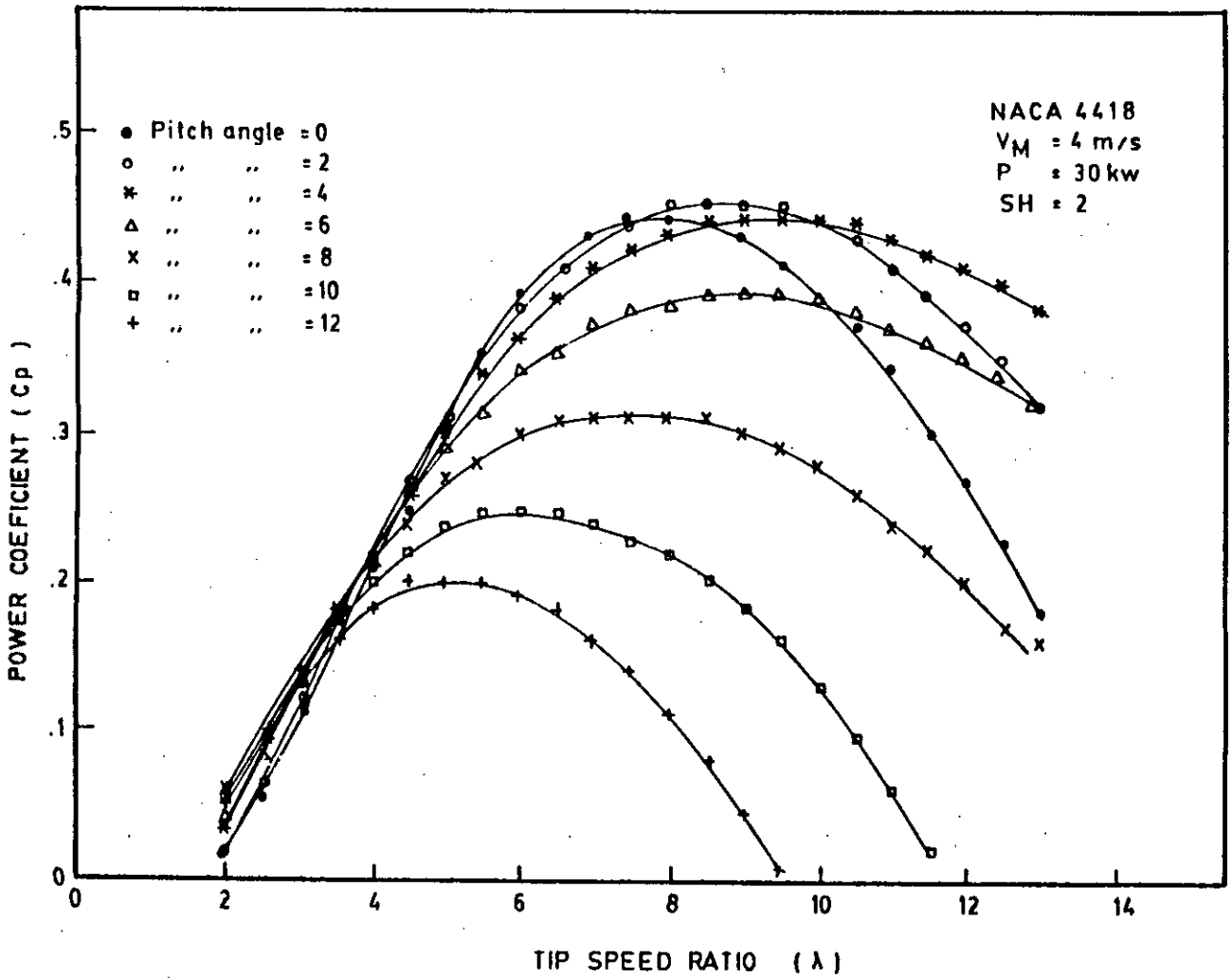
Fig. 5.1.4 Variation of power coefficient with tip speed ratio
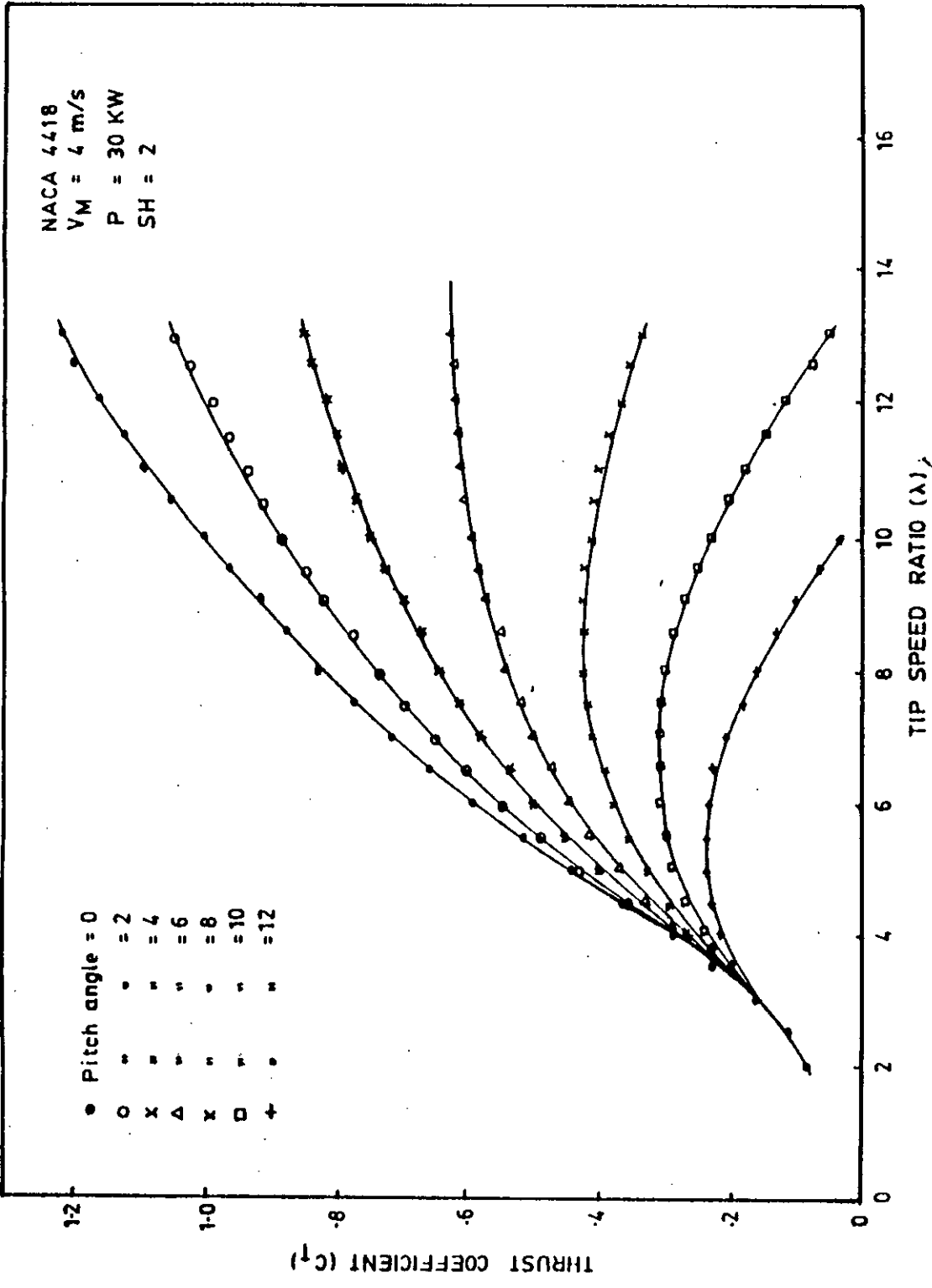
Fig.5.1.5 Effect of pitching on thrust coefficient
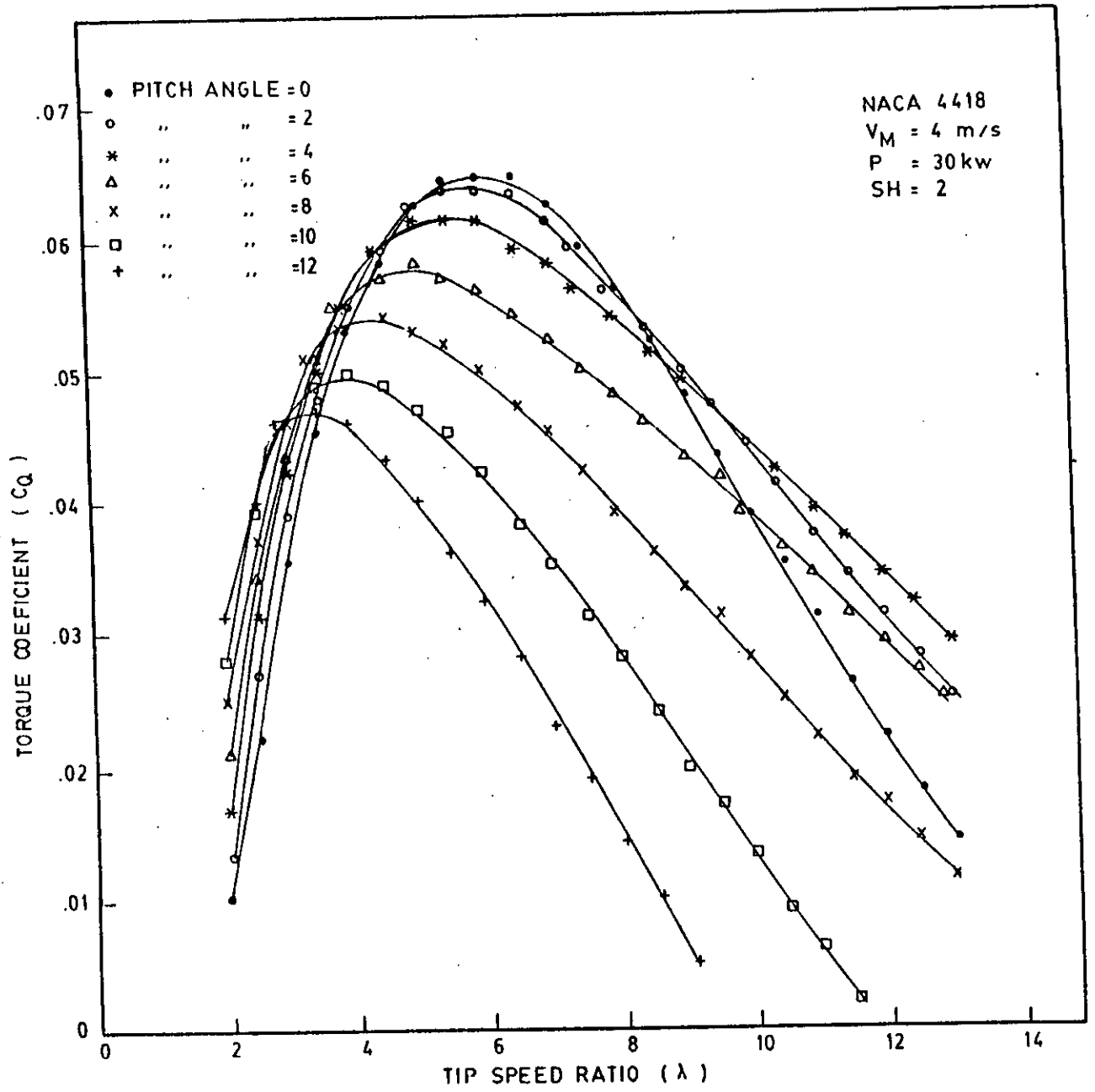
Figure.5.1.6. Variation of Torque Coefficient with tip speed ratio.
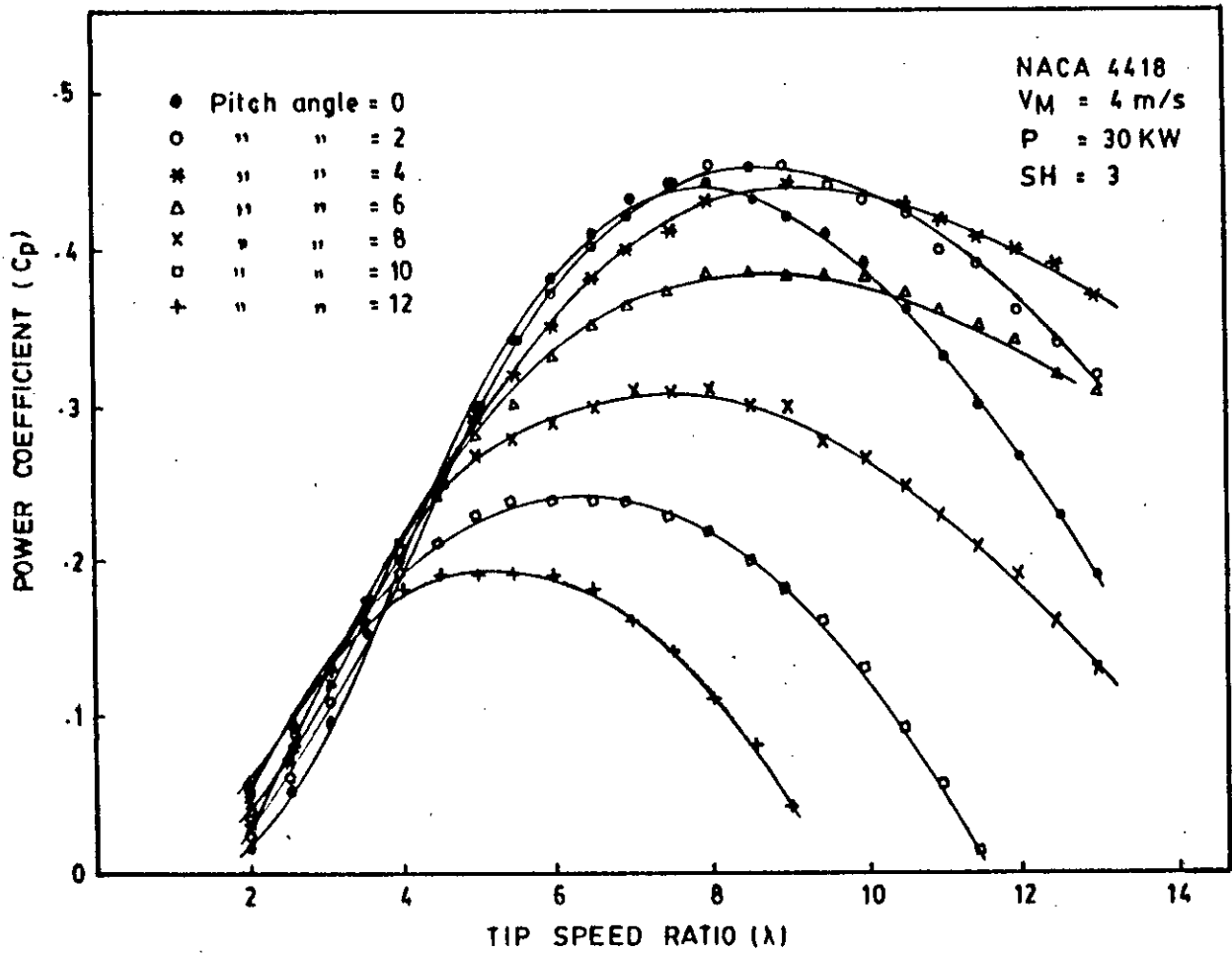
Fig.5.1.7 Variation of power coefficient with tip speed ratio
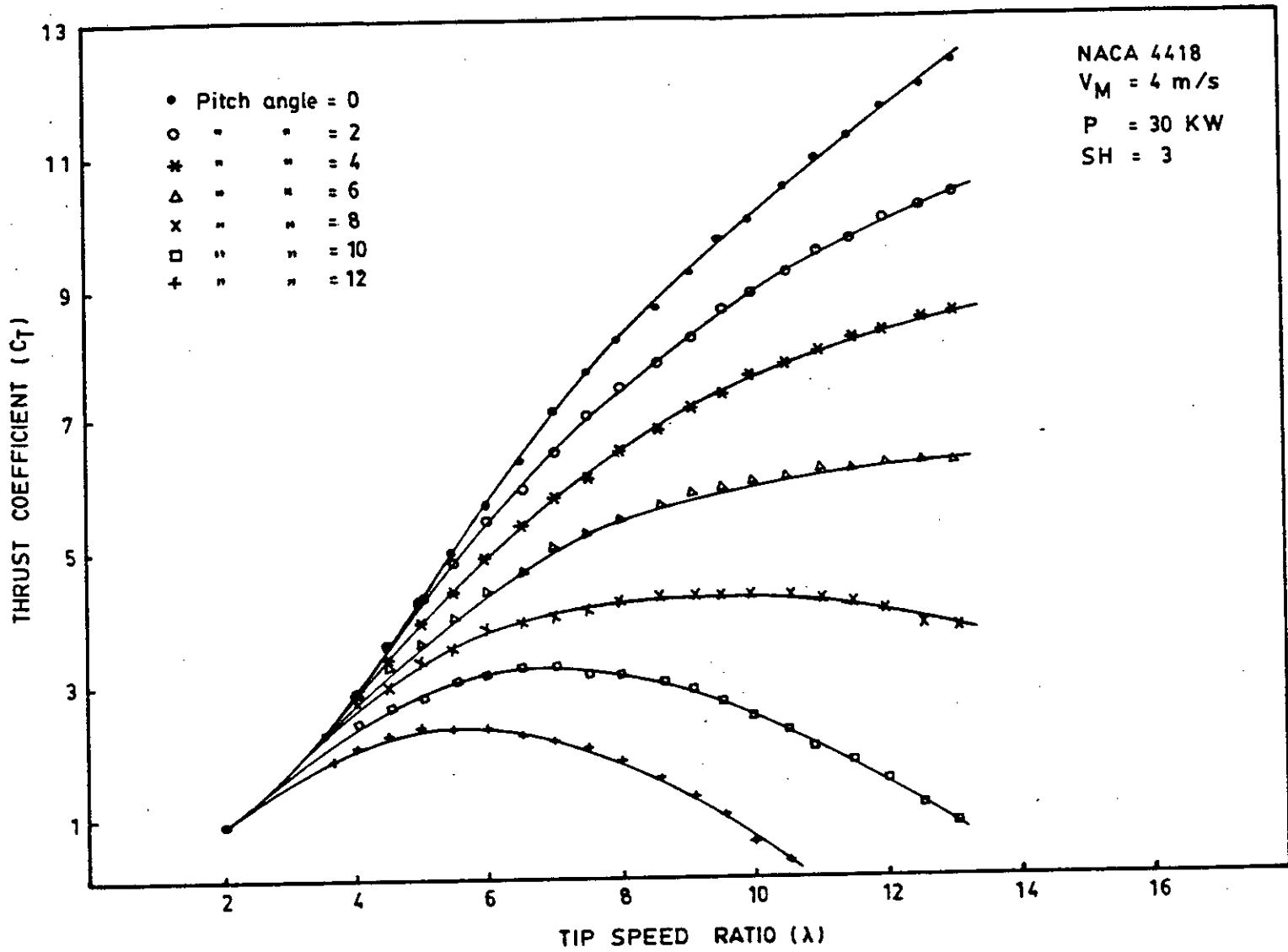
Fig. 5.1.8 Effect of pitching on thrust co-efficient
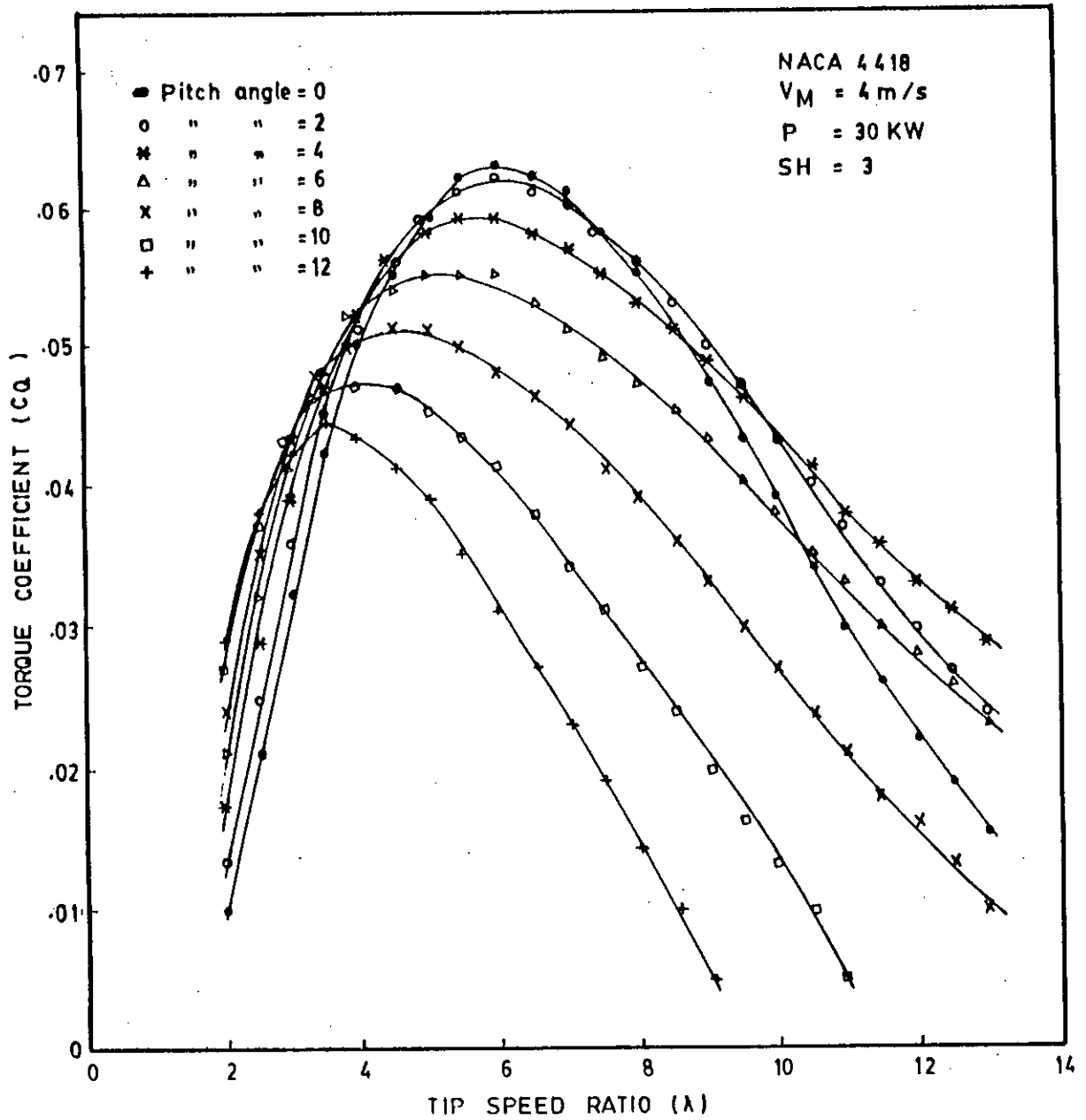
Fig.5.1.9 Variation of torque coefficient with tip speed ratio
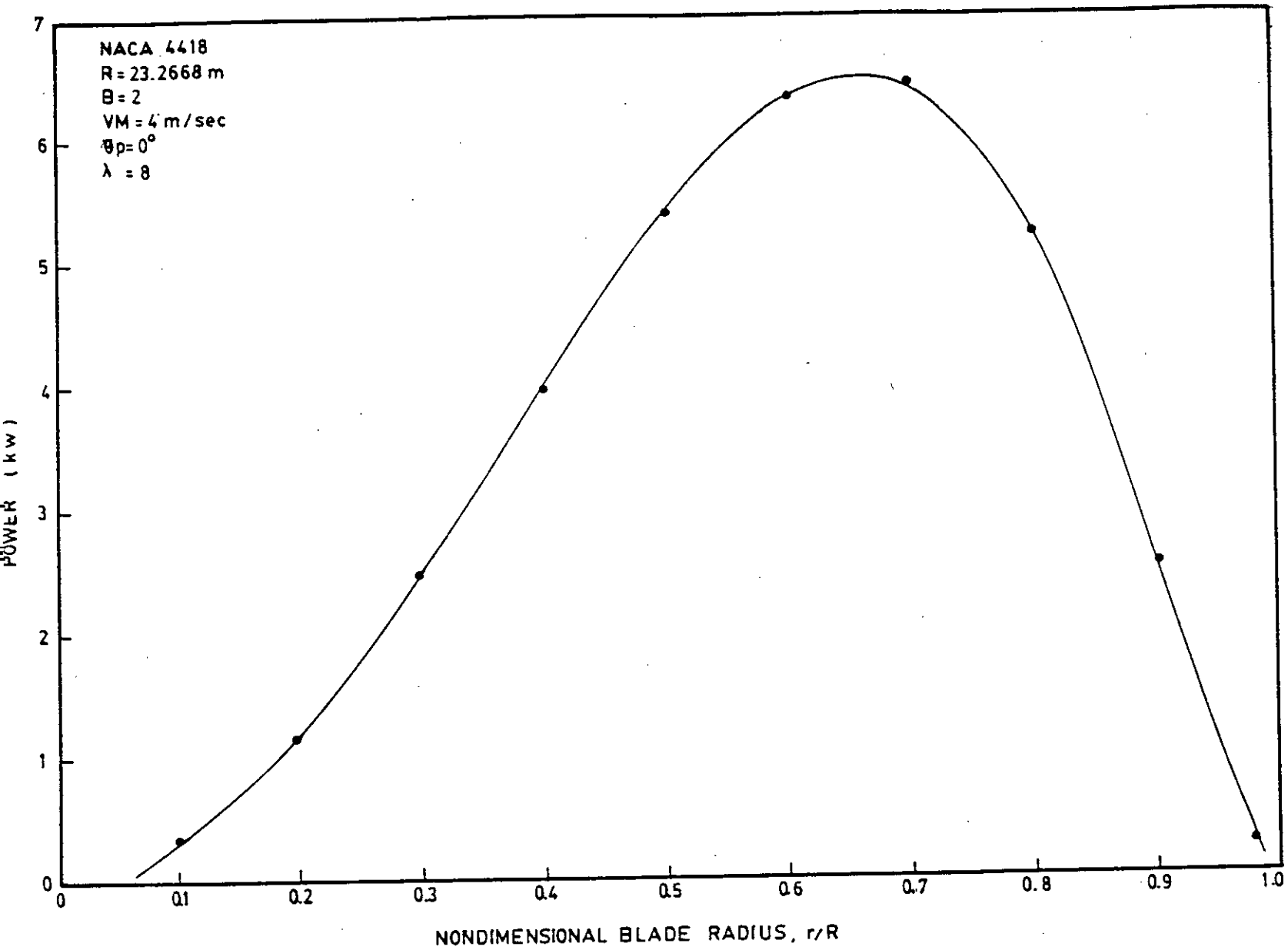
Fig.5.1.10 Radial variation of extracted power
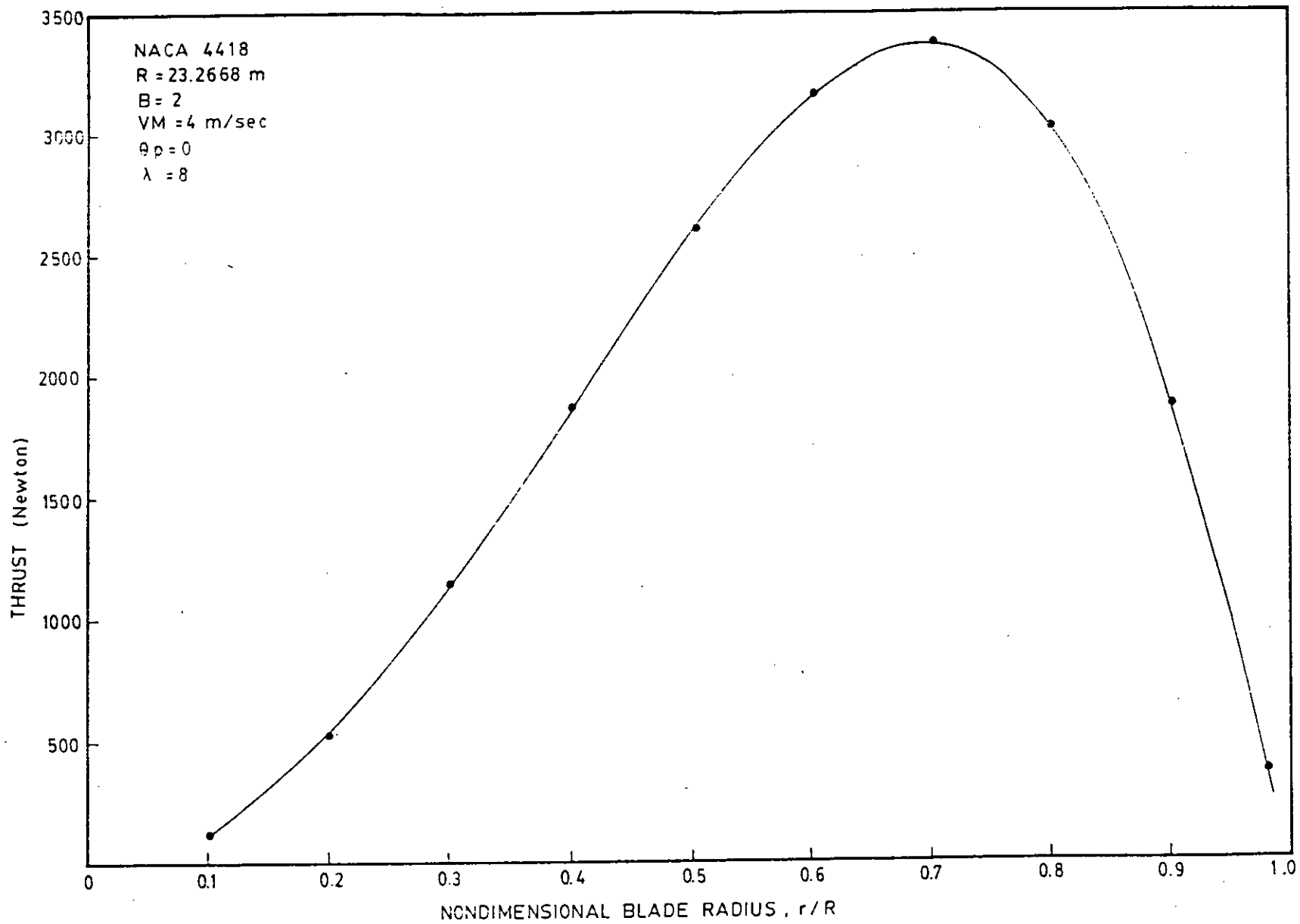
Fig. 5.1.11. Radial variation of thrust force.

NACA 4418
R = 23.2668 m
B = 2
VM = 4 m/sec.
θp = 0
λ = 8
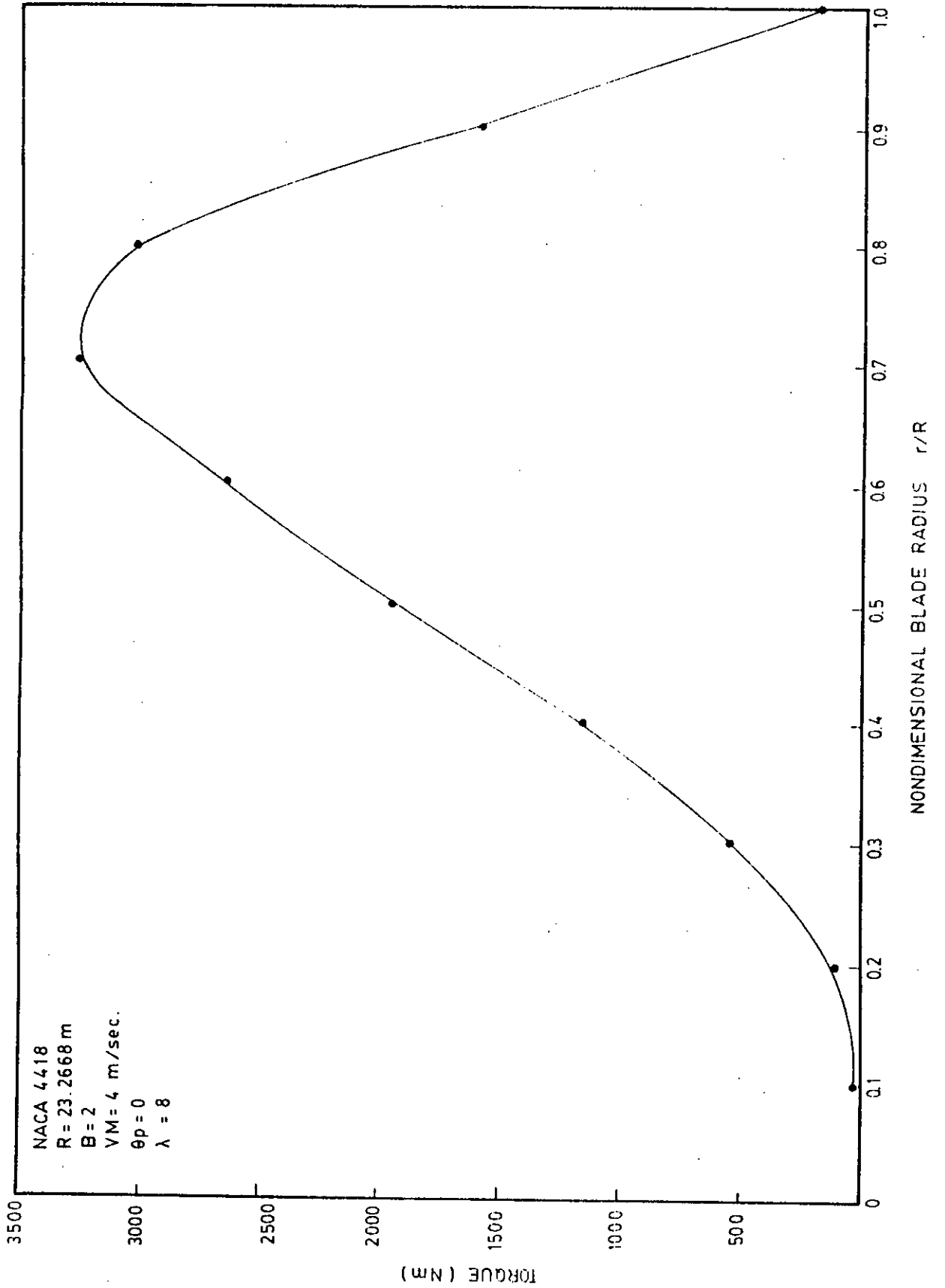
Fig. 5.1.12 Radial variation of torque.
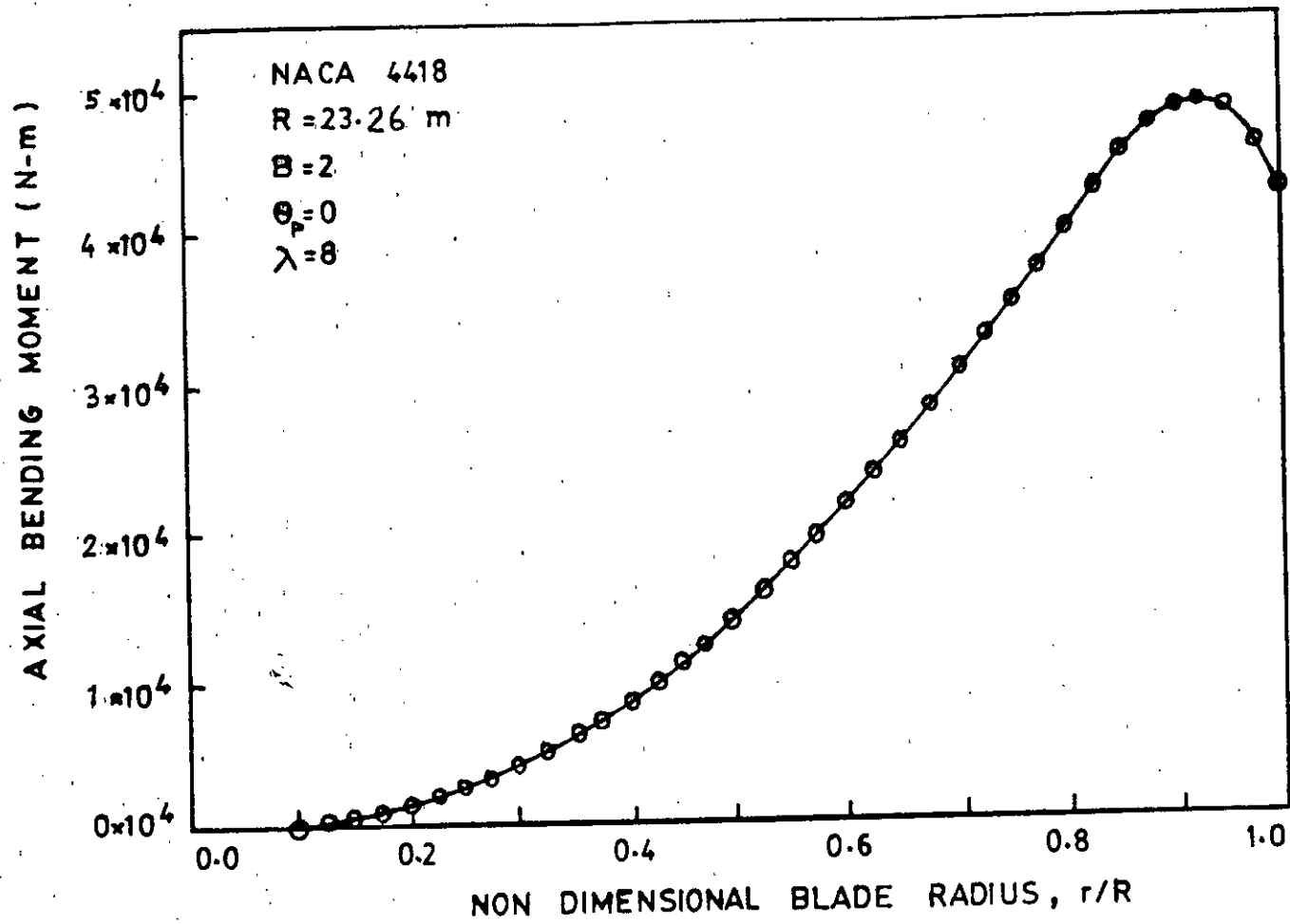
FIG. 5.1.13 : Radial Variation of Axial Bending Moment
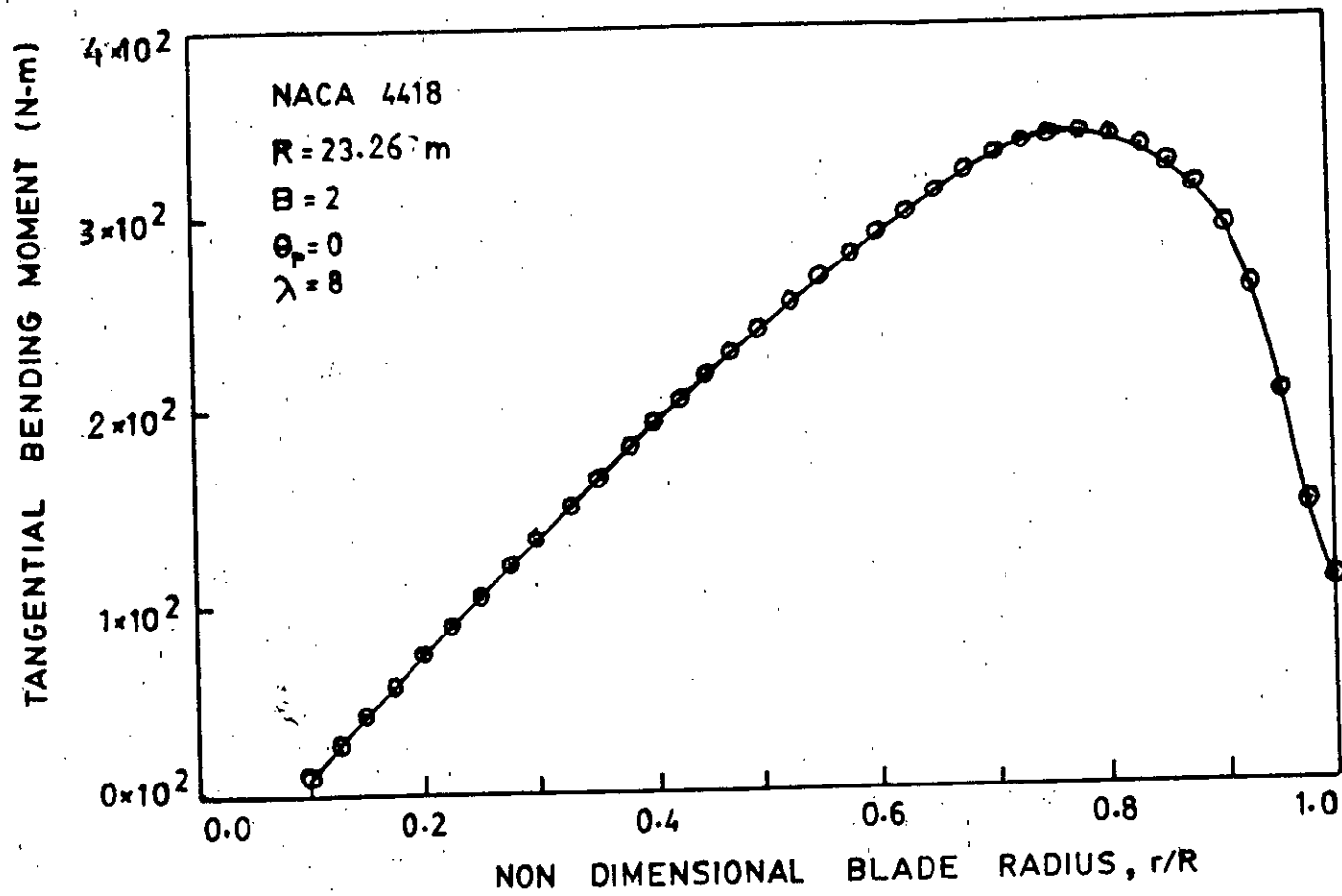
FIG. 5.1.14 : Radial Variation of Tangential Bending Moment
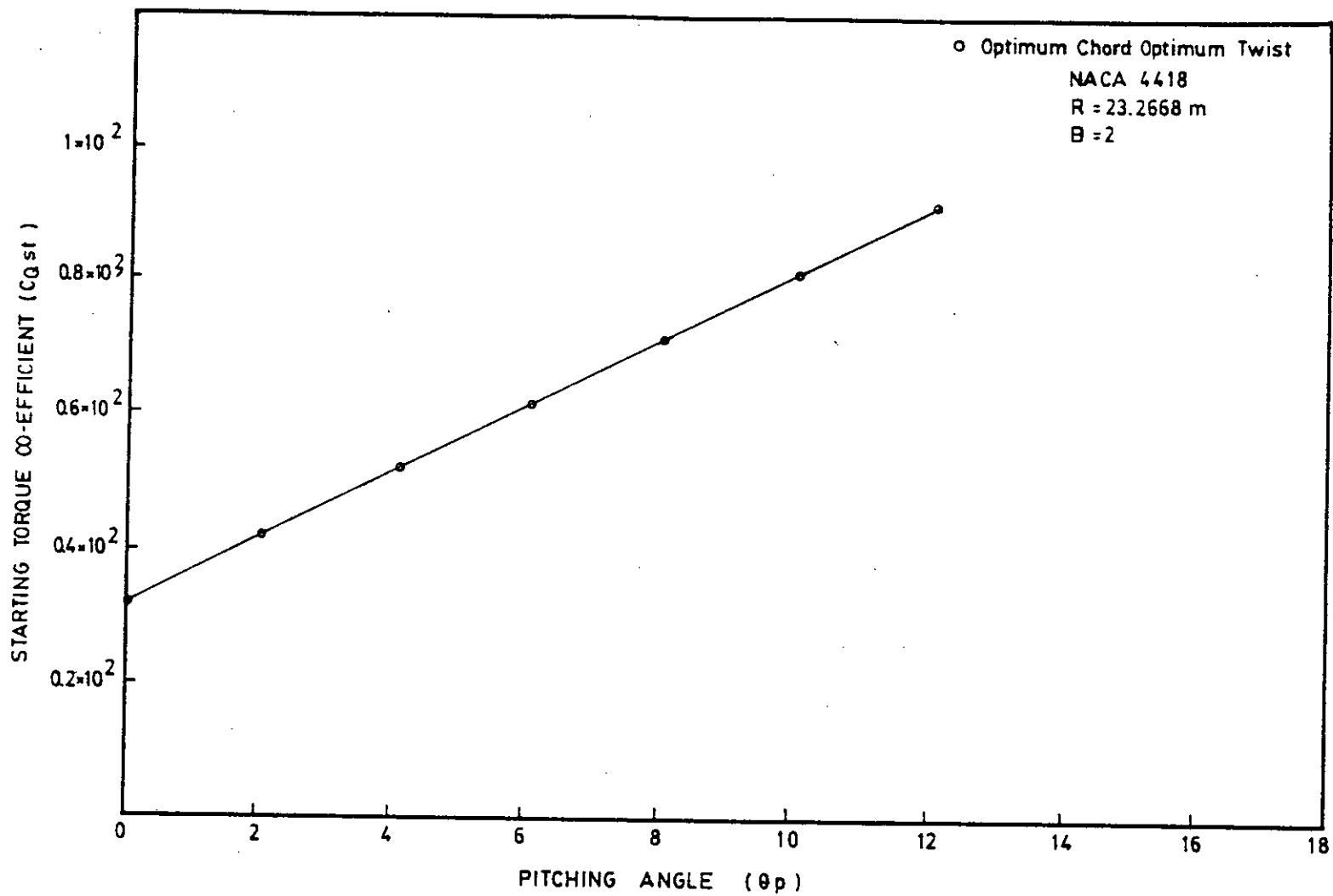
Fig. 5.1.15 Starting torque co-efficient as a function of pitch angle
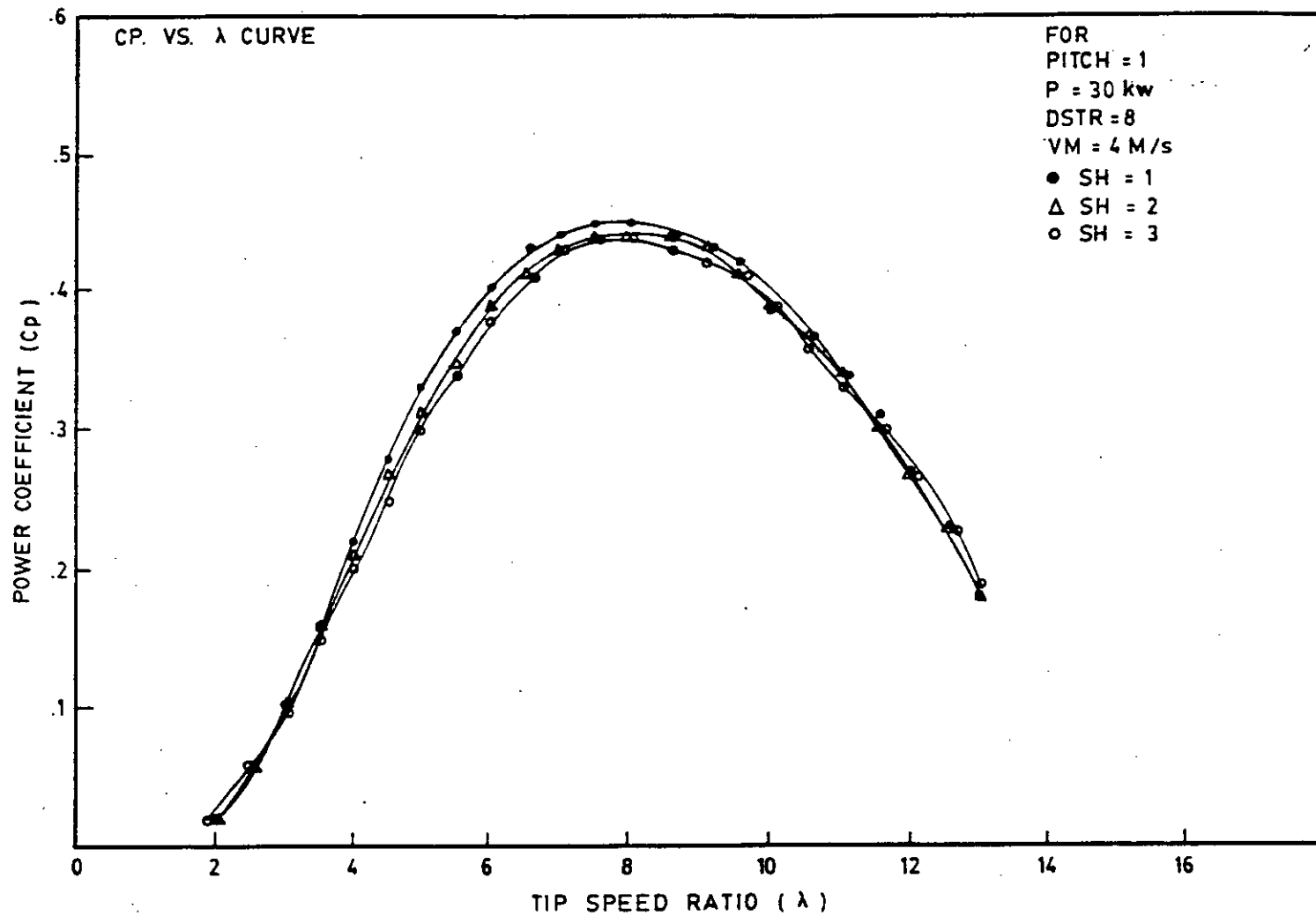
Fig.5.1.16 Variation of power co-efficient with tip speed ratio for optimum & linearized blade
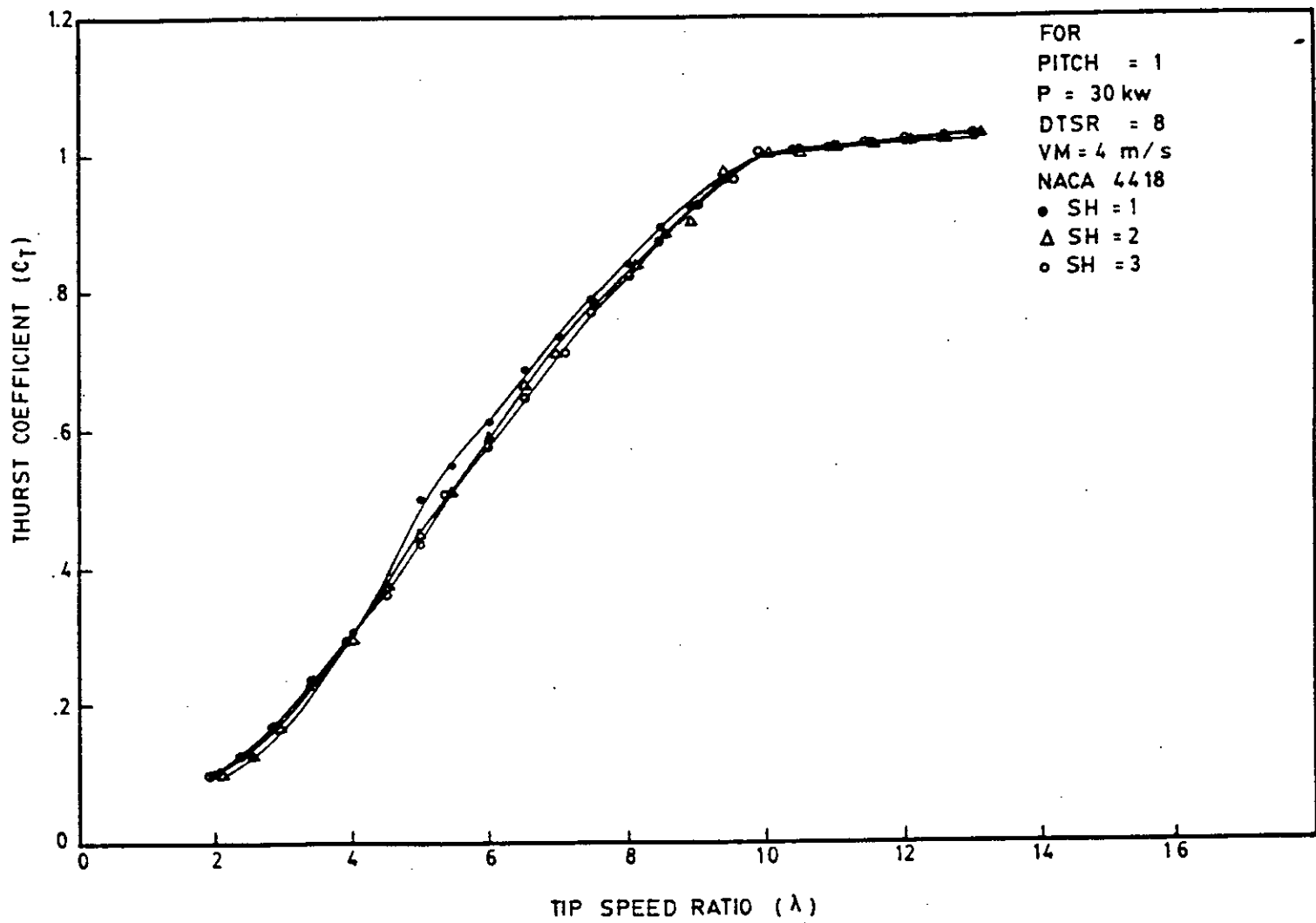
Fig.5.1.17 Variation of thrust co-efficient with tip speed ratio for optimum & linearized blade

FOR
PITCH = 1
P = 30 kw
DTSR = 8
VM = 4 m/s
NACA 4418
● SH = 1
△ SH = 2
○ SH = 3

(154)
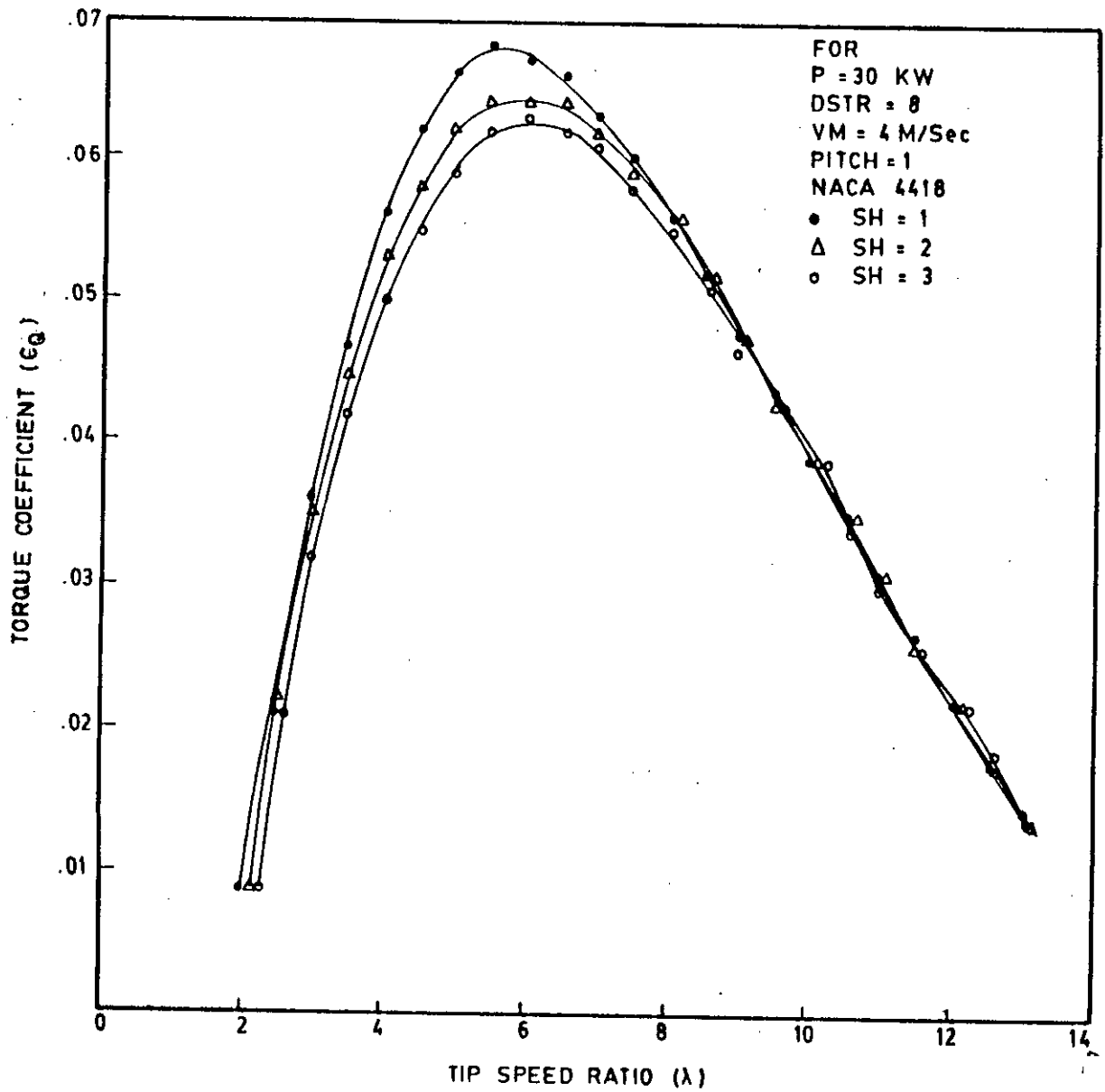
Fig.5.1.18 Variation of torque co-efficient with tip speed ratio for optimum & linearzed blade
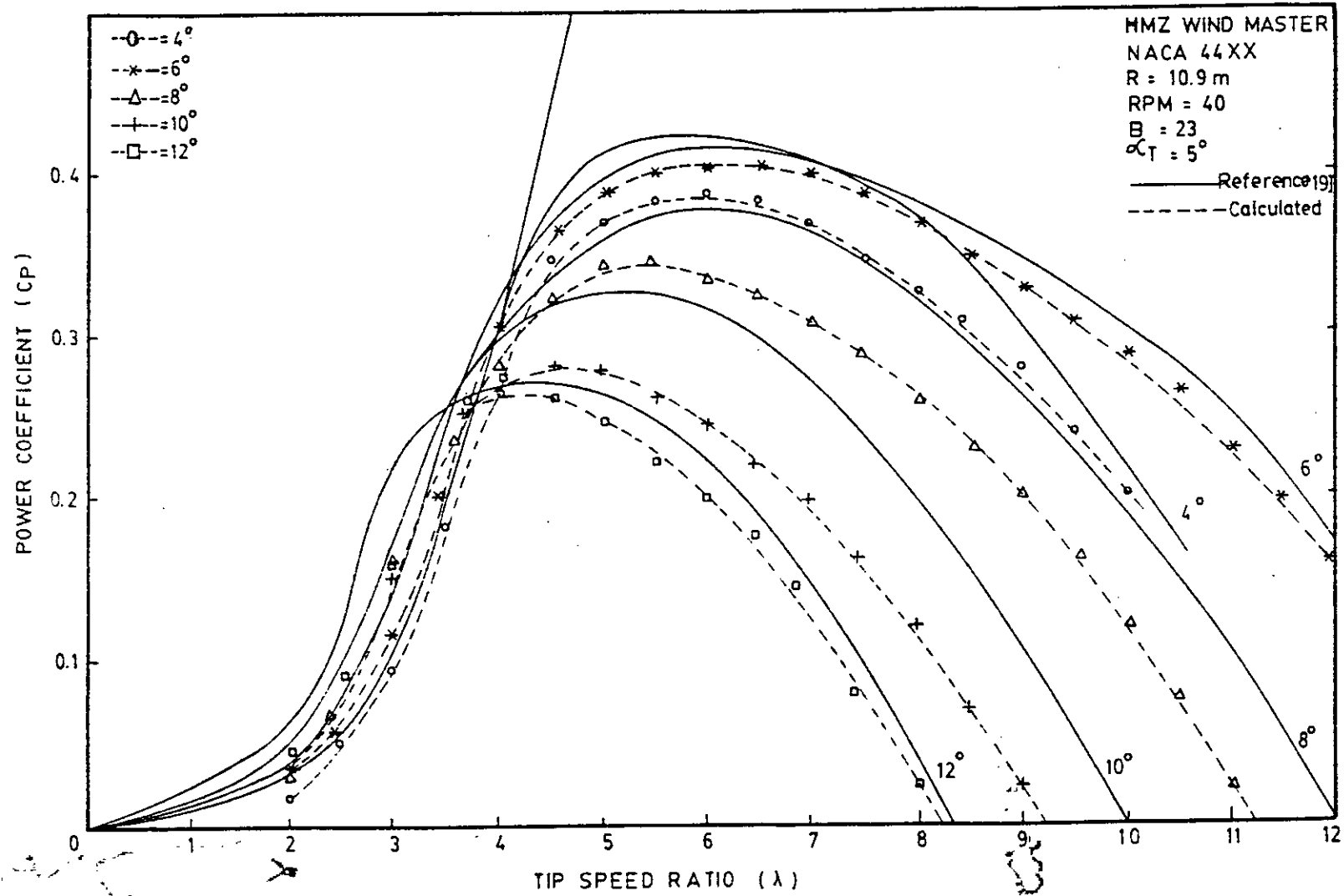
Figure 5.2.1. Calculated power coefficient of HMZ windmaster wind turbine
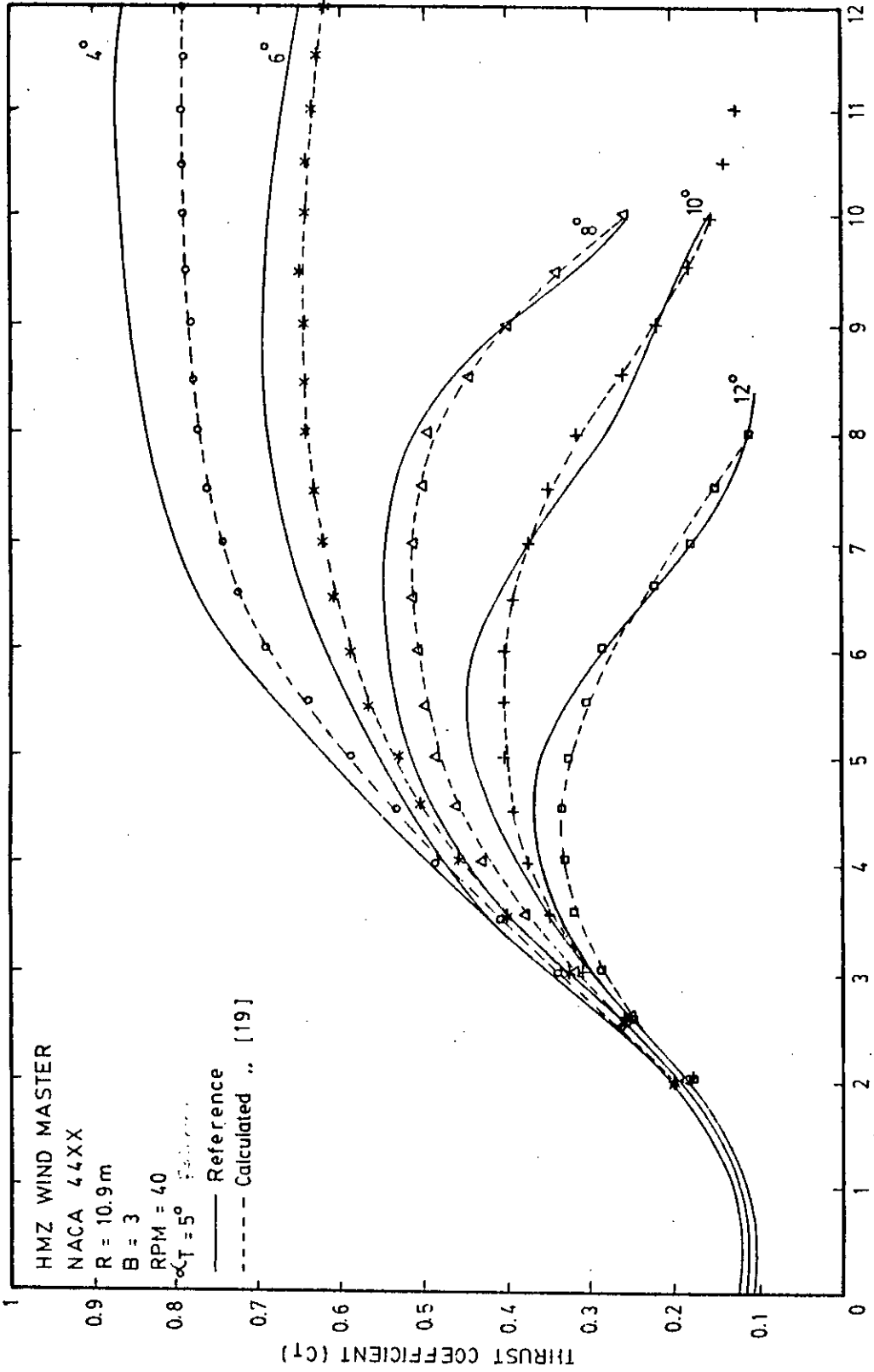
Figure 5.2.2. Predicted thrust coefficient of HMZ windmaster wind turbine

HMZ WIND MASTER
NACA 44XX
R = 10.9 m
B = 3
RPM = 40
$\alpha_T = 5°$

——— Reference
----- Calculated ,, [19]

TIP SPEED RATIO (λ)

THRUST COEFFICIENT (c_t)
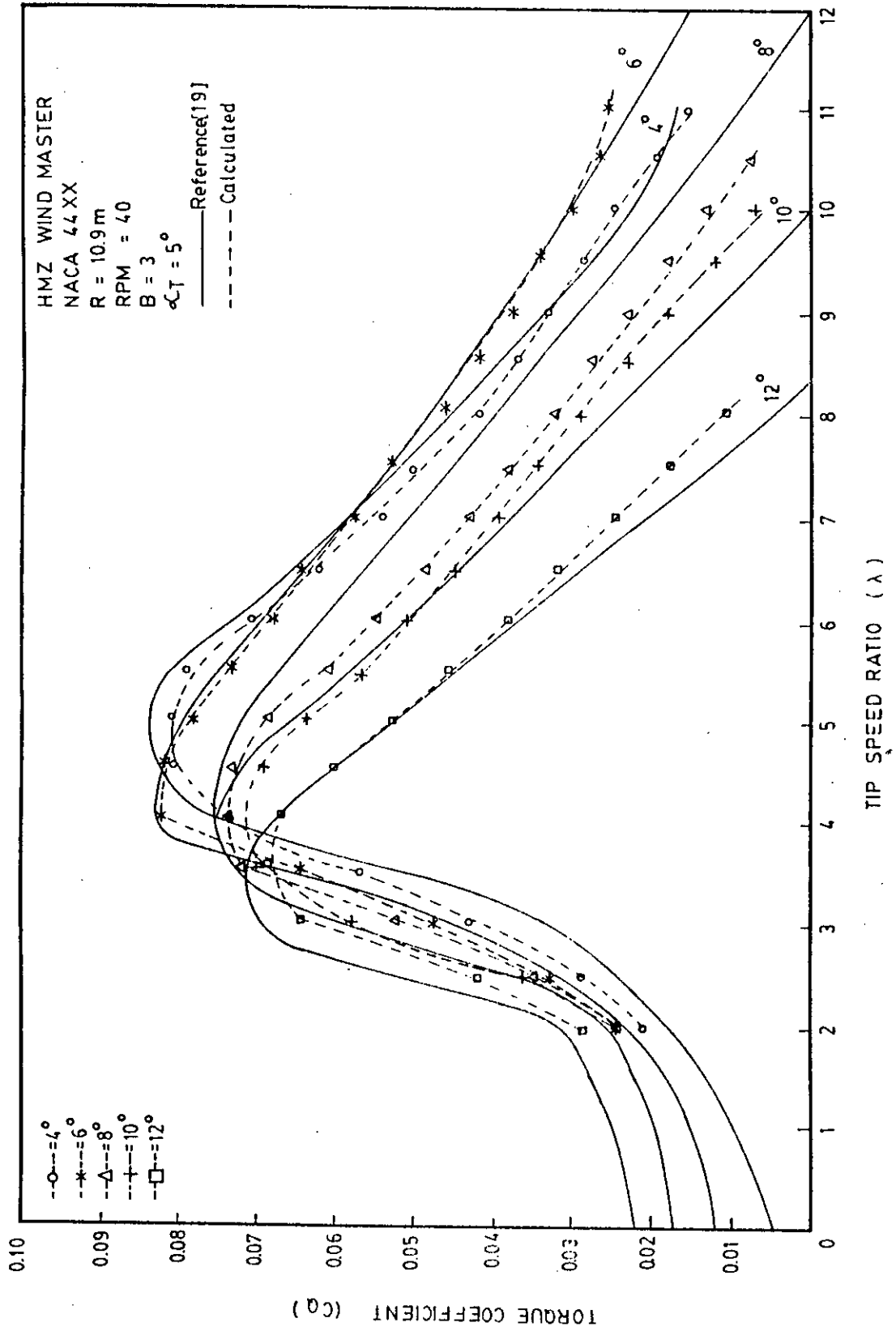
Figure 5.2.3 Predicted torque coefficient of HMZ windmaster wind turbine
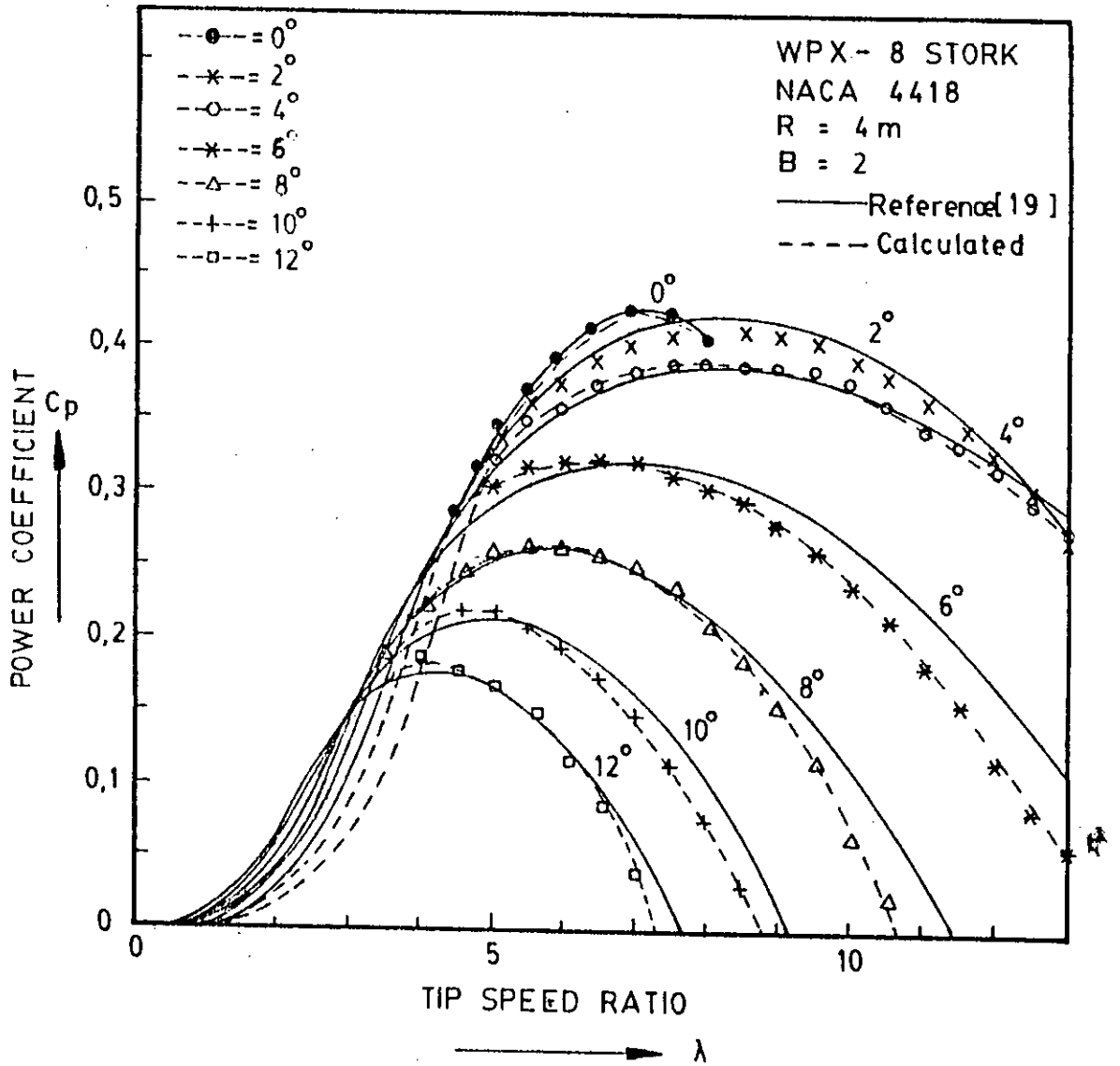
Figure 5.2.4: Comparison of calculated power coefficients at WPX- 8 stork wind turbine for 2 blade configuration
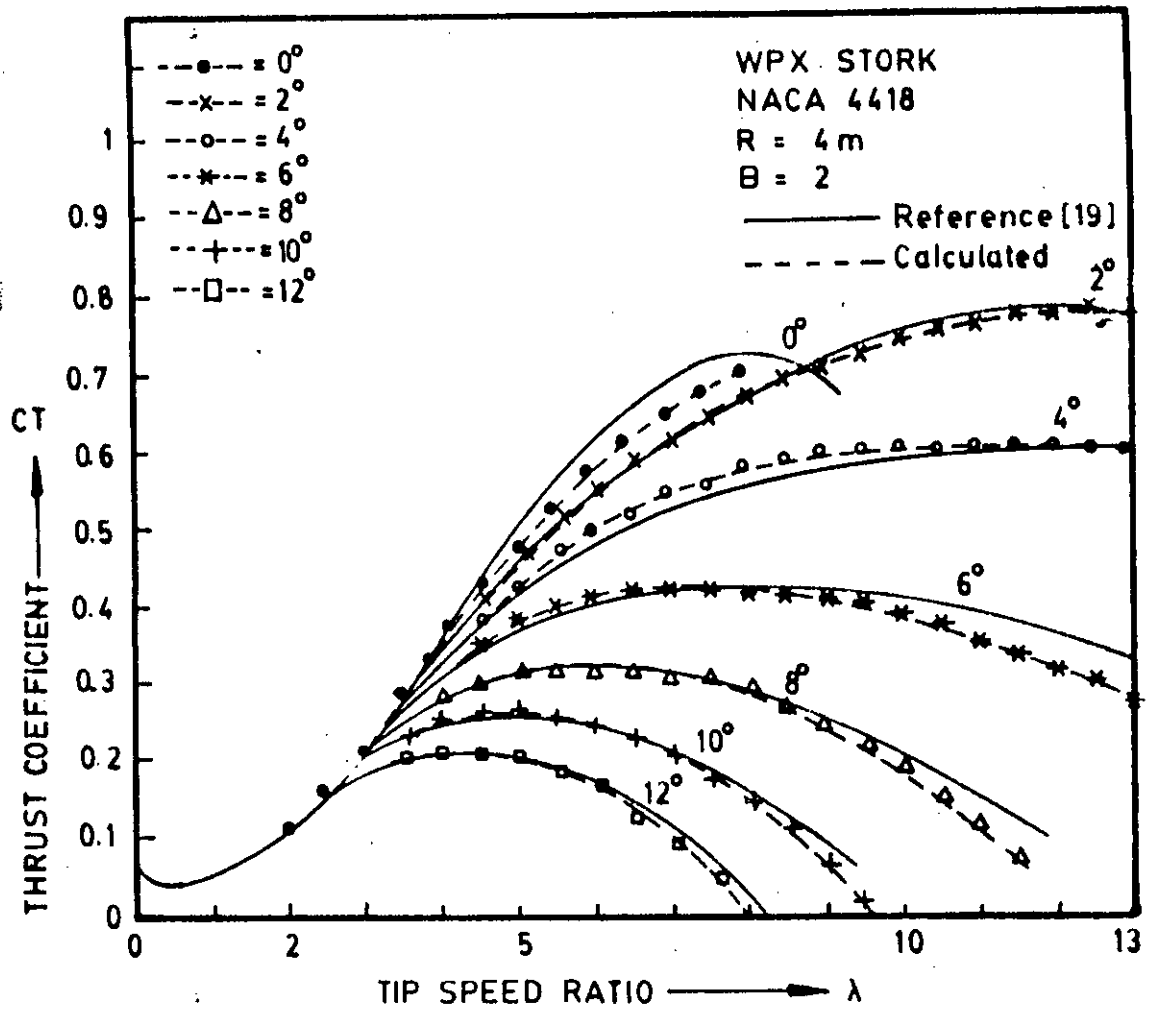
Figure 5.2.5. Comparison of predicted thrust coefficient of WPX-8 stork wind turbine for 2 blade configuration
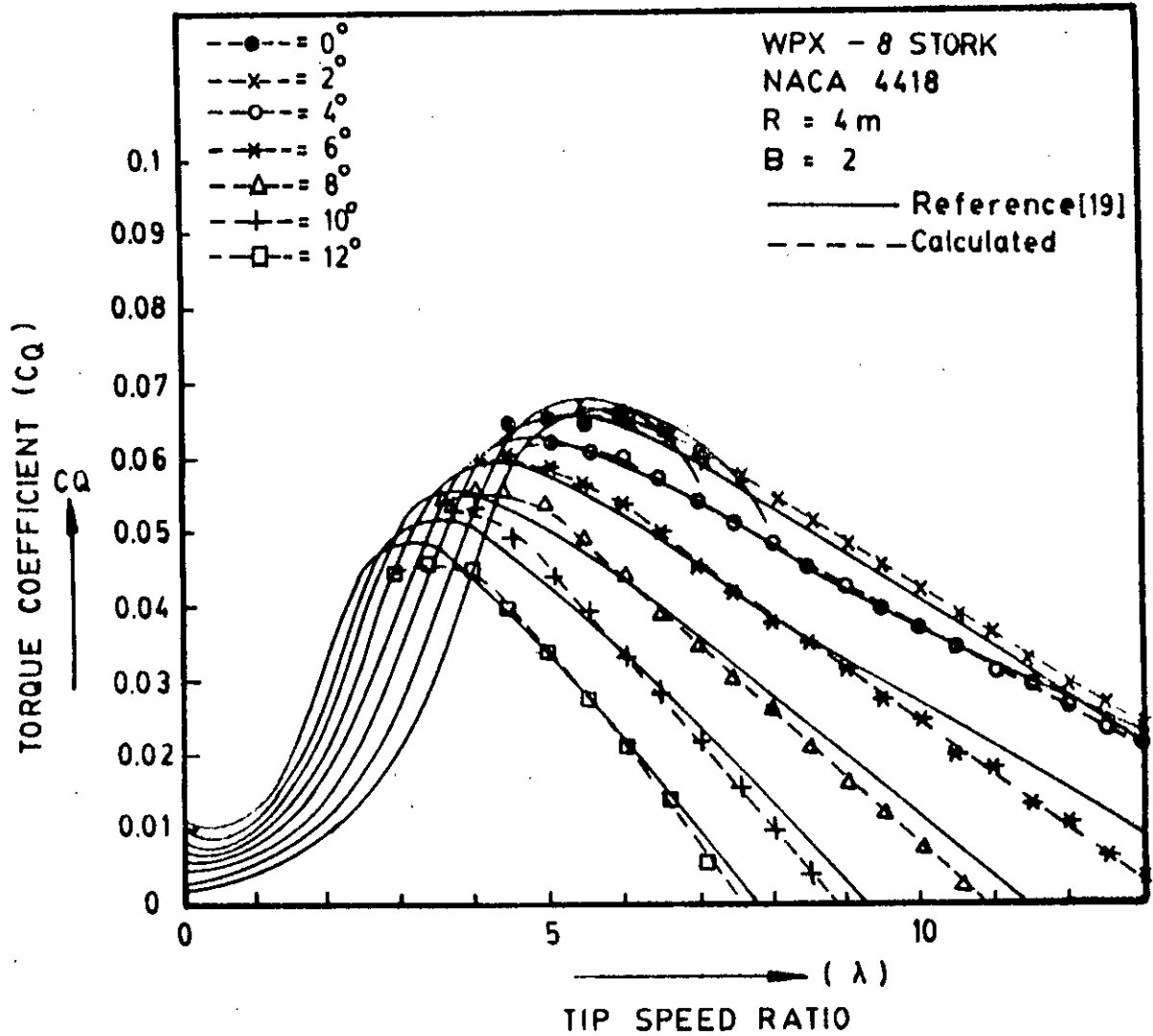
Figure 5.2.6. Comparison of predicted torque coefficients of WPX - 8 stork wind turbine for 2 blade configuration
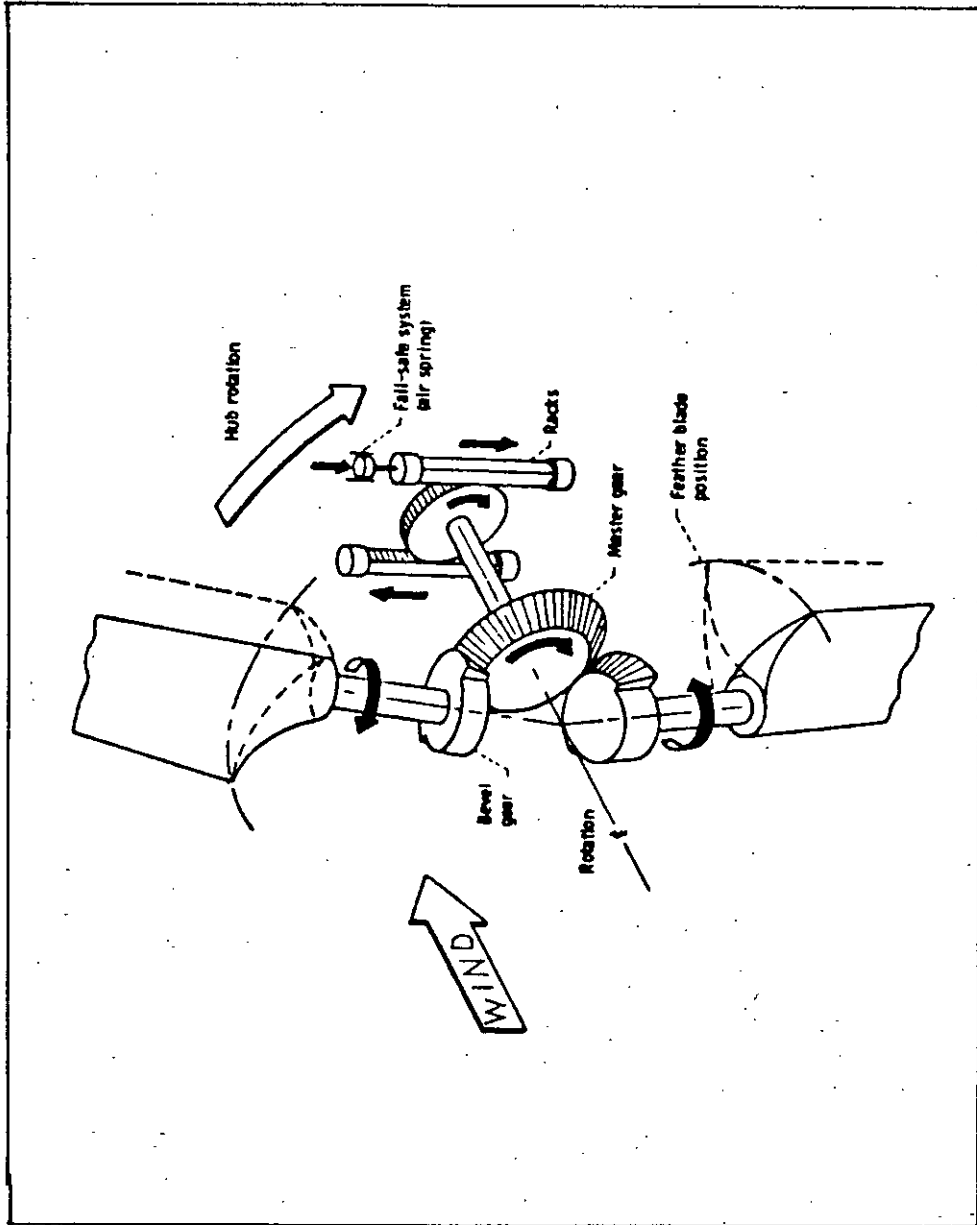
Fig 5.2.7: Blade Pitch Changing Mechanism; Reference [2]

WINDMILL	DIAM. m	RATED POWER kW	NO. OF BLADES	BLADE PROFILE	RPM	CONING ANGLE (Deg.)	TILT ANGLE (Deg.)	BLADE LOCATION
AEROSTAR (Denmark)	7	9	3	NACA 44XX	120	3.5		Upwind
GRP KALKUGNEN (Sweden)	18	60	2/3	NACA 643-618	77	7.5		Upwind
HAWT 1.5M (Holland)	1.5	.75	4	STEEL PLATE	330			Upwind
HAWT 3M (U.K)	3	2	2	NACA 4412	286	5		Upwind
HMZ WIND-MASTER (Belgium)	21.8	50	3	NACA 44XX	40		5	Upwind
ITDG 6M (U.K)	6	5	3/4/6	ARCHED PLATE	120			Upwind
LM17.2 (Denmark)	17.2	50.3	3	NACA 63-212/ 63-224	50		5	Upwind
MOD-0 (U.S.A)	38.1	100	2	NACA 23024	32/40	3.8		Up/Down
MOD-0A (U.S.A)	38.1	200	2	NACA 230XX	40	7		Downwind
MOD-1 (U.S.A)	61	2000	2	NACA 230XX/ 44XX	34.7	9		Downwind
RIISAGER (Denmark)	10.24	20	3	CLARK-Y	61		5	Upwind
SMITH-PUTNAM (U.S.A)	53.35	1250	2	NACA 4418	28.7			Downwind
STORK WPX-8 (Holland)	8	23	2/3	NACA 4418	190			Upwind
VESTAS-15 (Denmark)	15.34	55	3	NACA 4416-4424	50.3		5	Upwind

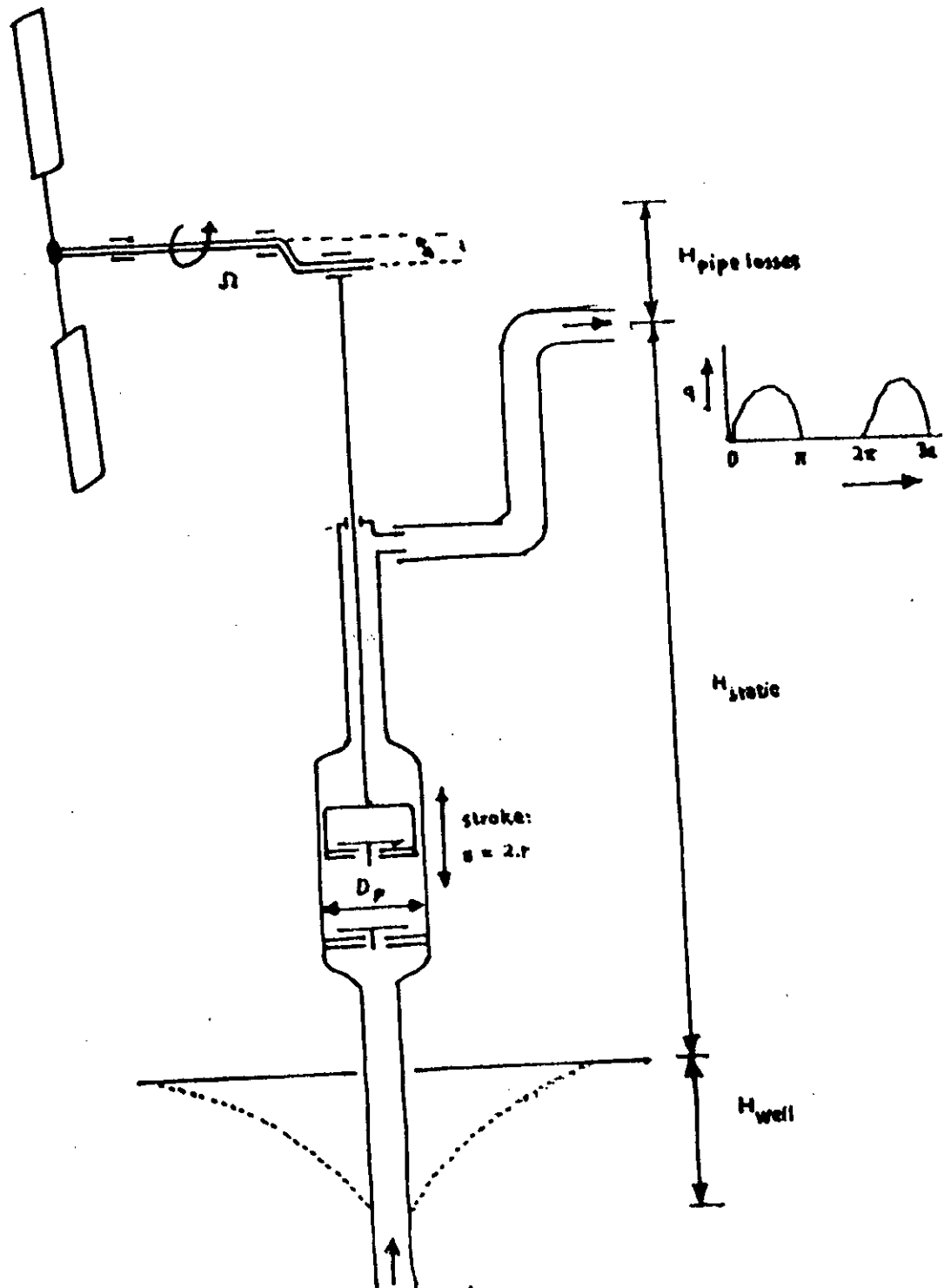Table 5.2.8: List of Wind Turbines. /¯19_7

Fig. 6.1 : Schematic drawing of a reciprocating
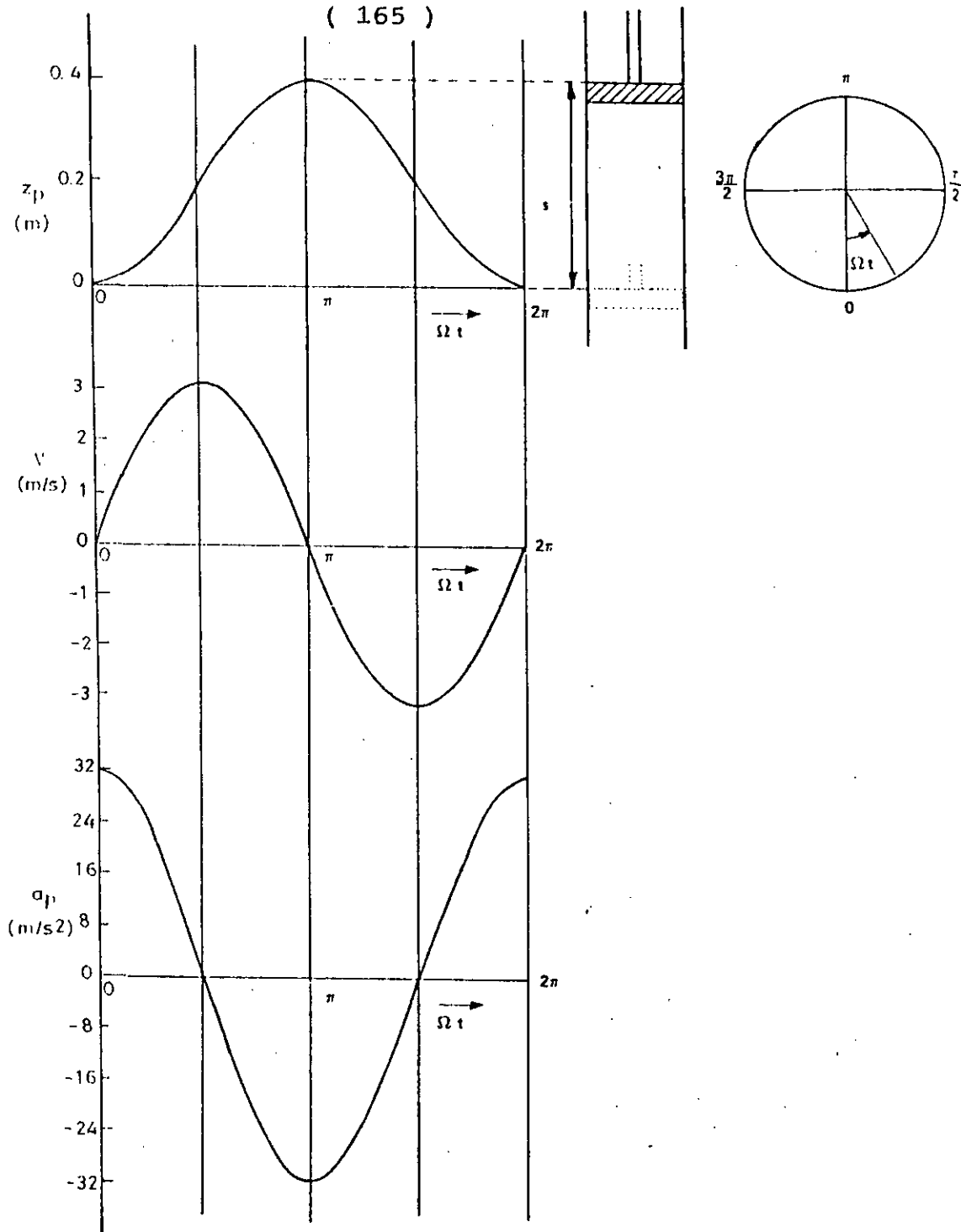piston pump connected to a wind rotor.

Fig. 6.2 : The displacement, velocity and acceleration of an ideal piston
pump with following characteristics:

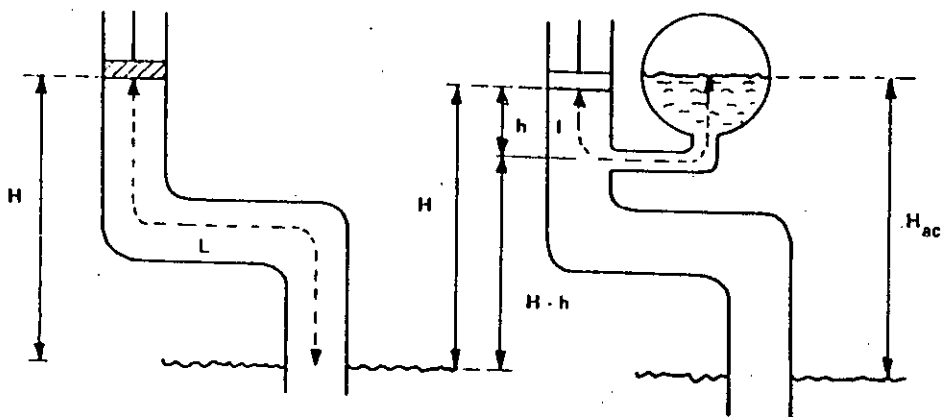$$s = .425 \text{ m.}$$
$$\Omega = 1.378 \text{ rps}$$

Fig. 6.3: Idealised piston pump   Fig. 6.4: Idealised piston pump
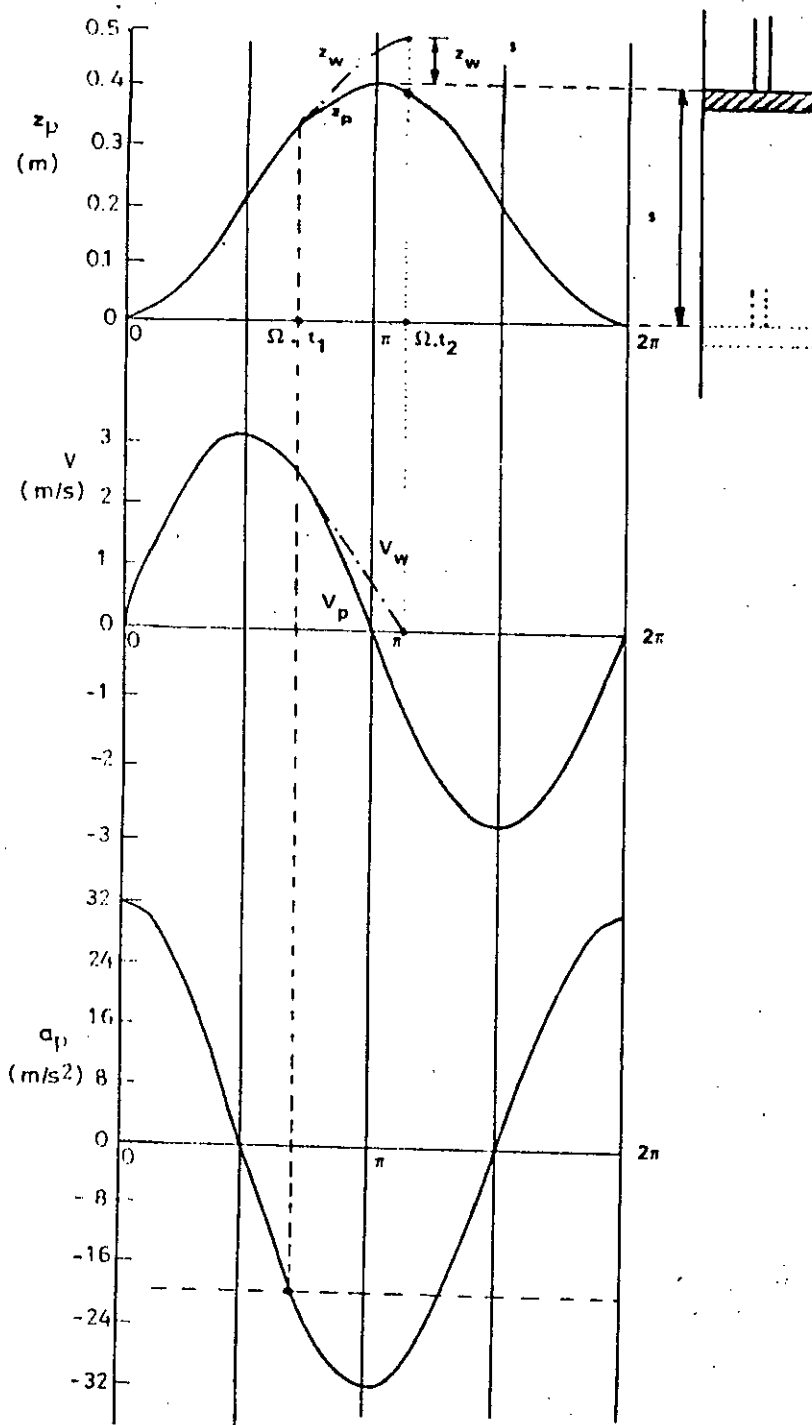without air chamber.   with suction air chamber.

Fig. 6.5: The displacement velocity and acceleration of an ideal piston pump.
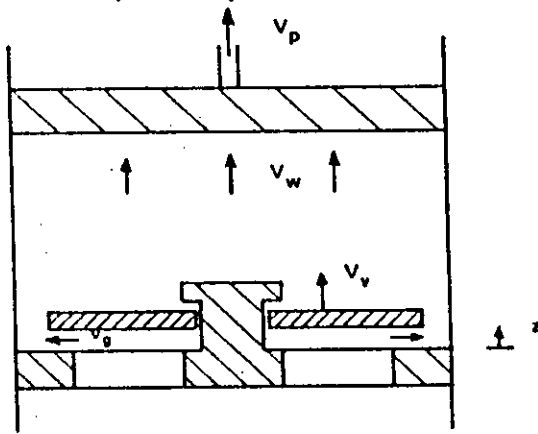
Fig. 6.6 : Schematic drawing of the foot valve of a
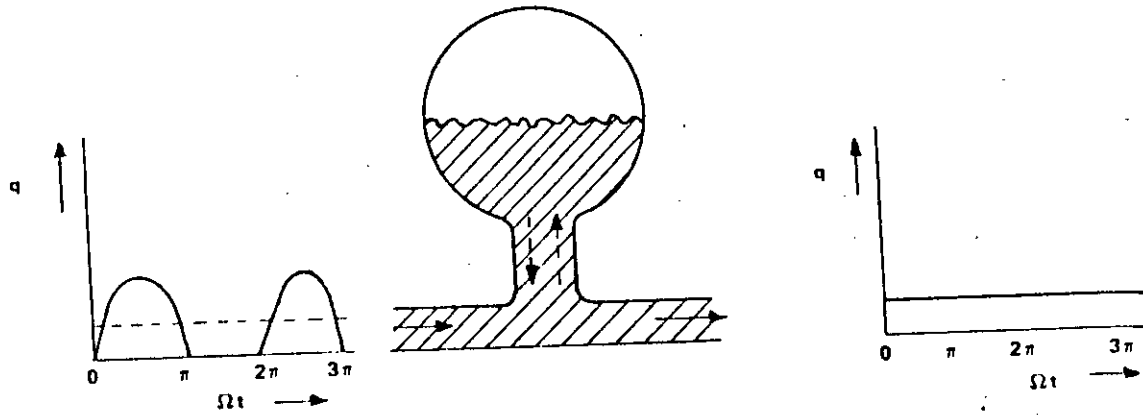reciprocating piston pump (27).

Fig. 6.7 : The in and outgoing flow of an ideal air
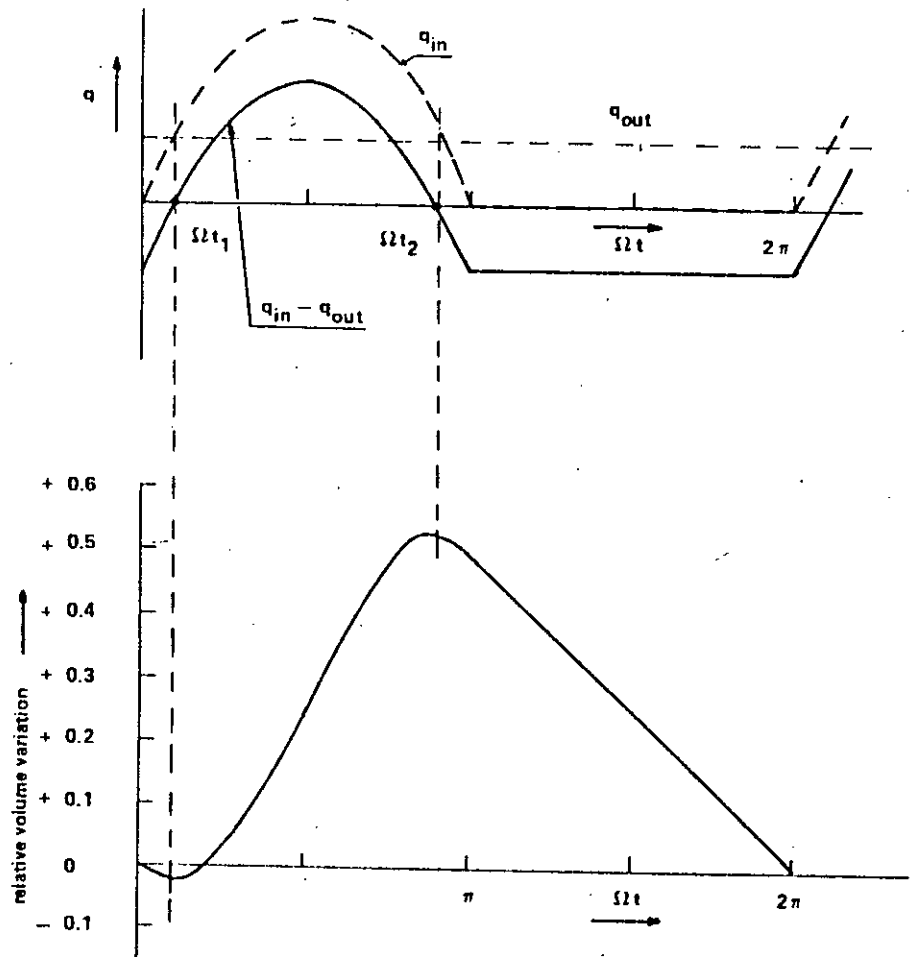chamber coupled to a single-acting piston pump.

Fig. 6.8 : Determination of volume variations of the ideal air chamber, i.e. with a constant outgoing flow.
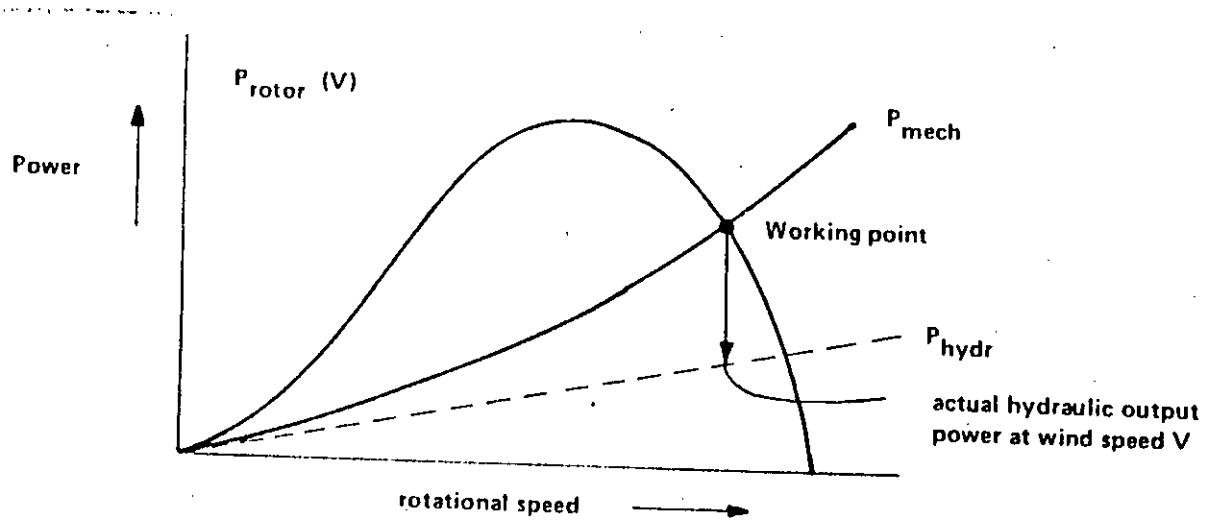
Fig. 7.1 : Working point of a rotor-pump combination at a given wind speed V.
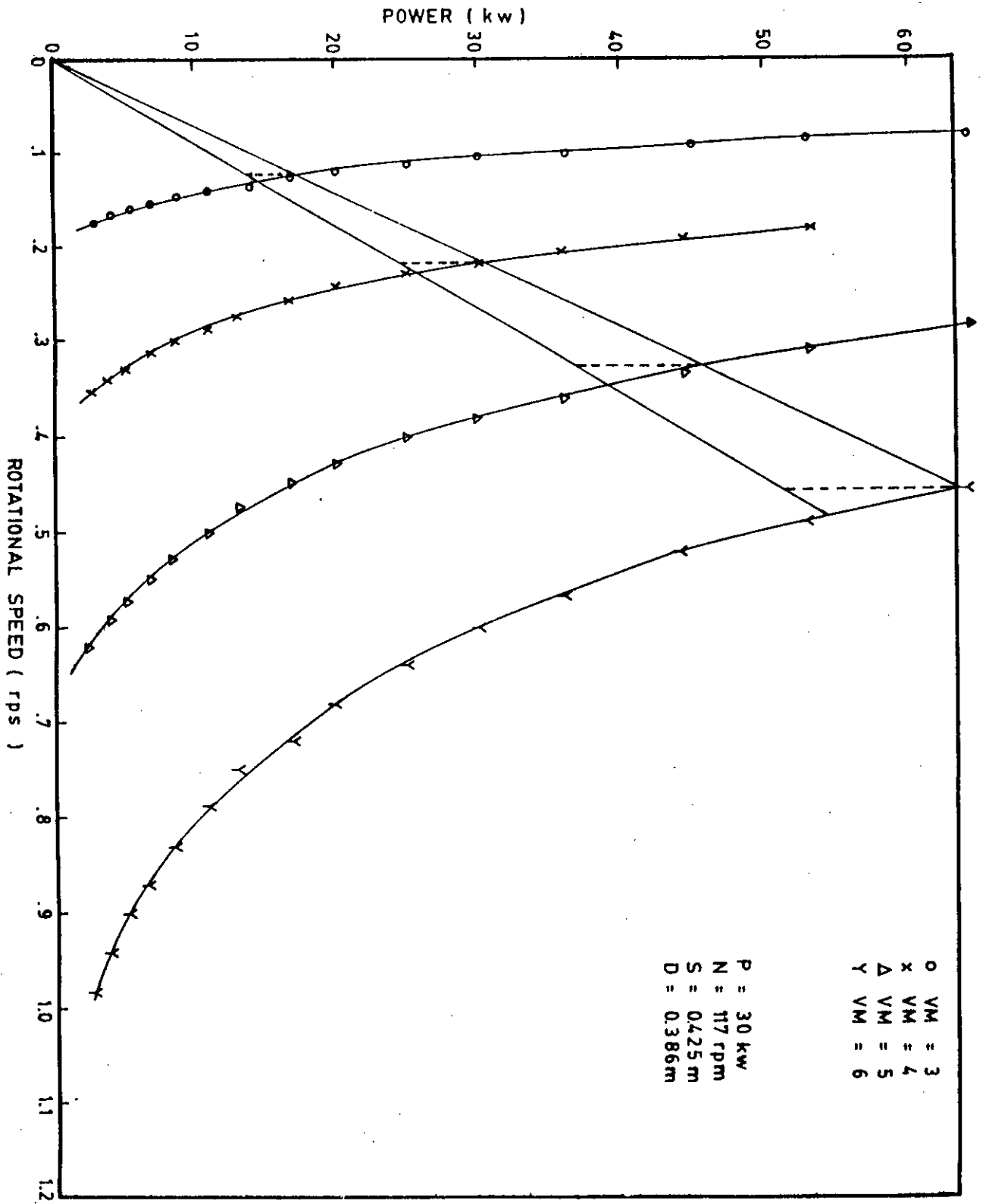
Fig. 7.2: Working point of rotor-pump combination at different wind speed

POWER (kw)

ROTATIONAL SPEED (rps)

o VM = 3
x VM = 4
△ VM = 5
Y VM = 6

P = 30 kw
N = 117 rpm
S = 0.425 m
D = 0.386 m

Fig. 7.3: Hydraulic output as a function of wind speed

P = 30 kw
N = 117 rpm
S = 0.425m
D = 0.386m
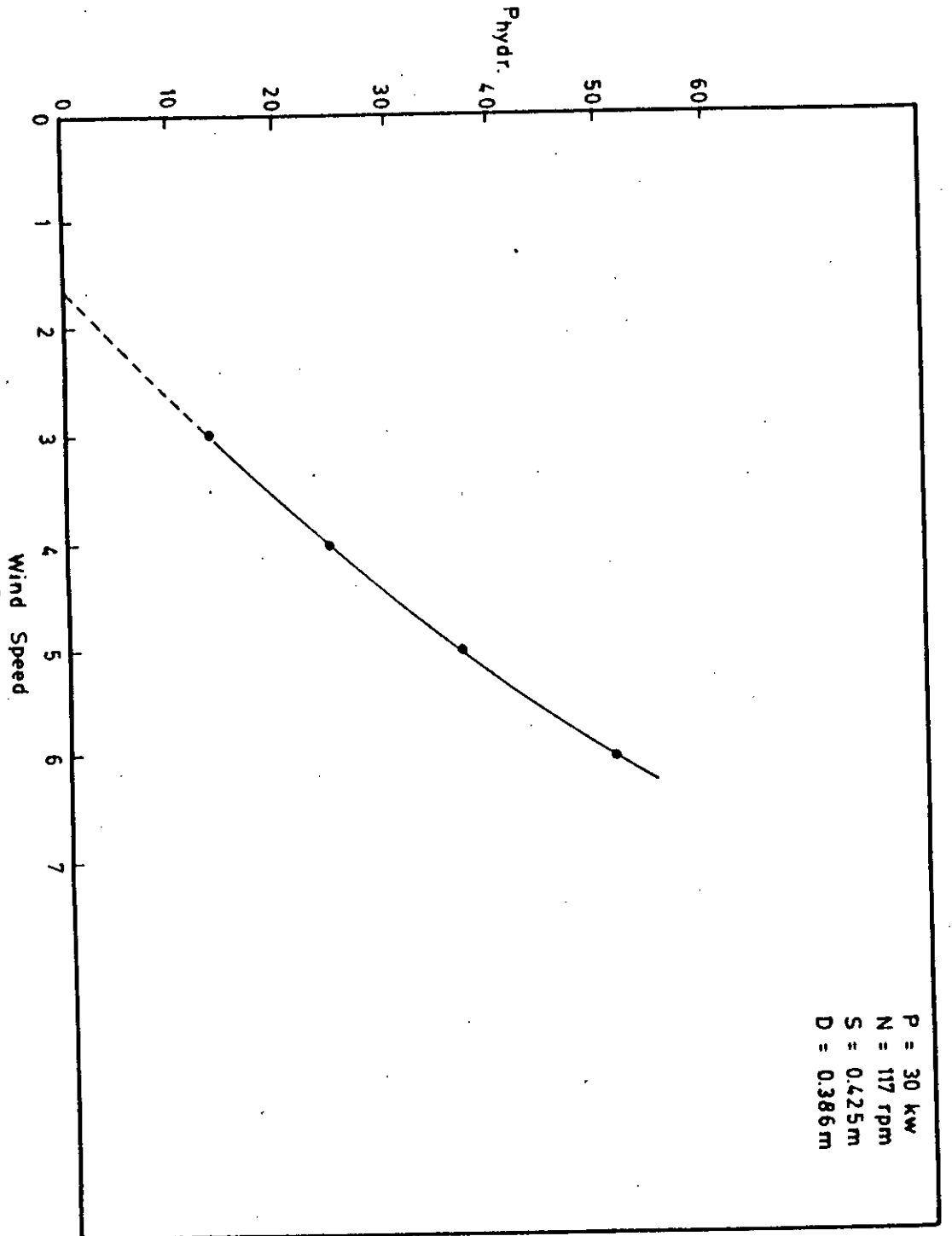
Fig. 7.4: TORQUE FOR SINGLE ACTING PUMP. (THREE PUMPS COUPLED IN
SINGLE WITH 120° P ASE DIFFERENCE)

Fig. 7.5 : Schematic drawing of a piston with a leakhole
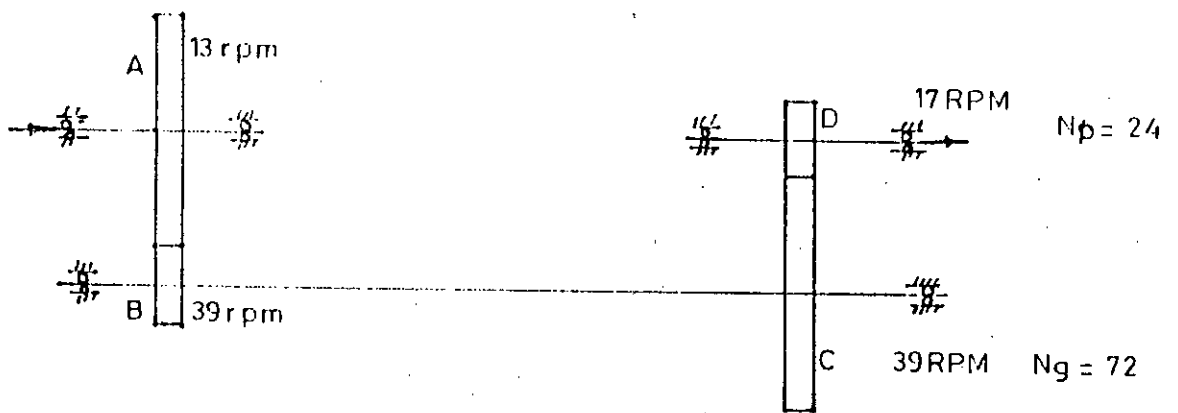
Fig. 7.6:   Gear Design.

APPENDICES

Appendix - A

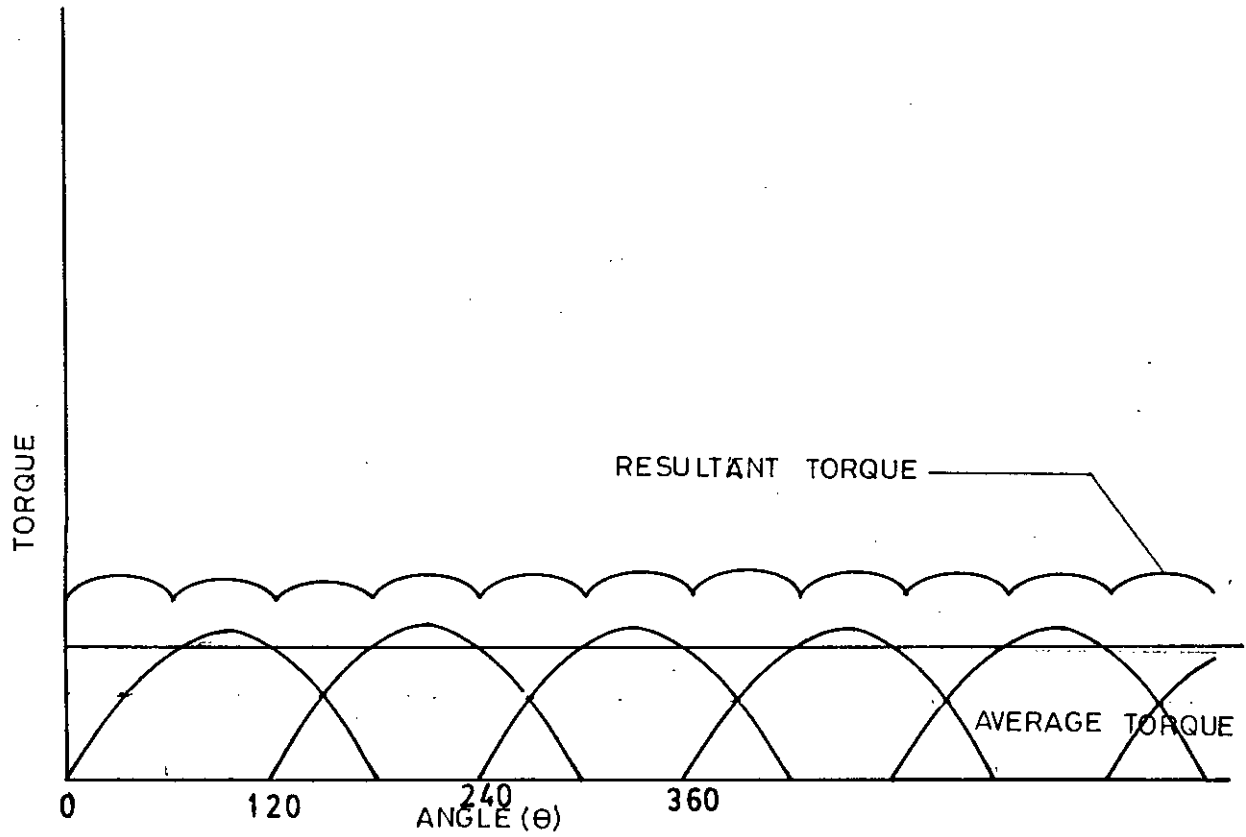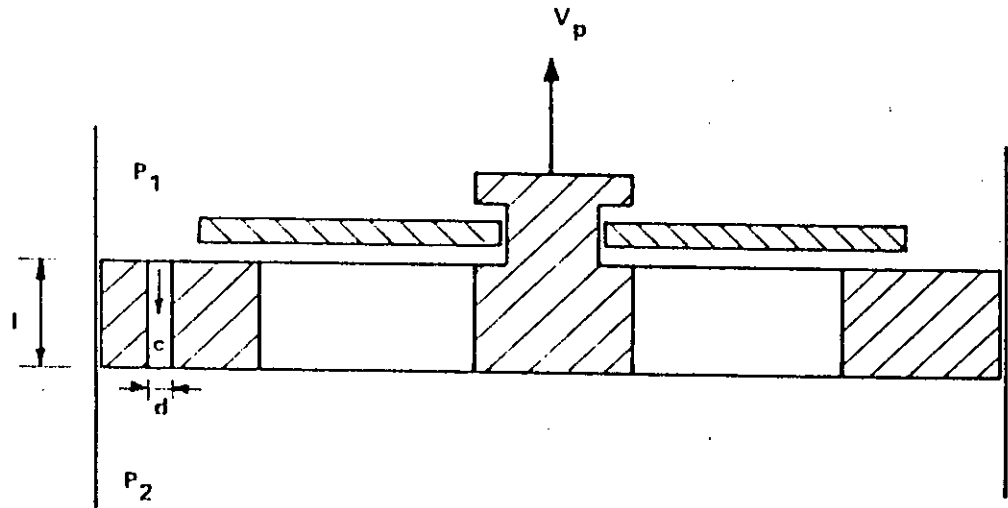Ten stations from all over Bangladesh analysed the availability of wind velocity. The following stations are found to have good potential for the use of wind power $\sqrt{28}$_7

	Stations	Potential month for power generation by windmill	Average wind speed
1.	Chittagong	March to September	4 m/sec.
2.	Dhaka	March to October	3.2 m/sec.
3.	Khepupara	February to September	3.5 m/sec.
4.	Comilla	March to September	2.8 m/sec.
5.	Teknaf	June to September	2.3 m/sec.
6.	Jessore	April to September	2.1 m/sec.
7.	Cox's Bazar	May to August	2 m/sec.
8.	Hatiya	Ends of April to July	1.9 m/sec.
9.	Dinajpur	March to August	2 m/sec.
10.	Rangamati	April and May	1.9 m/sec.

Appendix - C : Relation between a & a^1

$$C_p = \frac{8}{\lambda^2} \int_0^\lambda (1 - a') a' \; r^3 \; d\lambda r \qquad \boxed{\text{From Eqn.3.1.27}}$$

$$\frac{dc_p}{da} = \frac{da'}{da}(1 - a) - a' = 0$$

$$\frac{da'}{da} \qquad \frac{a'}{1-a}$$

$$a(1-a) = a'(1+a') \lambda_r^2 \qquad \boxed{\text{From Eqn. 3.1.21}}$$

$$1-2a = \boxed{(1+a')\frac{da'}{da} + a' \frac{da'}{da}} \lambda_r^2$$

$$1-2a = (1+2a') \frac{da'}{da} \lambda_r^2$$

$$1-2a = (1+2a') \frac{a'}{1-a} \lambda_r^2$$

$$= (1+2a') \frac{a'}{(1-a)} \; \frac{a(1-a)}{a'(1+a')}$$

$$1-2a = \frac{(1+2a')a}{1+a'}$$

$$(1-2a)(1+a') = (1+2a')a$$

$$1-2a+a'-2aa' = a+2aa'$$

$$1-3a = 4aa' \Leftarrow a'(4a-1)$$

$$a' = \frac{1-3a}{4a-1}$$

Appendix - B : Selection of Design Parameters

For the design of a horizontal axis wind turbine it is important to find the values of design lift coefficient from graphs that correspond with a minimum value of C_D/C_L ratio. To carry out the iteration procedures for the blade configuration, estimation of design power coefficient is also important. Determination of these parameters are discussed in the following sections :

B.1. Determination of Minimum C_D/C_L Ratio

The lift and drag coefficients of a given airfoil for a given Reynolds number are shown in Figure B.1.1. In the C_D/C_L graph a tangent is drawn through $C_D = C_L = 0$. From the point where the tangent touches the curve indicates the minimum C_D/C_L ratio. This ratio determines the maximum power coefficients that can be reached, particularly at high tip speed ratios. From the $C_L - \alpha$ curve corresponding to minimum C_D/C_L ratio the values of lift coefficient and angle of attack are found. The C_L and α values found in this way are known as design lift coefficient, C_{L_d} and design angle of attack, α_d and these are very important parameters in the design process.

APPENDIX.

NACA 4418

(Stations and ordinates given in
per cent of airfoil chord)

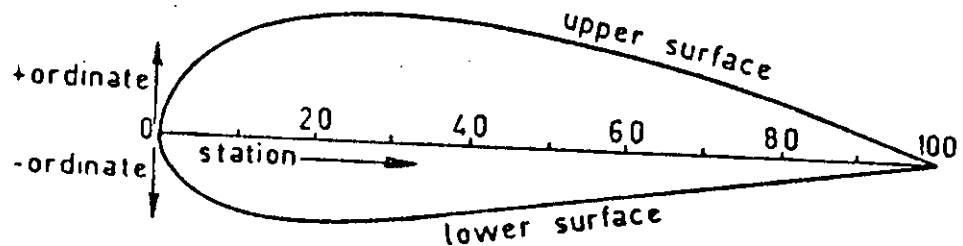| Upper surface		Lower surface	
Station	Ordinate	Station	Ordinate
0	.....	0	0
1.25	3.76	1.25	− 2.11
2.5	5.00	2.5	− 2.99
5.0	6.75	5.0	− 4.06
7.5	8.06	7.5	− 4.67
10	9.11	10	− 5.06
15	10.66	15	− 5.19
20	11.72	20	− 5.56
25	12.10	25	− 5.19
30	12.76	30	− 5.26
40	12.70	40	− 4.70
50	11.85	50	− 4.02
60	10.41	60	− 3.21
70	8.55	70	− 2.45
80	6.22	80	− 1.67
90	3.46	90	− 0.93
95	1.89	95	− 0.55
100	(0.19)	100	(− 0.19)
100	.....	100	0

Fig. B 1.4: Stations and ordinates are shown in
percent of airfoil NACA 4418 Chord (20).
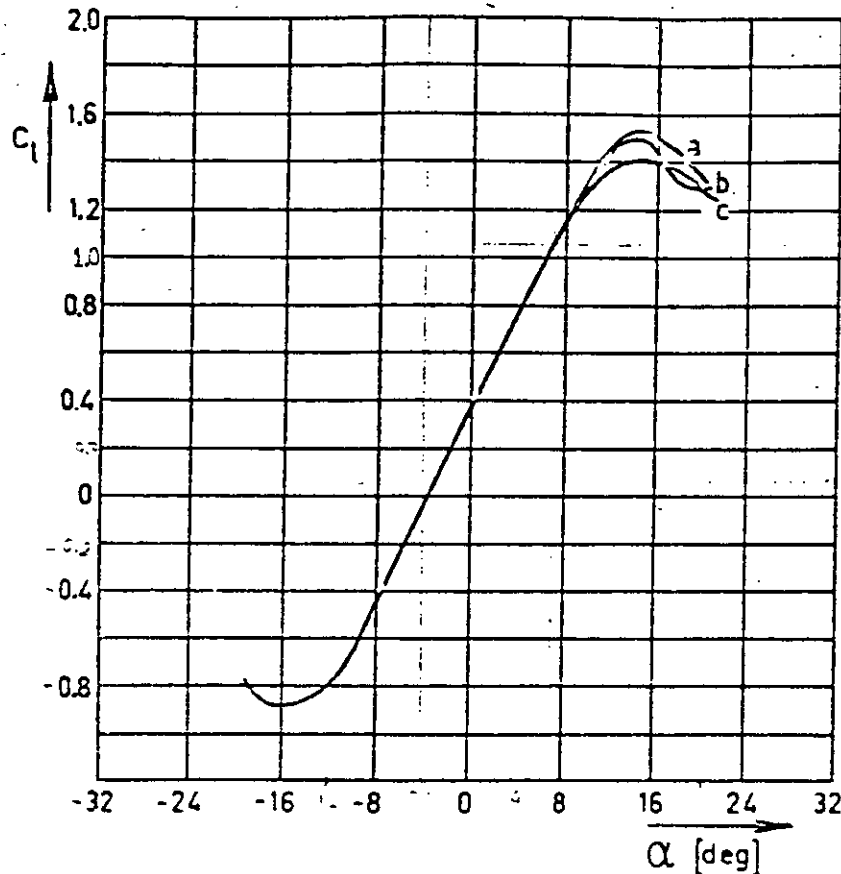
Fig. B 1.1: $C_L - \alpha$ Curve for a NACA 4418
airfoil section

a. $Re = 9 \cdot 10^6$
b. $Re = 6 \cdot 10^6$
c. $Re = 3 \cdot 10^6$

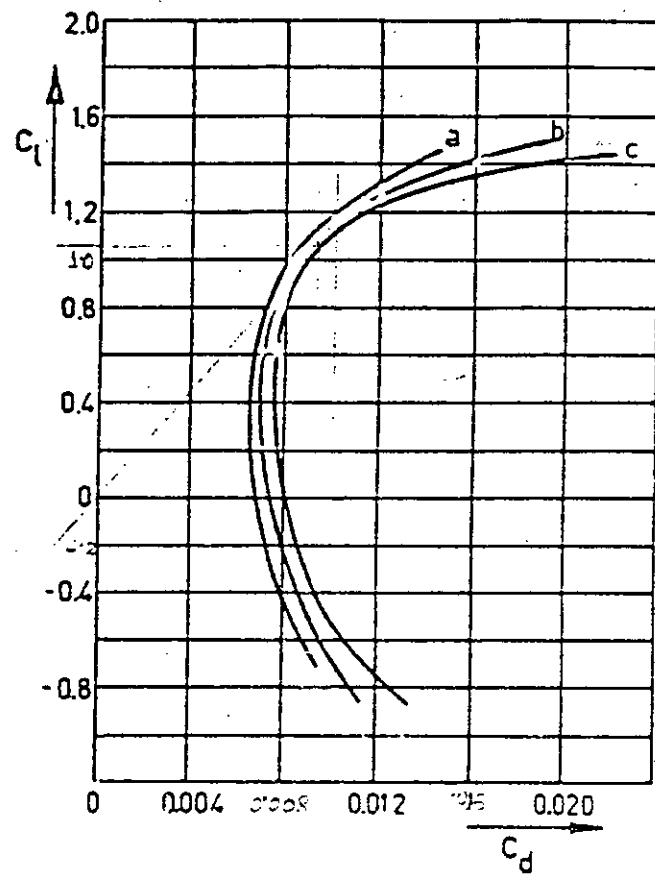Fig. B1.2: $C_L - C_D$ Curve for a Given Airfoil
Section (20).
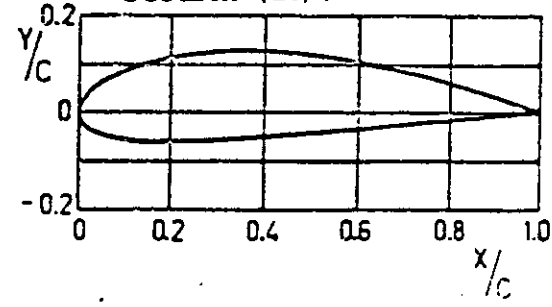
NACA 4418

Fig. B1.3: NACA 4418 Profile.

B.2 Determination of Design, C_p

The power coefficient is affected by the profile drag via the C_D/C_L ratio. The reduction of the maximum power coefficient is proportional to the tip speed ratio and to the C_D/C_L ratio. The result is shown in Figure B.2.1. The curves show for each λ the maximum attainable power coefficient with the number of blade and C_D/C_L ratio as a parameter. In this collection of maximum power coefficients it is seen that for a range of design tip speed ratio from 1 to 10 the maximum theoretically attainable power coefficients lie between 0.30 to 0.50.

Now we can design a windmill rotor for a given wind-speed $V_{\&}$ and a power demand. First the minimum C_D/C_L ratio of an airfoil is to be determined. The procedure for selection of number of blades, B and the design tip speed ratio λ has been explained in chapter 3. From Figure B.2.1. the maximum expected power coefficient can be found out. For conservative design the design C_p is calculated as $\boxed{20}$

$$C_p = 0.8 \, {}^{*}C_{p_{max}}$$

(B 2.1)

Appendix - D

$$C = a_1 r + a_2 \qquad\qquad (D.1)$$

$$\beta_r = a_3 r + a_4 \qquad\qquad (D.2)$$

$$C_{90} = {}^\cdot 9Ra_1 + a_2 \qquad\qquad (D.3)$$

$$C_{50} = {}^\cdot 5Ra_1 + a_2 \qquad\qquad (D.4)$$

From (C.3) & (C.4)

$$a_1 = \frac{2{}^\cdot 5\,(C_{90} - C_{50})}{R}$$

$$a_2 = C_{90} - {}^\cdot 9Ra_1$$

$$= C_{90} - {}^\cdot 9\cancel{R} \times \frac{2{}^\cdot 5(C_{90} - C_{50})}{\cancel{R}}$$

$$= C_{90} - 2{}^\cdot 25C_{90} + 2{}^\cdot 25C_{50}$$

$$= 2{}^\cdot 25C_{50} - 1{}^\cdot 25C_{90}$$

Putting a_1 & a_2 in eqn (C.1)

The eqn becomes

$$C = 2.5\,(C_{90} - C_{50})\,\frac{r}{R} + 2{}^\cdot 25C_{50} - 1{}^\cdot 25C_{90}$$

Similarly

$$\beta = 2{}^\cdot 5(\beta_{90} - \beta_{50})\,\frac{r}{R} + 2{}^\cdot 25\,\beta_{50} - 1{}^\cdot 25\,\beta'_{90}.$$

Appendix E

E.1 Piston pumps with a leakhole

For most of the leakholes, the length l is only a few times the diameter d, or sometimes even smaller than d. This means that pipe flow formulas cannot be used, but that the expressions for orifice flow must be used. The pressure difference over the leakhole is :

$$P_1 - P_2 = f * \tfrac{1}{2} \rho_w c^2 \qquad (E.1)$$

The friction factor f is slightly dependent on the Reynolds number but for values of Re 10^4 a value of f = 2.75 is a good approximation.

At low piston speeds the velocity C of the flow in the leakhole is given by the continuity of mass flow :

$$C = \frac{D_p^2}{d^2} V_p \qquad (E.2)$$

If the speed of the piston increases, C will increase and consequently the pressure, $(P_1 - P_2)$ to sustain the flow. At a given speed $V_p = V_o$, the pressure difference $(P_1 - P_2)$ equals the pressure head :

$$P_1 - P_2 = \rho_w gH \qquad (E.3)$$

With equation (E.1) the speed in the leakhole becomes :

$$C = (\frac{2 \, g \, H}{f}) \qquad (B.4)$$

The discharge of the pump starts if the speed of the piston $V_p \, / \! / \, V_o$ with:

$$V_o = \frac{d^2}{D_p^2} * \sqrt{(\frac{2 \, g \, H}{f})} \qquad\qquad (E.5.)$$

The speed is at its highest value if $\theta = \frac{\pi}{2}$, so the minimum rotational speed to pump water is given by:

$$\Omega_o = \frac{V_o}{\tfrac{1}{2} \, s} = \frac{d^2}{\tfrac{1}{2} \, s \, D_p^2} * \sqrt{(\frac{2 \, g \, H}{f})} \qquad\qquad (E.6.)$$

At higher (constant) rotational speeds the discharge starts at angles θ_o smaller than $\frac{\pi}{2}$

$$\tfrac{1}{2} \, s \, \sin \theta_o = \Omega_o \, \tfrac{1}{2} \, s \qquad\qquad (E.7.)$$

$$\theta_o = \sin^{-1} \frac{\Omega_o}{\Omega}$$

The torques to drive the pump at speeds below or above Ω_o are calculated as follows:

$$Q_p = (P_1 - P_2) * \tfrac{1}{2} \, V_s * \sin \theta \quad (\, \Omega / \Omega_o) \qquad (E.8)$$

Using equations (E.1), (E.2) and (E.8) one finds:

$$Q_p = \tfrac{1}{2} \, \rho_w \frac{D_p^4}{d^4} \, V_p^2 * f * \tfrac{1}{2} \, V_s * \sin \theta$$

With $V_p = \Omega \tfrac{1}{2} s \sin \theta$, equation(E.5) and equation(E.6) this transforms into :

$$Q_p = \rho_w \, g \, H * \frac{\Omega^2}{\Omega_o^2} * \tfrac{1}{2} V_s * \sin^3 \theta$$

or $\quad Q_p = \bar{Q}_{id} * \pi * \dfrac{\Omega^2}{\Omega_o^2} * \sin^3 \theta \quad (\Omega \le \Omega_o)$ $\qquad$ (E.9.)

The average torque $\bar{Q}_p$ for $\Omega \angle \Omega_o$ can be calculated with:

$$\frac{1}{2\pi} \int_o^\pi \sin^3 \theta \, d\theta = \frac{2}{3\pi} \qquad \text{(E.10)}$$

Resulting in:

$$\bar{Q}_p = \bar{Q}_{id} * \frac{2}{3} \frac{\Omega^2}{\Omega_o^2} \qquad (\Omega \angle \Omega_o) \qquad \text{(E.11)}$$

$$\bar{Q}_p = \frac{\bar{Q}_{id}}{2\pi} * 2 \int_o^{\theta_o} \frac{\Omega^2}{\Omega_o^2} \sin^3 \theta \, d\theta + \frac{Q_{id}}{2\pi} \int_{\theta_o}^{\pi - \theta_o} \pi \sin \theta \, d\theta \quad \text{(E.12)}$$

The result is:

$$\bar{Q}_p = \bar{Q}_{id} \left\{ \frac{2}{3} \frac{\Omega^2}{\Omega_o^2} + \frac{2}{3} \left(1 - \frac{\Omega^2}{\Omega_o^2} \right) * \sqrt{\left(1 - \frac{\Omega_o^2}{\Omega^2} \right)} \right\} (\Omega \rangle \Omega_o) \qquad \text{(E.13)}$$

The discharge of the pump, taking place between θ_o and $\pi - \theta_o$ has to be subtracted by the flow through the leakhole:

$$q_{leak} = \frac{\pi}{4} d^2 * C \qquad (E.14)$$

$$q_{leak} = \frac{\pi}{4} d^2 * \sqrt{(\frac{2 \, g \, H}{f})} \qquad (E.15)$$

with the equation 4.53 and 4.54 this reduces to

$$q_{leak} = \Omega_o * \frac{1}{2} \nabla_s \qquad (E.16)$$

or with,

$$\bar{q}_{id} = \frac{\Omega}{2\pi} \nabla_s$$

$$q_{leak} = \bar{q}_{id} * \pi \frac{\Omega_o}{\Omega} \qquad (E.17)$$

The instantanous flow discharge by the pump becomes(Fig. E.2)

$$q = \bar{q}_{id} (\pi \sin \theta - \pi \frac{\Omega_o}{\Omega}) \qquad (E.18)$$

The average flow is:

$$\bar{q} = \frac{\bar{q}_{id}}{2\pi} \int_{\theta_o}^{\pi - \theta_o} (\pi \sin \theta - \frac{\Omega_o}{\Omega}) \, d\theta$$

resulting in:

$$\bar{q} = \bar{q}_{id} \left\{ \sqrt{(1 - \frac{\Lambda_o^2}{\Lambda_2})} - \frac{\Lambda_o}{\Lambda} (\frac{\pi}{2} - \theta_o) \right\} \qquad (E.19)$$

The volumetric efficiency due to the effect of the leakhole is equal to the ratio of $\bar{q}$ and $\bar{q}_{id}$:

$$\eta_{leak, vol} = \sqrt{(1 - \frac{\Lambda_o^2}{\Lambda_2})} - \frac{\Lambda_o}{\Lambda} (\frac{\pi}{2} - \sin^{-1} \frac{\Lambda_o}{\Lambda}) \qquad (E.20)$$

The mechanical efficiency due to the effect of the leakhole is found with equation (4.8):

$$\eta_{leak, mech} = \eta_{leak, vol} \frac{\bar{Q}_p}{\bar{Q}_{id}} \qquad (E.21)$$

E.2 Calculating the diameter of a leak hole

$$R \quad = \quad 23 \cdot 2668 m$$

$$C_{p_{max}} \quad = \quad 0 \cdot 45$$

$$\eta_{mech} \quad = \quad 0.82$$

$$\eta_{vol} \quad = \quad 1 \times 0 \cdot 9 = 0 \cdot 9$$

$$\lambda_d \quad = \quad 8$$

$$D_p \quad = \quad 0 \cdot 386 \qquad \qquad f = 2 \cdot 75 \text{ (for submersed orifice flow)}$$

$$S \quad = \quad 0 \cdot 425$$

$$d^2 \quad = \quad \frac{(0 \cdot 386)^3}{30.8} \quad X \quad \left(\frac{0 \cdot 9 \ X \ (\cdot 425)^3 \ X \ 8^3}{\cdot 45 \ X \ \cdot 82 \ X \ (23 \cdot 266)^5} \right)^{\frac{1}{2}} X \ \frac{1000 \ X \ 2 \cdot 75}{8 \ \pi \ X \ 1 \cdot 225}$$

$$d \quad = \quad 8 \cdot 17 \ X \ 10^{-3} m$$

$$\quad = \quad 8 \cdot 17 mm$$

with a piston diameter of $0 \cdot 386$ and a stroke of $0 \cdot 425 m$

the leak hole must have a diameter of $8 \cdot 17 mm$.

E.3[2] To calculate Ω_o

$$\Omega_o \quad = \frac{d^2}{\frac{1}{2} D_p^2 S} \quad X \ \sqrt{\frac{2 \ gH}{f}}$$

$$\Omega_0 = \frac{(\cdot 00817)^2}{\frac{1}{2} \times \cdot 425 \times (\cdot 386)^2} \times \sqrt{\frac{2 \times 9 \cdot 81 \times 8 \cdot 5}{2 \cdot 75}}$$

$$= 0 \cdot 0164427$$

$$\Omega^* = 1 \cdot 3754 \times 9 = 12 \cdot 3786$$

$$\frac{\Omega^*}{\Omega_0} = \frac{12 \cdot 3786}{0 \cdot 0164427} = 752 \cdot 83$$

The discharge starts at angles θ_0

$$\theta_0 = \sin^{-1} \frac{\Omega_0}{\Omega^*} = 0 \cdot 07590 .^{o}$$

$\frac{\Omega}{\Omega_o}$	$\frac{\overline{Q}_p}{\overline{Q}_{id}}$	$\eta_{leak, mech}$	$\eta_{leak, vol}$
1	0.667	0	0
2	0.935	0.366	0.342
3	0.972	0.548	0.532
4	0.984	0.649	0.639
5	0.990	0.713	0.706
6	0.993	0.757	0.752
7	0.995	0.790	0.786
8	0.996	0.815	0.811
9	0.997	0.834	0.832
10	0.997	0.850	0.848
11	0.998	0.863	0.861
12	0.998	0.874	0.872
13	0.998	0.883	0.882
14	0.999	0.891	0.890
15	0.999	0.898	0.897
16	0.999	0.905	0.904
17	0.999	0.910	0.909
18	0.999	0.915	0.914
19	0.999	0.919	0.919
20	0.999	0.923	0.923
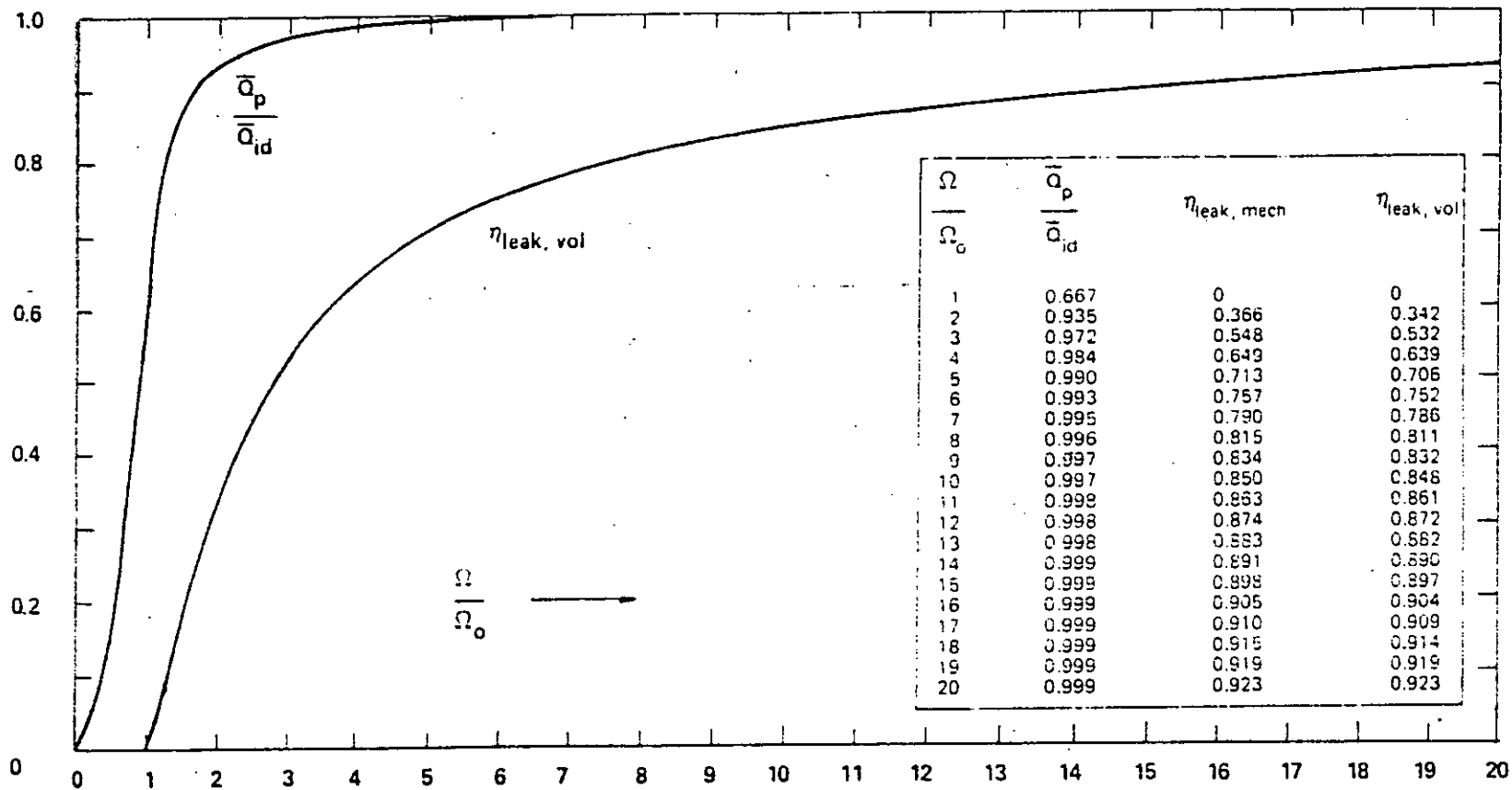
Fig. E1.1: The average torque and efficiencies of a piston pump, due to the effect of a leakhole, as a function of the relative speed. The rotational speed Ω_o is the speed at which the pumps starts pumping water. (27).

(213)

Appendix - F : Program Operation

The design analysis programme utilizes the modified strip theory discussed in chapter two. It was written by Stel N.Walker and Robert E. Wilson in the Fortran IV programme language and developed under the OS - 3 operating package for a CDC 3500 digital computer at Oregon State University and later modified for operation on a CDC 6600 computer. $\sqrt{45\_7}$

Thereafter it is modified to implement on IBM 370 VM/Sp release system in BUET computer center. This system with an interactive mode has no facility to plot curves and hence extensive print/write statements are inserted in the programme to have the values appear in output.

Computer Code "PROP" is a programme designed to calculate the performance of a horizontal axis wind turbine. This computer programme package used for analysis and utilizes simpson's rule of numerical integration.

Program Organisation

In this program unit 11 and unit 12 refer to the input file and output file respectively. This computer program consists of a main program and fifteen subroutines. The functions of them are discussed below.

1. **MAIN (PROP)**

    It is the main program, which performs input – output functions as well as the numerical integration of various performance quantities over the rotor blades.

2. **TITLES**

    A subroutine that outputs the program, input information in a descriptive form for reference.

3. **SEARCH**

    The subroutine that calculates the chord and twist angle at a given position on the blade utilizing a linear interpolation scheme on geometry data imputted.

4. **CALC**

    At each station, this subroutine determines the induced flow factors (axial and angular interference factors), the angle of attack and call the subroutine which determine the lift, drag and torque coefficients.

5. **TIPLOS**

    This subroutines determines tip and hubless factors based on Prandle's or Goldsterns formula.
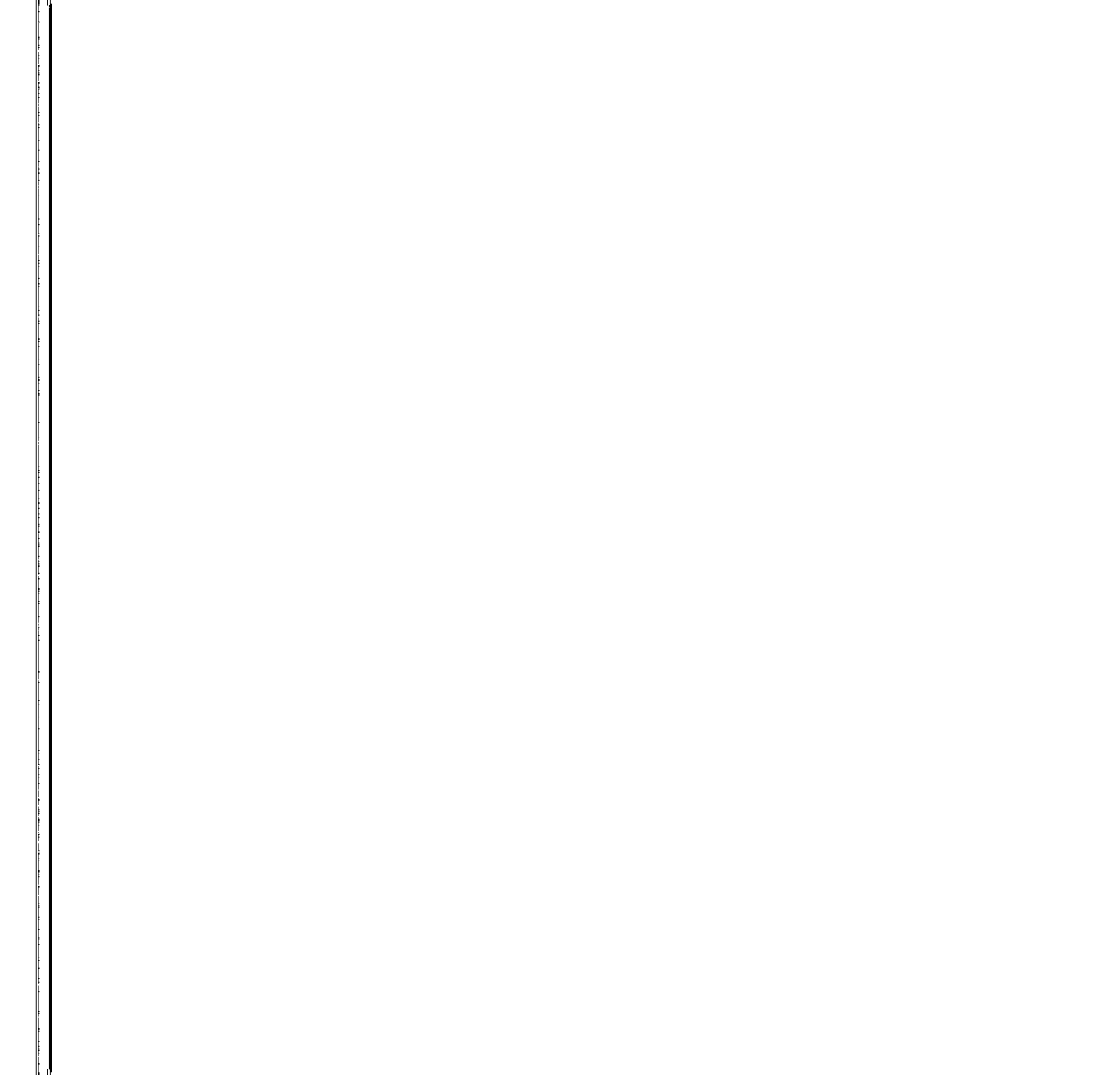
6. <u>BESSEL</u>

A subroutine that calculates modified Bessel functions for the Goldstein Tiploss Model.

7. <u>NACAOO</u>

The subroutine that determines the lift and drag coefficients at a given angle of attack for a NACAOO 12 airfoil series (Re = 6 X 10^6)

8. <u>NACA 44</u>

A subroutine that determine the loft and drag coefficients at a given angle of attack for a NACA 4418 airfoil series (Re = 6 X 10^6)

9. <u>NACA XX</u>

This subroutine is designed to use curvefit relations for airfoil designations not included by NACA00 and NACA44 without other program changes.

10. <u>NACA TT</u>

A subroutine that determines the lift and drag coefficients at a given angle of attack for tabular airfoil data inputted using linear interpolution.

11. **CLCD**

   A subroutine that determines the lift and drag coefficient at any profile.

12. **NACA 24**

   A subroutine that determine the lift and drag coefficients for NACA 23024.

13. **NACA 15**

   A subroutine that determine the lift and drag coefficients for NACA 0015 airfoil as a function of angle of attack .

14. **SOLIDI**

   The subroutine that determines the total solidity of the wind turbine design.

$$O = \int_{R_{Hrb}}^{R_{TIP}} \frac{BC}{R^2} \, dr.$$

where B is the number of blades, C is the local chord and r is the local radious.

15. **ACTIVI**

   A subroutine that determines the activity factor of a particular wind turbine design.

$$AF = \frac{10,000}{16} \int_{Hob}^{TIP} \frac{B}{D} \left(\frac{r}{R}\right)^3 d\left(\frac{r}{R}\right).$$ where D = diameter
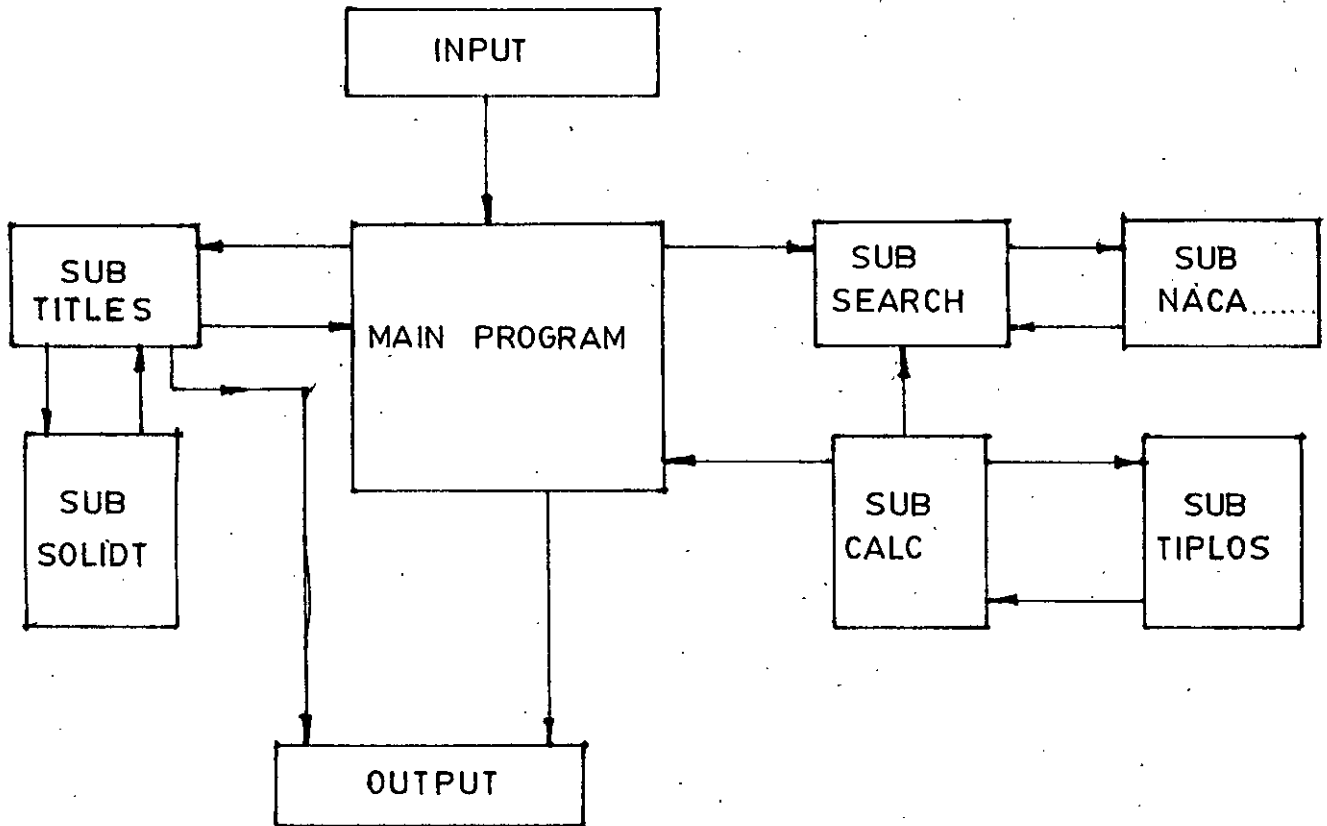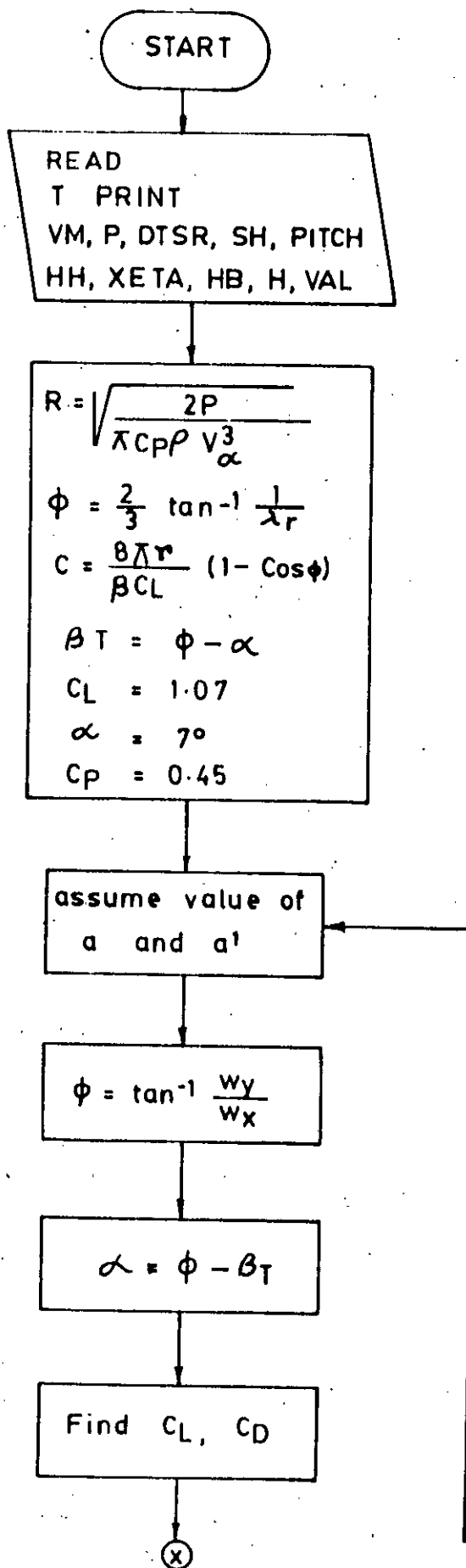
Fig. F.1. PROGRAM FLOW DIAGRAM.

$$\boxed{\text{START}}$$
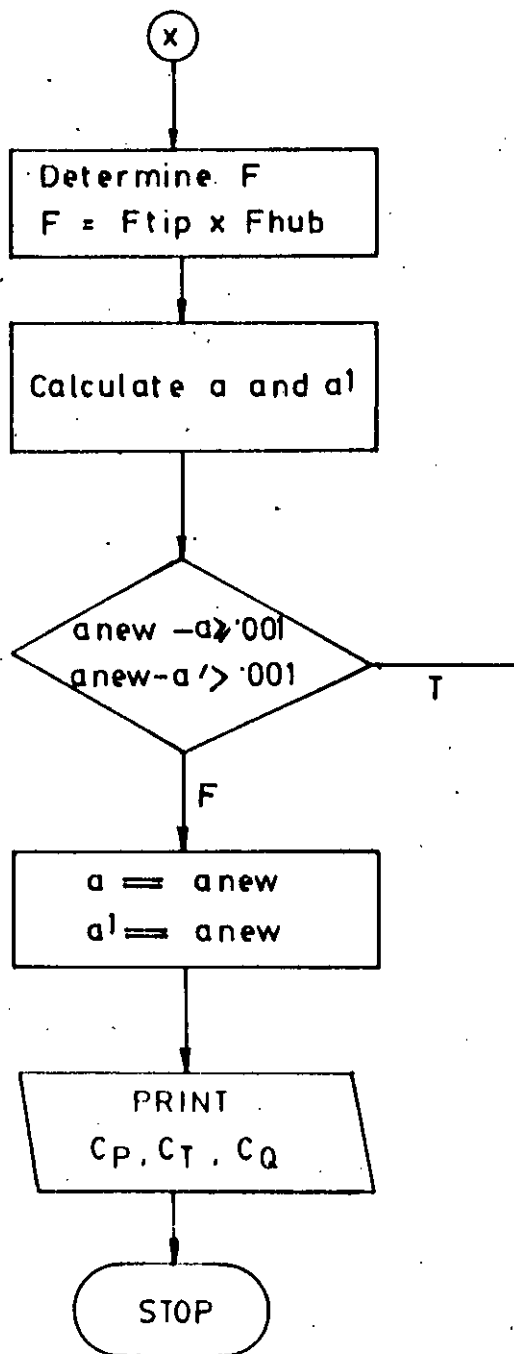
READ
T PRINT
VM, P, DTSR, SH, PITCH
HH, XETA, HB, H, VAL

$$R = \sqrt{\frac{2P}{\pi C_P \rho \, V_\alpha^3}}$$

$$\phi = \frac{2}{3} \tan^{-1} \frac{1}{\lambda_r}$$

$$C = \frac{8 \pi r}{\beta C_L} (1 - \cos\phi)$$

$$\beta T = \phi - \alpha$$

$$C_L = 1.07$$

$$\alpha = 7°$$

$$C_P = 0.45$$

assume value of
a and a'

$$\phi = \tan^{-1} \frac{w_y}{w_x}$$

$$\alpha = \phi - \beta_T$$

Find C_L, C_D

$$\bigotimes$$

FIG. 2 PROGRAM FLOW CHART

Appendix G : DETERMINATION OF CONING ANGLE AND MASS DISTRIBUTION.

Mass destribution is calculated by balancing the centrifugal force with aerodynamic lift force considering a certain coning angle. According to Figure G.1.1, for a small differential element, the relation between elementary lift dL and differential mass dm can be obtained by the following equation.

$$\frac{dL}{dr} = \Omega^2 r \cos\beta \, \sin\beta \, \left(\frac{dm}{dr}\right)$$

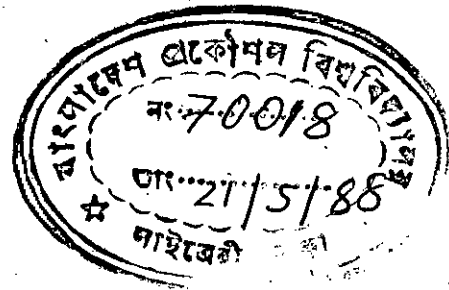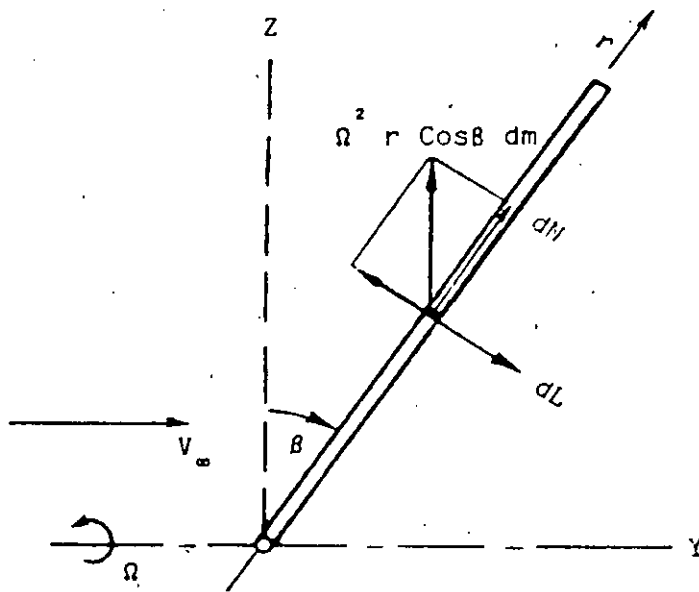It is assumed that the blade characterstics number of blades and airfoil sections are known.

Fig. G 1.1 : Lift and Centrifugal Forces on a Blade Element.